Supporting Information

Multifaceted role of silver salts as ligand scavengers and different behavior of nickel and palladium complexes: Beyond halide abstraction

Ignacio Pérez-Ortega and Ana C. Albéniz*
IU CINQUIMA/Química Inorgánica. Universidad de Valladolid. 47071 Valladolid (Spain).

1. Experimental details

1.1- General Considerations.

^{1}H, $^{13}C\{^{1}H\}$, $^{31}P\{^{1}H\}$ and ^{19}F NMR spectra were recorded on Bruker AV-400 or Agilent MR-500 spectrometers at the LTI-UVa Research Facilities. Chemical shifts (in δ units, ppm) were referenced to $SiMe_4$ (^{1}H and ^{13}C), $CFCl_3$ (^{19}F) and H_3PO_4 (85%, ^{31}P) The spectroscopic data were recorded at 293 K unless otherwise noted. Homonuclear (^{1}H-COSY and ^{1}H-NOESY) and heteronuclear (^{1}H-^{13}C HSQC and HMBC) experiments were used to help with the signal assignments. Size exclusion chromatography (SEC, also gel permeation chromatography, GPC) was carried out using a Waters SEC system on a three-column bed (Styragel 7.8x300 mm columns: 50-100000, 5000-500000 and 2000-4000000 Da) and a Waters 410 differential refractometer. SEC samples were run in $CHCl_3$ at 313 K and calibrated to polystyrene standards. Elemental analyses were carried out in a Carlo Erba 1108 microanalyser at the Vigo University, Spain or in a Thermo Fisher Sci. EA Flash 2000 microanalyser at the PCT, University of Burgos.

CH_2Cl_2 and THF were dried using a solvent purification system SPS PS-MD-5, toluene was dried with Na, distilled and stored over 4 Å molecular sieves. Acetone was dried using $CaSO_4$ and distilled. CD_2Cl_2 and $CDCl_3$ were dried using CaH_2 and distilled. All commercial reagents and solvents were used as received unless otherwise indicated.

All catalytic reactions were conducted under a N_2 atmosphere employing Schlenk techniques. A solution of norbornene was prepared dissolving the appropriate amount in dry CH_2Cl_2 (3.8 M). The solution was kept under N_2 at -35 ºC and titrated by ^{1}H NMR with $C_6H_3Br_3$ as internal standard.

Norbornene, magnesium, $AgBF_4$, PPh_3, HBF_4(aq) (48 % wt.), $HBF_4{\cdot}Et_2O$ $MeCOCH_2C(OH)Me_2$, $MeCOCH_2C(SMe)Me_2$, 1-bromo-2-(trifluoromethyl)benzene and 1-iodo-2-(trifluoromethyl)benzene are commercially available and were purchased from Sigma-Aldrich, Acros Organics and Fluorochem. $[NiBr_2(PPh_3)_2]$,[1] $[Pd(PPh_3)_4]$,[2] and $[PdCl_2(PPh_3)_2]$[3] were prepared according to the literature methods.

1.2- Synthesis of nickel(II) complexes.

Synthesis of [Ni(*o*-CF_3-C_6H_4)Br(PPh_3)$_2$] (1). Complex **1** was reported previously. We describe here a synthetic method following the Jamison procedure.[1a] Magnesium turnings (0.16 g, 6.58 mmol) were placed in a round-bottom flask under N_2 and activated with an iodine crystal. The magnesium was suspended in 25 mL of dry THF and 1-bromo-2-(trifluoromethyl)benzene (0.46 mL, 3.36 mmol) was added. The suspension was heated to reflux for 1h. The initial colorless solution turns to a light-grey suspension. In another Schlenk tube was placed [$NiBr_2(PPh_3)_2$] (2.5 g, 3.37 mmol) under N_2 and it was suspended in 10 mL of dry THF. The green suspension was cooled to 0 ºC in an ice bath. The light-grey solution of the aryl Grignard reagent was transferred via cannula to the green suspension and it was stirred for 15 min at 0 ºC. After this time, the greenish solution was evaporated to dryness and 10 mL of MeOH were added. The yellow solid generated was stirred for 10 min at room temperature. The solid was filtered off, washed with cold MeOH (2 x 10 mL) and air-dried (2.2 g, 81.5% yield.). ^{1}H NMR (499.73 MHz, δ, CD_2Cl_2): 7.56 (m, 12H, H_{meta}, H_{ortho} Ph PPh_3), 7.50 (d, J = 8, 1H, H^6), 7.38 (m, 6H, H_{para} Ph PPh_3), 7.24 (m, 12H, H_{meta}, H_{ortho} Ph PPh_3), 6.60 (d, J = 8 Hz, 1H, H^3), 6.47 (vt, J = 8 Hz, 1H, H^4), 6.42 (vt, J = 7.6 Hz, 1H, H^5). ^{13}C{^{1}H} (125.67 MHz, δ, CD_2Cl_2): 153 (t, J_{C-P} = 34 Hz, C^1), 137.5 (C^6), 135.4 (m, $^2J_{C-F}$ = 29 Hz, C^2), 134.6, 127.6 (C_{meta}, C_{ortho}, Ph PPh_3), 131.7 (vt, J_{C-P} = 27 Hz, C^{ipso} PPh_3), 129.6 (C_{para} Ph PPh_3), 127.6 (C^5), 127.4 (q, $^1J_{C-F}$ = 273 Hz, C^7), 127.3 (C^3), 121.6 (C^4). ^{19}F NMR (470.17 MHz, δ, CD_2Cl_2): -58.8 (t, J_{P-F} = 6 Hz, CF_3). ^{31}P{^{1}H} (202.31 MHz, δ, CD_2Cl_2): 20.1 (q, J_{P-F} = 5 Hz, 2P).

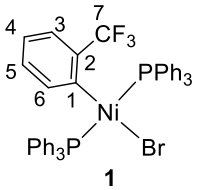

1

Synthesis of [Ni(*o*-CF_3-C_6H_4)(OH_2)(PPh_3)$_2$](BF_4) (2). In a Schlenk tube the dimeric complex **4** (75 mg, 0.0776 mmol) and PPh_3 (41 mg, 0.156 mmol) were placed under N_2. The mixture was dissolved in 5 mL of dry CH_2Cl_2 and the orange solution was cooled to 243 K in an acetone bath for 10 min until constant temperature. Subsequently, a solution of $HBF_{4(aq)}$ (25 μL, 0.194 mmol; 48 % wt) was added. Immediately, the

solution turned yellow and it was stirred for 20 min at 243 K. After this time, the yellow solution was evaporated to dryness. The residue was redissolved in 4 mL of CH_2Cl_2 and 12 mL of dry hexane were added inducing the formation of a yellow solid. The solid was decanted and the supernatant solution was transferred via cannula. The same process was repeated twice. The yellow solid was dried in vacuo (0.1 g, 77% yield). ^{1}H NMR (499.73 MHz, δ, 243 K, CD_2Cl_2): 7.52 (m, 6H, H_{para}, Ph PPh_3), 7.39 (m, 12H, H_{meta} Ph PPh_3), 7.29 (m, 12H, H_{ortho}, Ph PPh_3), 7.21 (d, 1H, J = 7.6, 1H, H^6), 6.70 (vt, J = 7.6, 1H, H^4), 6.61 (d, J = 7.6, 1H, H^3), 6.58 (vt, J = 7.6, 1H, H^5), 2.76 (s, 2H, OH_2). ^{13}C{^{1}H} (125.67 MHz, δ, 243 K, CD_2Cl_2): 139.4 (t, J_{C-P} = 35 Hz, C^1), 136.3 (C^6), 134.6 (q, $^2J_{C-F}$ = 29 Hz, C^2), 134 (C_{ortho}, Ph PPh_3), 129.1 (C_{meta}, Ph PPh_3), 131.3 (C_{para} Ph PPh_3), 126.4 (vt, J_{C-P} = 22 Hz, C^{ipso} PPh_3), 128.7 (C^5), 128.5 (q, $^1J_{C-F}$ = 276 Hz, C^7), 128.2 (C^3), 123.10 (C^4). ^{19}F NMR (470.17 MHz, δ, 243 K, CD_2Cl_2): -59.7 (t, J_{P-F} = 6 Hz, CF_3), -150.7 (BF_4). ^{31}P{^{1}H} (202.31 MHz, δ, 243 K, CD_2Cl_2): 18 (q, J_{P-F} = 6 Hz, 2P). Analysis calc. for $C_{43}H_{36}BF_7OP_2Ni$: C, 61.98; H, 4.35; found: C, 61.81; H, 4.42.

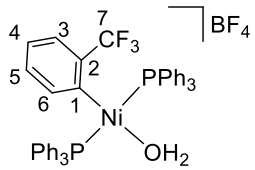

2

Synthesis of [Ni(*o*-CF_3-C_6H_4)(μ-OH)(PPh_3)]$_2$ (4). Complex **4** was synthesized following a reported method for analogous complexes.[4] In a 100 mL round-bottom flask complex **1** (1.86 g, 2.30 mmol) was dissolved in 28.5 mL of THF. KOH (2.6 g, 47 mmol) in pellets was grounded and added to the orange solution. In addition, 1 mL of H_2O was added and the mixture was stirred vigorously for 24 h at room temperature. After this time, the aqueous phase was removed and the organic solution was evaporated to dryness. The residue was redissolved in the minimal amount of THF and filtered off through a plot of Celite. The orange solution was evaporated to dryness. The residue was triturated with 5 mL of pentane and stirred for 30 min at room temperature inducing the formation of an orange solid. The solid was filtered off, washed with pentane (2 x 5 mL) and then air-dried (0.95 g, 89% yield).

In dry $CDCl_3$, complex **4** is a mixture of three isomers, resulting from the different arrangement of the phosphines (*cis* or *trans*) and CF_3 group (*syn* or *anti*) (Figure S1). By analogy to other hydroxo dimers,[4] the isomers with the two OH with similar

chemical shifts (-4.0 ppm and -4.2 ppm in ^{1}H NMR, Figure S2) are assigned to the *trans*-**4** isomers The two *cis* isomers are conformed by two OH groups with very different chemical shifts but a priory is not possible assigned to which isomer (*cis-anti*-**4** or *cis-syn*-**4**) correspond each OH signal. Because of the higher steric hindrance in the isomer with the two CF_3 in *syn* disposition, we tentatively assigned the minor isomer to the *cis-syn*-**4**. The molecular structure of *cis-anti*-**4** was determined by X-ray diffraction (see section 2).

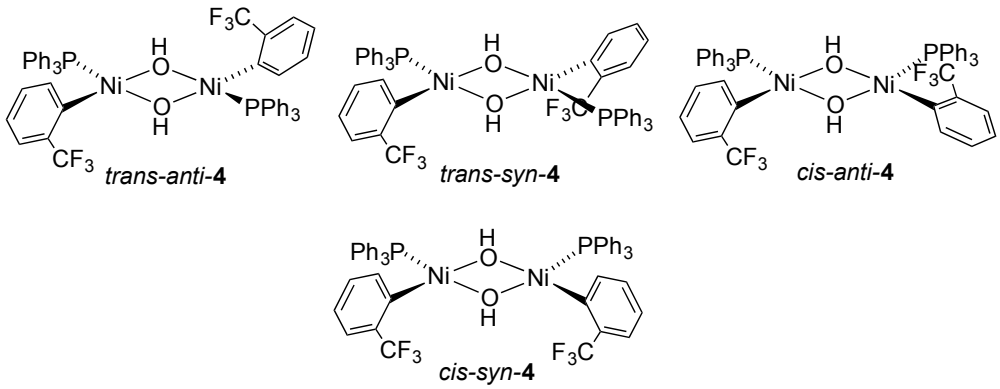

Figure S1. Isomers for complex **4**.

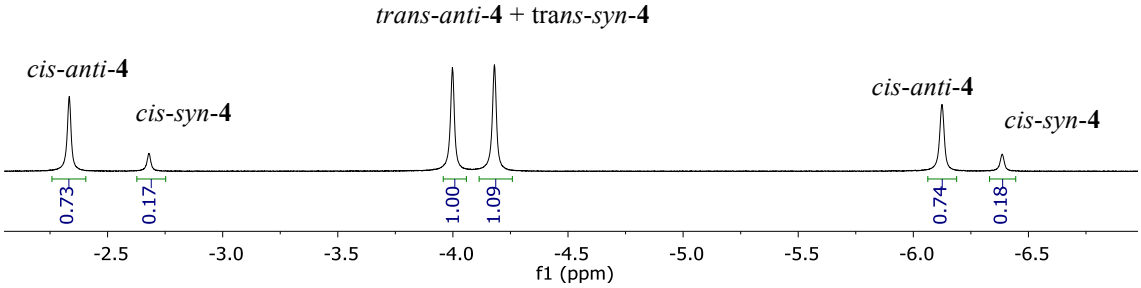

Figure S2. ^{1}H NMR spectrum of complex **4** in $CDCl_3$ at 298 K showing only the region of the OH groups.

4: ^{1}H NMR (499.73 MHz, δ, $CDCl_3$): 8.03, 7.94, 7.83 (d, $^{1}J_{H\text{-}H}$ = 8 Hz, H^6, $H^{6'}$), 7.56-7.19 (m, PPh_3), 6.9, 6.8, 6.77 (d, $^{1}J_{H\text{-}H}$ = 8 Hz, H^3, $H^{3'}$), 6.75-6.60 (m, H^4, $H^{4'}$) 6.61 (m, H^5, H^5), -2.7 (s, 1H, OH, *cis-syn*-**4**), -2.33 (s, 1H, OH, *cis-anti*-**4**), -4 (s, 1H, OH, *trans-syn/anti*-**4**), -4.2 (s, 1H, OH′, *trans-syn/anti*-**4**), -6.1 (s, 1H, OH′, *cis-anti*-**5**), -6.4 (s, 1H, OH′, *cis-syn*-**4**). $^{13}C\{^{1}H\}$ (125.67 MHz, δ, $CDCl_3$): 146.5 (C^1, $C^{1'}$), 138.8, 138.5 (C^6, $C^{6'}$), 136.9 (C^2, $C^{2'}$), 133.9, 128 (C_{ortho}, C_{meta} Ph PPh_3), 129.91 (C_{ipso} Ph PPh_3), 128.06 (C_{para}, Ph PPh_3), 125.8 (q, $^{1}J_{C\text{-}F}$ = 273 Hz, C^7, $C^{7'}$), 126.5 (C^4, $C^{4'}$) 125.3 (C^3, $C^{3'}$), 121.8 (C^5, $C^{5'}$). ^{19}F NMR (470.17 MHz, δ, $CDCl_3$): -57.5 (d, $J_{P\text{-}F}$ = 5.3 Hz, CF_3 *trans-anti/syn*-**4**), -57.8 (d, $J_{P\text{-}F}$ = 5.3 Hz, CF_3' *trans-anti/syn*-**4**), -57.9 (d, $J_{P\text{-}F}$ = 5.3 Hz, CF_3, CF_3' *cis-*

anti-**4**, *cis-syn*-**4**). $^{31}P\{^{1}H\}$ NMR (202.31 MHz, δ, $CDCl_3$): 28.3 (m, 2P, *trans-anti*-**4** + *trans-syn*-**4**), 28 (m, 2P, *cis-anti*-**4**), 27.7 (m, 2P, *cis-syn*-**4**). Analysis calc. for $C_{50}H_{40}F_6O_2P_2Ni_2 \cdot C_4H_8O$: C, 62.46; H, 4.60; found: C, 62.67; H, 4.19.

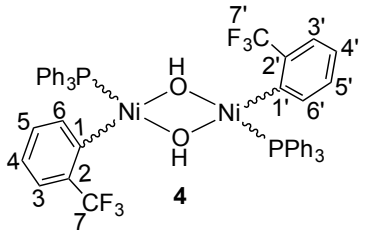

4

Synthesis of [Ni(*o*-CF_3-C_6H_4)( )(κ^2-O, S-$MeCOCH_2C(SMe)Me_2$)(PPh_3)](BF_4) (6). In an oven dry Schlenk tube complex **4** (150 mg, 0.155 mmol) was dissolved in 5 mL of dry CH_2Cl_2. The orange solution was cooled in an acetone bath at 243 K for 10 min until constant temperature. The ligand $MeCOCH_2C(SMe)Me_2$ (47 μL, 0.31 mmol) and $HBF_4 \cdot Et_2O$ (42 μL, 0.31 mmol) were added. The solution turned from orange to yellow and it was stirred for 15 min at 243 K. After this time, the solution was evaporated to dryness and the residue was redissolved in 2 mL of CH_2Cl_2. 10 mL of hexane were added inducing the formation of a yellow solid. The solid was decanted and the supernatant solution was transferred via cannula. The same process was repeated twice. The yellow solid was vacuum dried (0.19 g, 87.7 % Yield). ^{1}H NMR (499.73 MHz, δ, $CDCl_3$): 7.6 (d, 1H, $^{1}J_{H\text{-}H}$ = 8 Hz, H^6), 7.46 (m, 3H, H_{para} PPh_3), 7.37 (m, 12H, H_{meta}, H_{ortho} PPh_3), 6.99 (d, 1H, $^{1}J_{H\text{-}H}$ = 8 Hz, H^3), 6.85 (m, 2H, H^5, H^4), 3.53 (d, 1H, $^{1}J_{H\text{-}H}$ = 21 Hz, H^{10}), 2.89 (d, 1H, $^{1}J_{H\text{-}H}$ = 21 Hz, $H^{10'}$), 2.18 (s, 3H, SMe), 1.77 (s, 3H, H^9). 1.5 (CH_3), 1.41 (CH_3). $^{13}C\{^{1}H\}$ (125.758 MHz, δ, $CDCl_3$): 223.1 (C^8), 135.4 (C^6), 136.2 (C^2), 133.7, 128.8, (C_{ortho}, C_{meta}, PPh_3), 131 (C_{para}, C^{ipso}, PPh_3), 128.8, 123.8 (C^5, C^4), 127.7 (C^3), 49.7 (C^{10}), 40 (C^{11}), 33 (C^9), 27.2 (CH_3), 27.8 (CH_3), 12.4 (SMe).* ^{19}F NMR (470.17 MHz, δ, $CDCl_3$): -58.4 (d, $J_{P\text{-}F}$ = 5.7 Hz, CF_3), -152 (BF_4^-). $^{31}P\{^{1}H\}$ NMR (202.31 MHz, δ, $CDCl_3$): 19.5 (m, 1P). Analysis calc. for $C_{32}H_{33}BF_7OPSNi$: C, 54.98; H, 4.76; found: C, 54.76; H, 4.78.

*C^1 and C^7 could not be located.

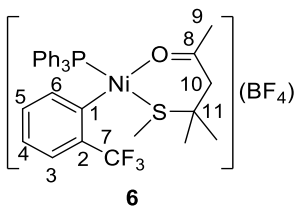

6

1.3- Synthesis of palladium(II) complexes

Synthesis of [Pd(*o*-CF_3-C_6H_4)Br(PPh_3)$_2$] (7). Complex **7** was synthesized following a reported method for analogous complexes.[5] In a Schlenk tube, [Pd(PPh_3)$_4$] (0.5 g, 0.432 mmol) was placed under N_2. The complex was dissolved in 8 mL of dry toluene. Subsequently, 1-bromo-2-(trifluoromethyl)benzene (1.2 mL, 8.81 mmol) was added. The light-yellow solution was stirred for 6 h at 100 ºC. After this time, the solution was evaporated to dryness. Et_2O (10 mL) was added to the residue inducing the formation of a white solid. The solid was filtered off, washed with Et_2O (2 x 10 mL) and air-dried (0.33 g, 89.2% yield). ^{1}H NMR (499.73 MHz, δ, CD_2Cl_2): 7.49 (m, 12H, H_{meta}, H_{ortho} Ph PPh_3), 7.38 (t, 6H, $^1J_{H-H}$ = 7 Hz, H_{para} Ph PPh_3), 7.28 (m, 12H, H_{meta}, H_{ortho} Ph PPh_3), 7.23 (d, $^1J_{H-H}$ = 8 Hz, 1H, H^6), 6.75 (d, $^1J_{H-H}$ = 8 Hz, 1H, H^3), 6.58 (t, $^1J_{H-H}$ = 8 Hz, 1H, H^4), 6.47 (t, $^1J_{H-H}$ = 8 Hz, 1H, H^5). ^{13}C{^{1}H} (125.67 MHz, δ, CD_2Cl_2): 156.2 (C^1), 137.6 (C^6), 132.2 (q, $^2J_{C-F}$ = 27 Hz, C^2), 134.7, 127.7 (C_{meta}, C_{ortho} Ph PPh_3), 131.2 (vt, J_{C-P} = 23 Hz, C^{ipso} PPh_3), 129.9 (C_{para} Ph PPh_3), 129.3 (C^5), 127.3 (q, $^1J_{C-F}$ = 273 Hz, C^7), 127 (C^3), 122.5 (C^4). ^{19}F NMR (470.17 MHz, δ, CD_2Cl_2): -59.7 (t, J_{P-F} = 5 Hz, CF_3). ^{31}P{^{1}H} (202.31 MHz, δ, CD_2Cl_2): 22.30 (q, J_{P-F} = 5 Hz).

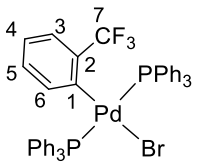

7

Synthesis of [Pd(*o*-CF_3-C_6H_4)(OH_2)(PPh_3)$_2$](BF_4) (8). In an oven-dried vial $AgBF_4$ (51 mg, 0.262 mmol) was placed under N_2. The solid was dissolved in 5 mL of dry toluene. In a Schlenk tube complex **7** (180 mg, 0.21 mmol) was dissolved in 3 mL of CH_2Cl_2. The vial and the Schlenk tube were cooled to 243 K during 10 min to ensure a constant temperature. The solution of $AgBF_4$ was transferred to the yellow solution of complex **6**. Immediately, a white solid (AgBr) appeared and the suspension was stirred for 15 min at 243 K. After this time, the solvent was evaporated to dryness. The residue was suspended in 2 mL of dry CH_2Cl_2 and the solution was transferred via cannula. *n*-Hexane (10 mL) was added to the clear yellow solution inducing the formation of a

white solid. The solid was decanted and the supernatant solution was transferred via cannula. The same process was repeated twice. The white solid was dried in vacuo (0.155 g, 84.2% yield). ^{1}H NMR (499.73 MHz, δ, 243 K, CD_2Cl_2): 7.5 (m, 6H, H_{para}, Ph PPh_3), 7.38 (m, 12H, H_{meta}/H_{ortho} Ph PPh_3), 7.25 (m, 12H, H_{meta}/H_{ortho} Ph PPh_3), 7.18 (d, J = 7.6, 1H, H^6), 6.83 (vd, J = 7.6, 1H, H^3), 6.8 (vt, J = 7.6, 1H, H^4), 6.65 (t, J = 7.6, 1H, H^5), 3.33 (s, 2H, OH_2). ^{13}C{^{1}H} (125.67 MHz, δ, 243 K, CD_2Cl_2): 142.8 (C^1), 136.1 (C^6), 134.2 (q, $^{2}J_{C-F}$ = 29 Hz, C^2), 133.8, 129 (C_{meta}, C_{ortho} Ph PPh_3), 131.3 (C_{para} Ph PPh_3), 127.5 (vt, J_{C-P} = 23 Hz, C^{ipso} PPh_3), 130.3 (C^5), 126.3 (q, $^{1}J_{C-F}$ = 273 Hz, C^7), 128.8 (C^3), 123.7 (C^4). ^{19}F NMR (470.17 MHz, δ, 243 K, CD_2Cl_2): -58.9 (t, J_{P-F} = 6 Hz, CF_3), -150.8 (BF_4^-). ^{31}P{^{1}H} (202.31 MHz, δ, 243 K, CD_2Cl_2): 21.2 (q, J_{P-F} = 6 Hz). Analysis calc. for $C_{43}H_{36}BF_7OP_2Pd$: C, 58.63 ; H, 4.12; found: C, 58.90; H, 4.25.

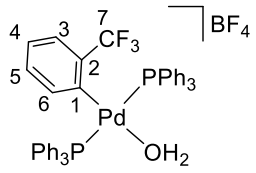

8

Synthesis of [Pd(o-CF_3-C_6H_4)(μ-OH)(PPh_3)]$_2$ (10). Complex **10** was synthesized following a reported method for analogous complexes.[6] In a 50 mL round-bottom flask [$PdCl_2(PPh_3)_2$] (1 g, 1.42 mmol) and KOH (4 g) were placed under N_2. The solids were suspended in a mixture of 20 mL of toluene and 4 mL of degassed H_2O. Immediately, 1-iodo-2-(trifluoromethyl)benzene (0.63 mL, 4.5 mmol) was added. The mixture was vigorously stirred for 3 h at 69 ºC under N_2. The suspension turns to a yellow solution with the formation of a little amount of palladium black. The organic phase was separated and the aqueous phase was washed with toluene (2 x 10 mL). Activated carbon was added to the combined organic phases and they were filtered off through a plot of Celite. The filtrate was evaporated to dryness. 5 mL of pentane were added to the yellow residue and the mixture was stirred for 30 min at room temperature. A yellow solid was generated, containing the desired complex **10** and PPh_3O. The solid was filtered off and recrystallized twice in a mixture of CH_2Cl_2/pentane (1:3). Complex **10** was obtained as a white solid (0.95 g, 89% yield).

In $CDCl_3$, complex **10** is a mixture of four isomers, resulting from the different disposition of the phosphines (*cis* or *trans*) and CF_3 groups (*syn* or *anti*) (Figure S3). We assigned the signals at -1.77 ppm and -2.05 ppm in the OH region of the ^{1}H NMR

spectrum to the *trans* isomers (Figure S4). In addition, we tentatively assigned the major isomer for the *cis* disposition of the phosphines to the compound where the CF_3 groups are in *anti* disposition (OH groups at -0.5 ppm and -3.57 ppm, Figure S4).

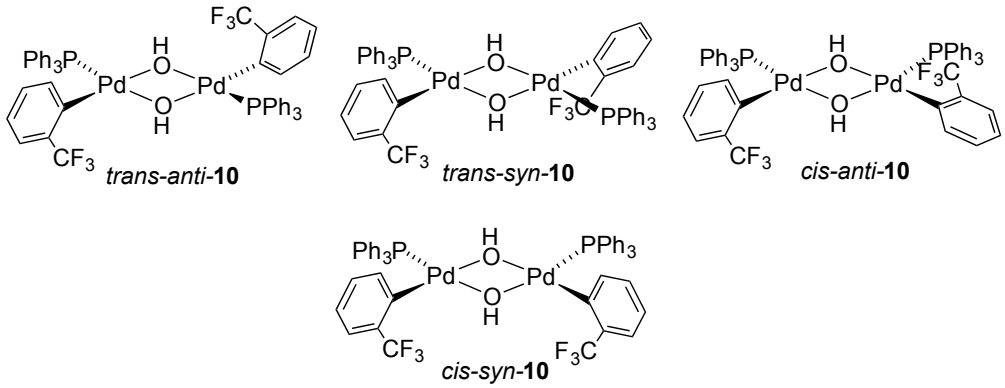

Figure S3. Four isomers for complex **10** detected in $CDCl_3$ at 298 K.

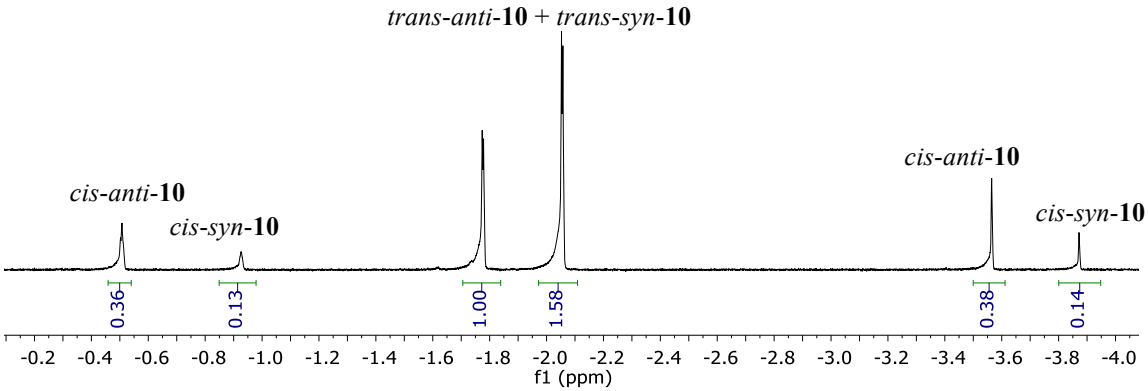

Figure S4. ^{1}H NMR of complex **10** in $CDCl_3$ at 298 K showing only the region corresponding to the OH groups.

10: ^{1}H NMR (499.73 MHz, δ, $CDCl_3$): 7.68, 7.59, 7.52 (m, H^6, $H^{6'}$), 7.5-7.1 (m, PPh_3), 7.10, 7.03, 6.99 (m, H^3, $H^{3'}$), 6.8-6.6 (m, H^5, $H^{5'}$, H^4, $H^{4'}$), -0.51 (s, 1H, OH , *cis-anti*-**10**), -0.93 (s, 1H, OH, *cis-syn*-**10**), -1.77 (s, 1H, OH, *trans-anti/syn*-**10**), -2.05 (s, 3H, OH, OH′, *trans-syn/anti*-**10**), -3.57 (s, 1H, OH′, *cis-anti*-**10**), -3.87 (s, 1H, OH′, *cis-syn*-**10**). $^{13}C\{^1H\}$ (125.67 MHz, δ, $CDCl_3$): 150, 149.2, 148.98, 148.16 (C^1, $C^{1'}$), 138.6-138.2 (C^6, $C^{6'}$), 135 (C^2, $C^{2'}$), 134.3, 128.2 (C_{ortho}, C_{meta} Ph PPh_3), 130.6 (C_{ipso} Ph PPh_3), 130.3 (C_{para}, Ph PPh_3), 127.2 (q, $^1J_{C\text{-}F}$ = 273 Hz, C^7, $C^{7'}$), 128.3, 126.1, 122.7 (C^5, $C^{5'}$, C^4, $C^{4'}$, C^3, $C^{3'}$). ^{19}F NMR (470.17 MHz, δ, $CDCl_3$): -60.6 (d, $J_{P\text{-}F}$ = 5 Hz, CF_3), -60.9

(d, J_{P-F} = 5 Hz, CF_3). -61.1 (d, J_{P-F} = 5 Hz, CF_3), -60.12 (d, J_{P-F} = 5 Hz, CF_3). $^{31}P\{^1H\}$ NMR (202.31 MHz, δ, $CDCl_3$): 27.7(m), 27.1(m).

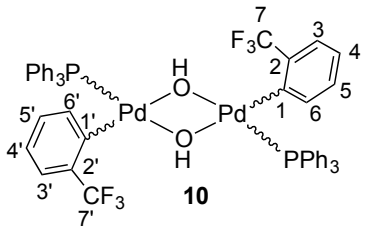

10

1.4- Study of the formation *in situ* of organometallic species starting from complexes **1**, **2** and **4**.

1.4.1- Effect of the amount of $AgBF_4$ in the formation of nickel cationic species in a mixture of CH_2Cl_2/toluene

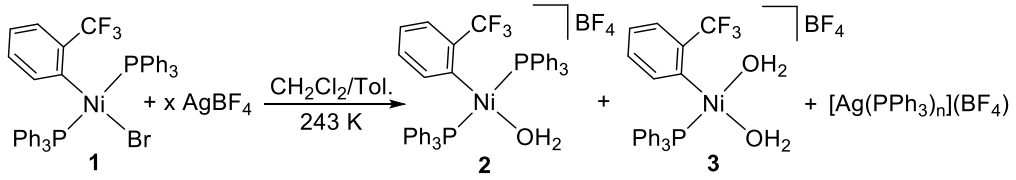

1 **2** **3**

A general procedure for the following experiments is described (mol ratio **1**:$AgBF_4$ = 1:1.25). In an oven dry vial $AgBF_4$ (6.1 mg, 0.031 mmol) was dissolved in 2 mL of dry toluene under N_2. The solution was cooled to 243 K for 10 min until constant temperature and then complex **1** (20 mg, 0.0247 mmol) dissolved in 1 mL of dry-cooled CH_2Cl_2 was added. Instantly, a white solid (AgBr) appeared and the suspension was stirred for 15 min at 243 K. The white solid was removed employing a PTFE 0.2 μm filter and the orange solution was transferred to an oven dry and cooled Schlenk tube. The solution was evaporated to dryness. The residue was redissolved in 0.6 mL of dry and cooled CD_2Cl_2 and checked by NMR spectroscopy.

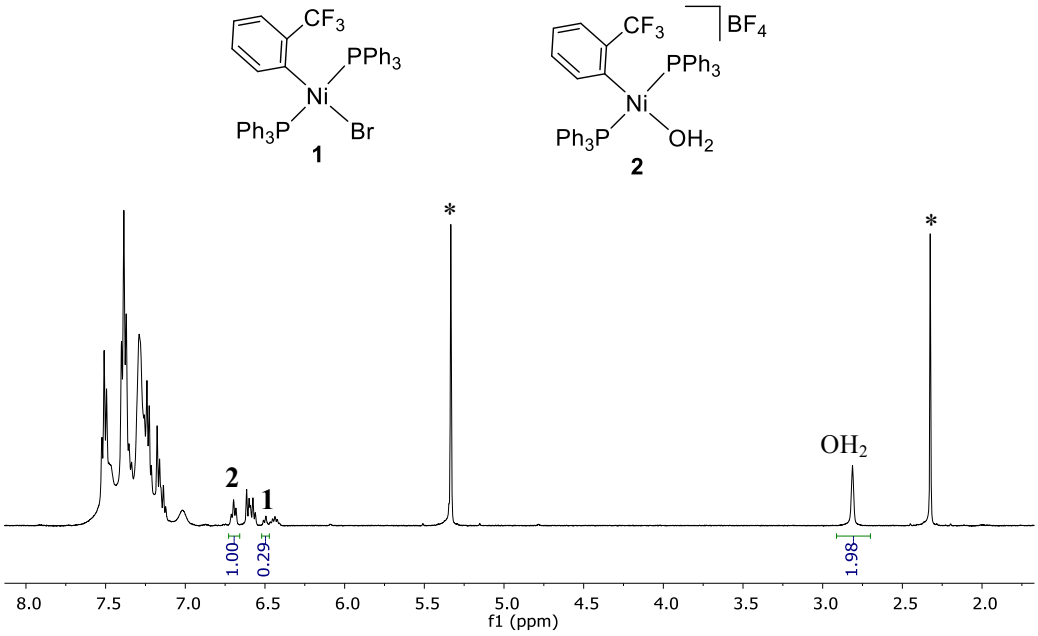

Figure S5. ^{1}H NMR (499.73 MHz, 243 K, CD_2Cl_2) of the organometallic species generated *in situ* from complex **1** and $AgBF_4$ in CH_2Cl_2/toluene (mol ratio $AgBF_4$:**1** = 1:1). *Signals corresponding to CH_2Cl_2 and toluene.

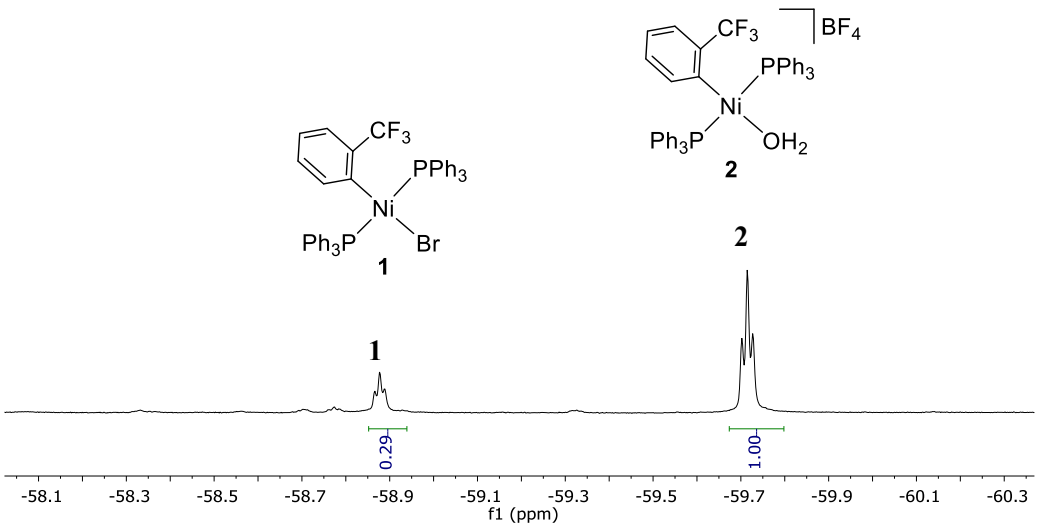

Figure S6. ^{19}F NMR (376.498 MHz, 243 K, CD_2Cl_2) of the organometallic species generated *in situ* from complex **1** and $AgBF_4$ (mol ratio $AgBF_4$:**1** = 1:1) in CH_2Cl_2/toluene. % Mol of **1** = 22.4; % mol of **2** = 77.6.

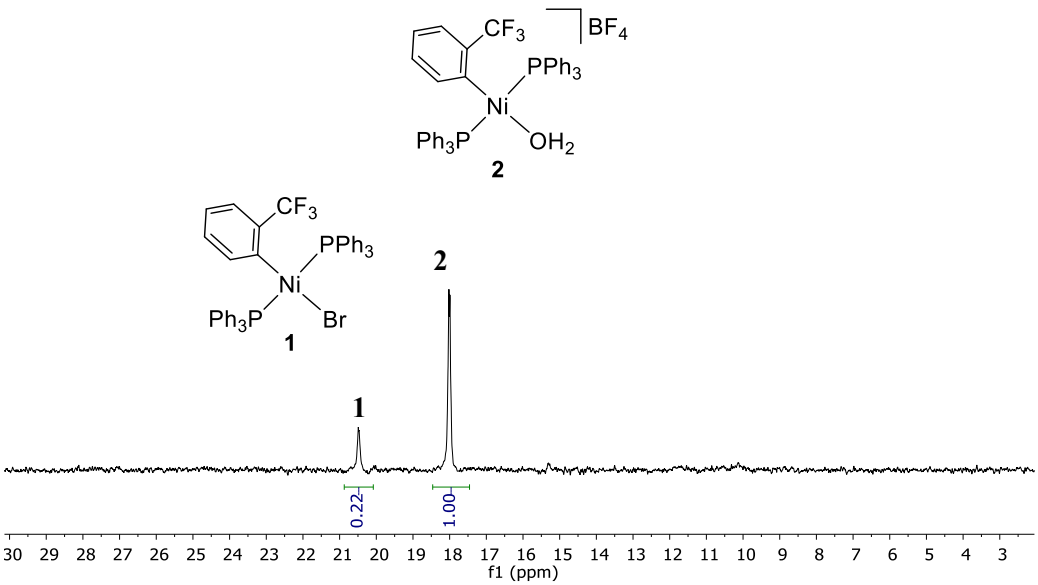

Figure S7. ^{31}P NMR (202.31 MHz, 243 K, CD_2Cl_2) of the organometallic species generated *in situ* from complex **1** and $AgBF_4$ in CH_2Cl_2/toluene (mol ratio $AgBF_4$:**1** = 1:1).

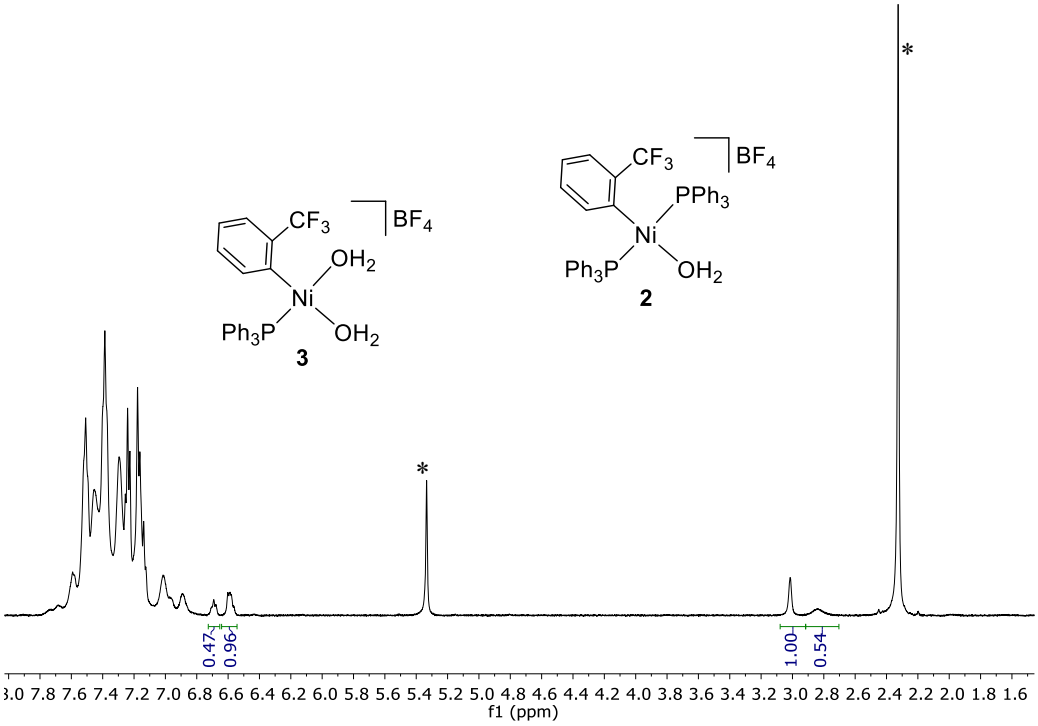

Figure S8. ^{1}H NMR (499.73 MHz, 243 K, CD_2Cl_2) of the organometallic species generated *in situ* from complex **1** and 1.25 eq. of $AgBF_4$ in CH_2Cl_2/toluene (mol ratio $AgBF_4$:**1** = 1.25:1). *Signal corresponding to CH_2Cl_2 and toluene.

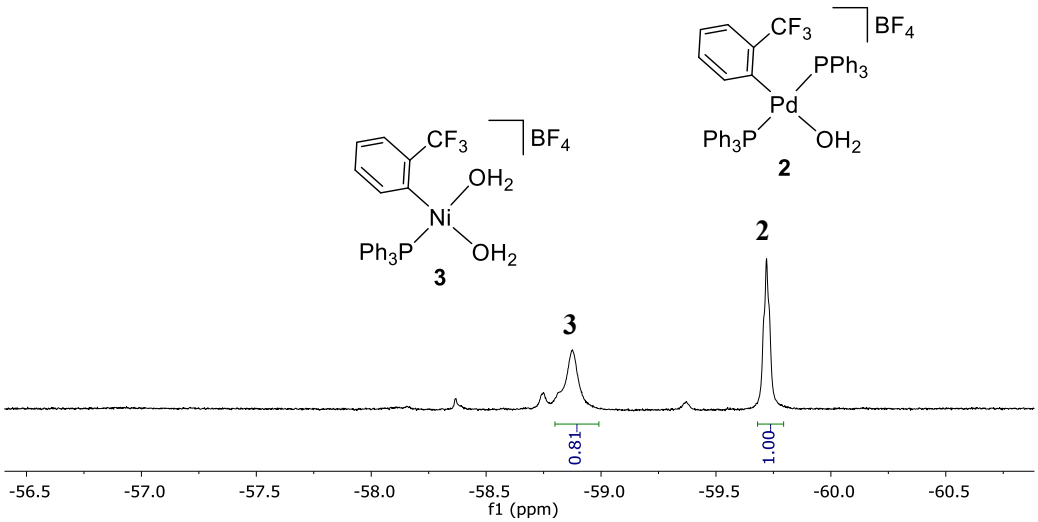

Figure S9. ^{19}F NMR (376.498 MHz, 243 K, CD_2Cl_2) of the organometallic species generated *in situ* with complex **1** and $AgBF_4$ in CH_2Cl_2/toluene (mol ratio $AgBF_4$:**1** = 1.25:1). % Mol of **2** = 55.3; % mol of **3** = 44.7.

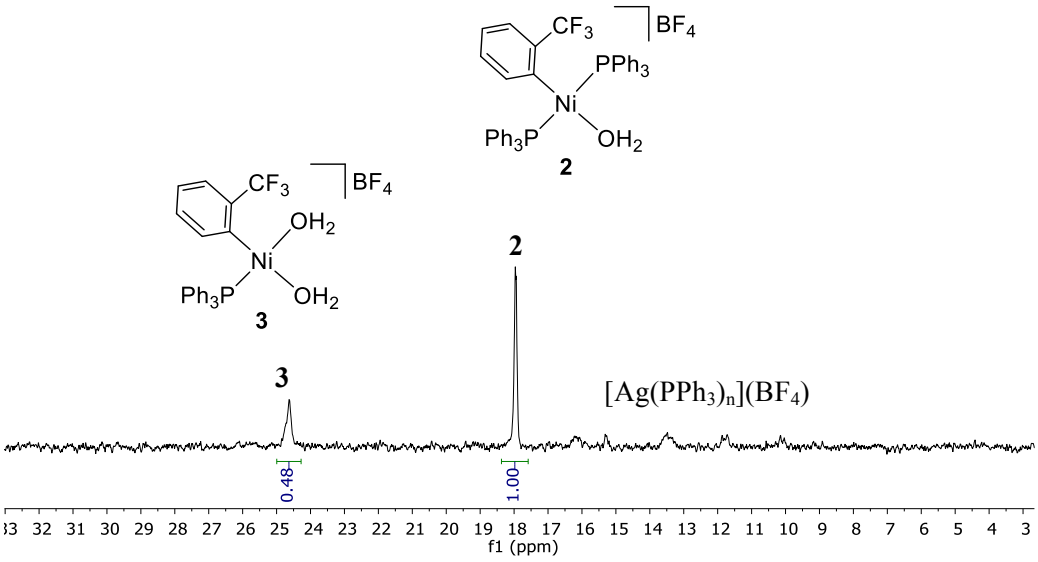

Figure S10. ^{31}P NMR (202.31 MHz, 243 K, CD_2Cl_2) of the organometallic species generated *in situ* with complex **1** and $AgBF_4$ in CH_2Cl_2/toluene (mol ratio $AgBF_4$:**1** = 1.25:1).

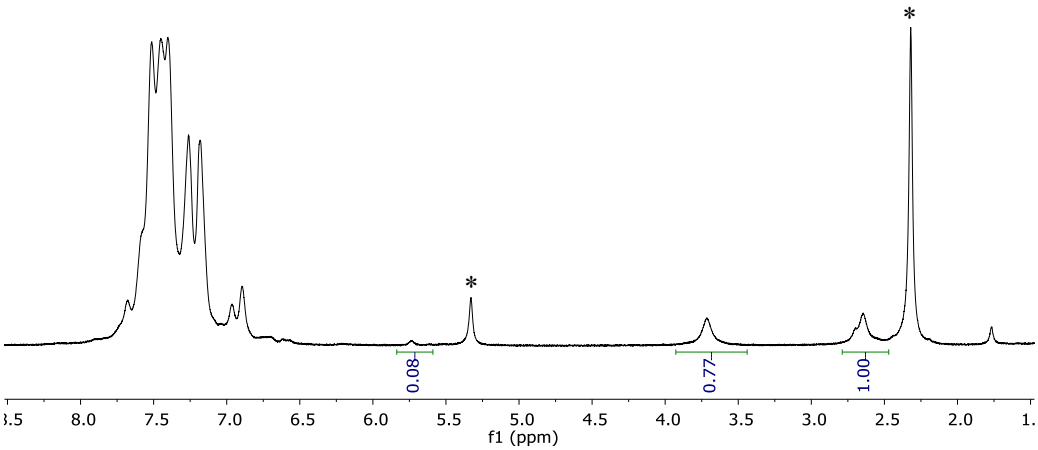

Figure S11. ^{1}H NMR (499.73 MHz, 243 K, CD_2Cl_2) of the organometallic species generated *in situ* with complex **1** and $AgBF_4$ in CH_2Cl_2/toluene (mol ratio $AgBF_4$:**1** = 1.75:1). *Signal corresponding to CH_2Cl_2 and toluene.

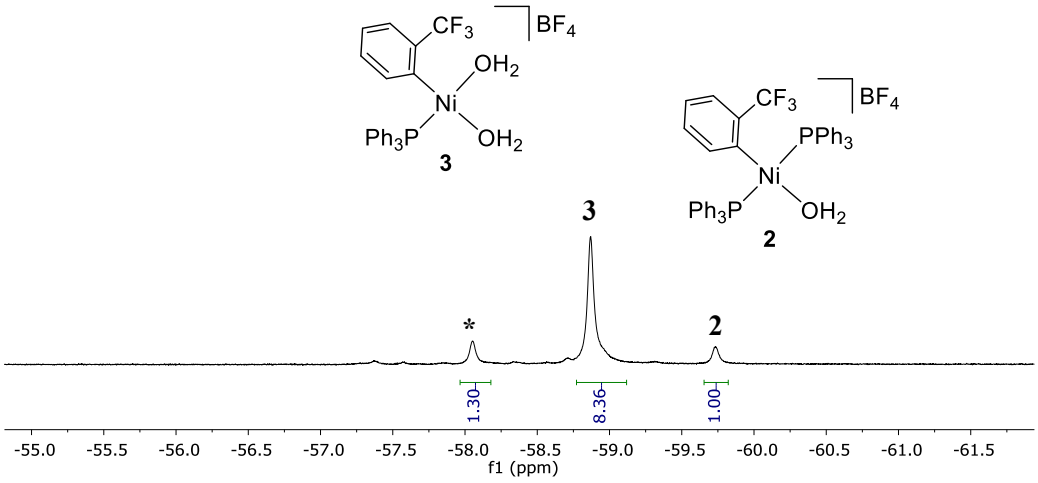

Figure S12. ^{19}F NMR (376.498 MHz, 243 K, CD_2Cl_2) of the organometallic species generated *in situ* from complex **1** and $AgBF_4$ in CH_2Cl_2/toluene (mol ratio $AgBF_4$:**1** = 1.75:1). % Mol of **3** = 78.4; % mol of **2** = 9.3; % mol of * = 12.3). *Unidentified complex.

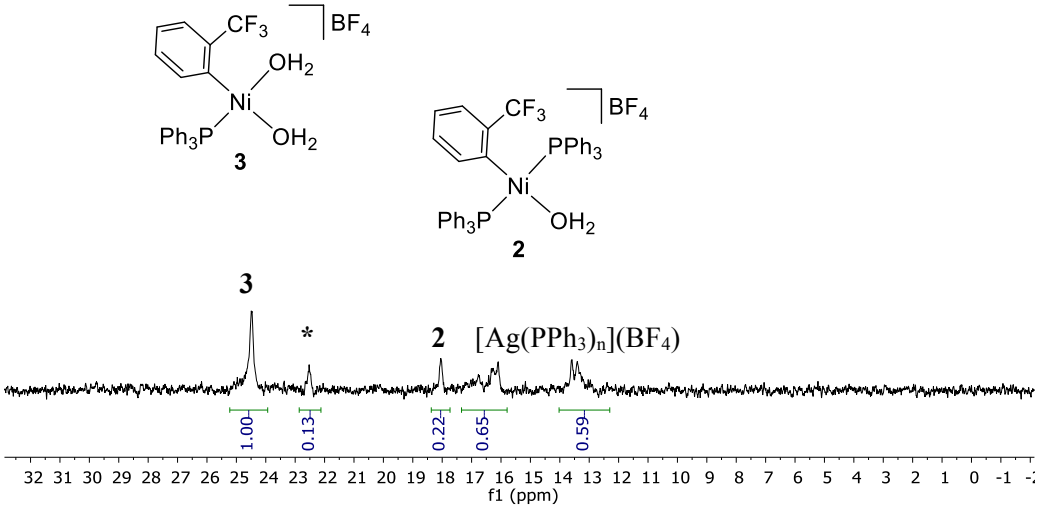

Figure S13. ^{31}P NMR (202.31 MHz, 243 K, CD_2Cl_2) of the organometallic species generated *in situ* from complex **1** and $AgBF_4$ in CH_2Cl_2/toluene (mol ratio $AgBF_4$:**1** = 1.75:1). *unidentified complex.

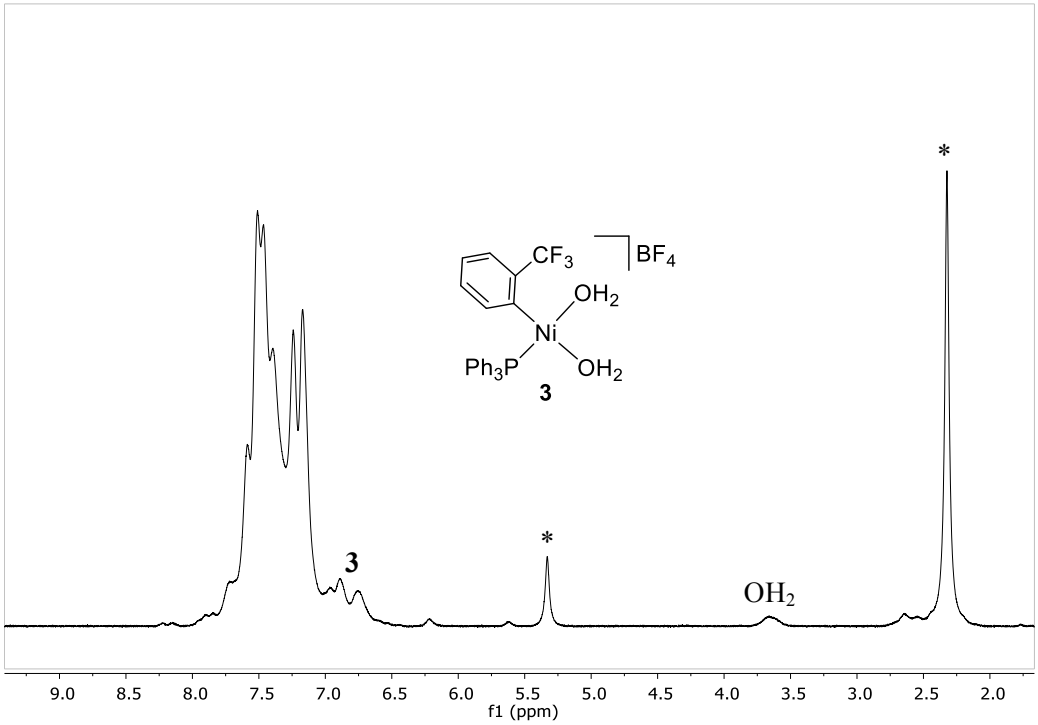

Figure S14. ^{1}H NMR (499.73 MHz, 243 K, CD_2Cl_2) of the organometallic species generated *in situ* from complex **1** and $AgBF_4$ in CH_2Cl_2/toluene (mol ratio $AgBF_4$:**1** = 2.25:1). *Signal corresponding to CH_2Cl_2 and toluene.

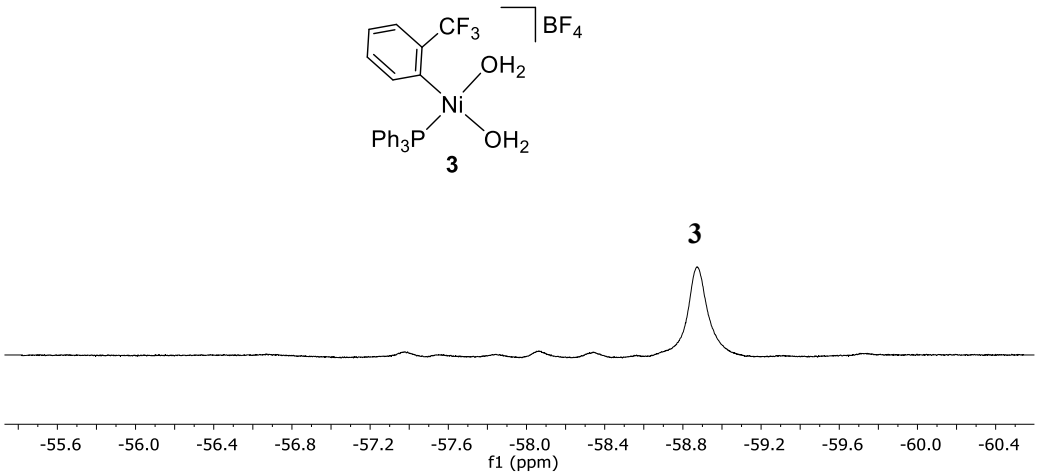

Figure S15. ^{19}F NMR (376.498 MHz, 243 K, CD_2Cl_2) of the organometallic species generated *in situ* from complex **1** and $AgBF_4$ in CH_2Cl_2/toluene (mol ratio $AgBF_4$:**1** = 2.25:1).

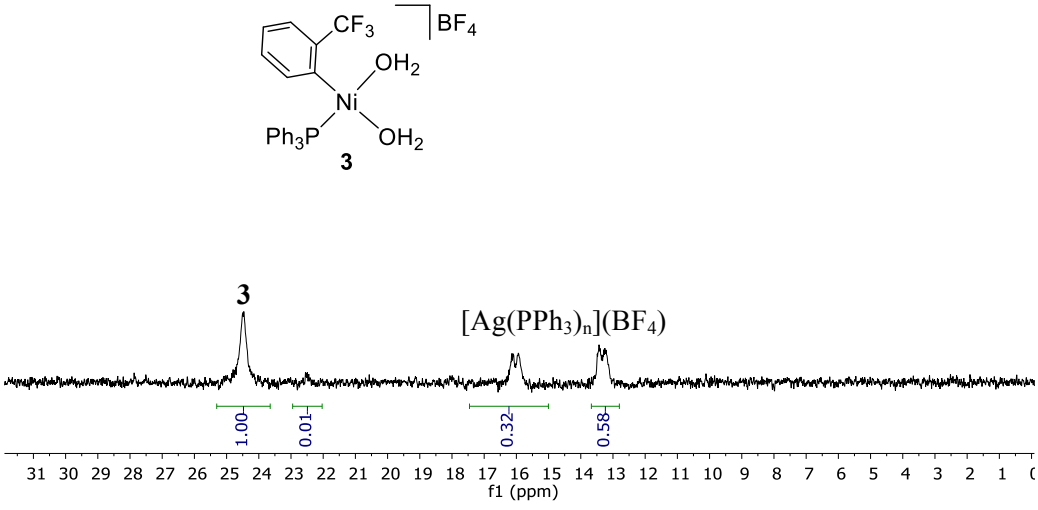

Figure S16. ^{31}P NMR (202.31 MHz, 243 K, CD_2Cl_2) of the organometallic species generated *in situ* from complex **1** and $AgBF_4$ in CH_2Cl_2/toluene (mol ratio $AgBF_4$:**1** = 2.25:1).

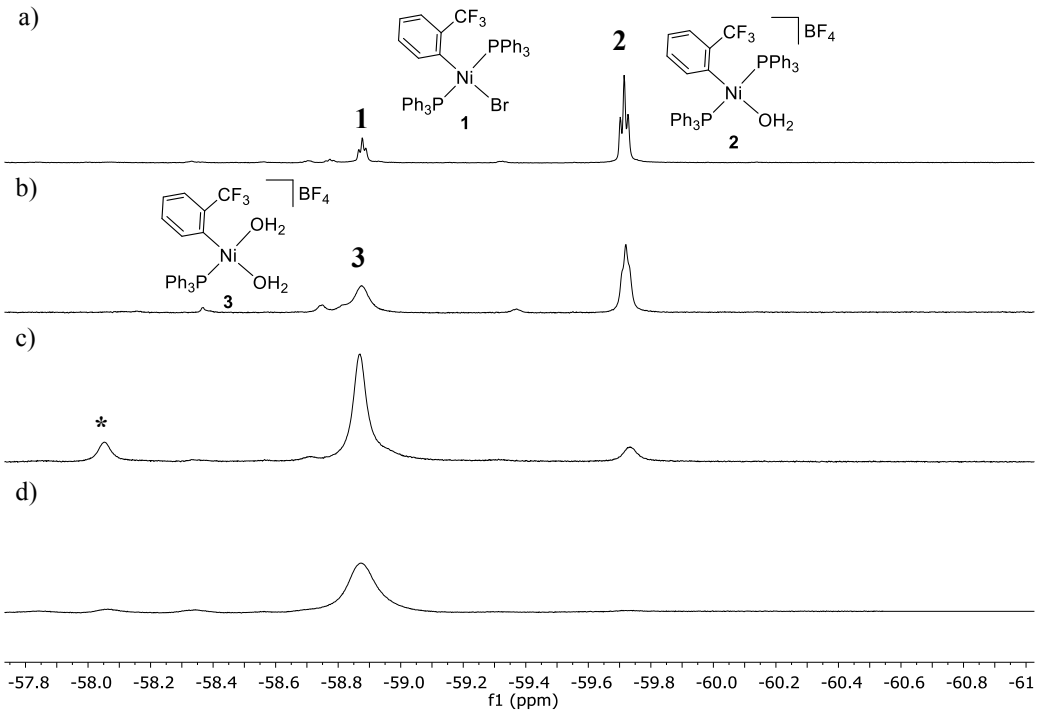

Figure S17. Comparative ^{19}F NMR (376.498 MHz, 243 K, CD_2Cl_2) spectra of the organometallic species generated *in situ* from complex **1** and different amounts of $AgBF_4$ in CH_2Cl_2/toluene: a) mol ratio $AgBF_4$:**1** = 1:1; b) mol ratio $AgBF_4$:**1** = 1.25:1; c) mol ratio $AgBF_4$:**1** = 1.75:1; d) mol ratio $AgBF_4$:**1** = 2.25:1. *unidentified complex.

To compare the species generated *in situ* at room temperature, we performed the abstraction of the bromine atom in complex **1** with $AgBF_4$ (mol ratio $AgBF_4$:**1** = 1:1.25) in CH_2Cl_2/toluene following the procedure mentioned above. The NMR spectra (Figures S18-S19) showed the formation of a similar mixture of the organometallic species detected at low temperature (Figures S9-S10). Note that the signals are very broad so the determination of the mol % of the species present is difficult. We decided to perform all experiments at low temperature to avoid the decomposition of the diaquo complex **3** that is highly unstable at room temperature.

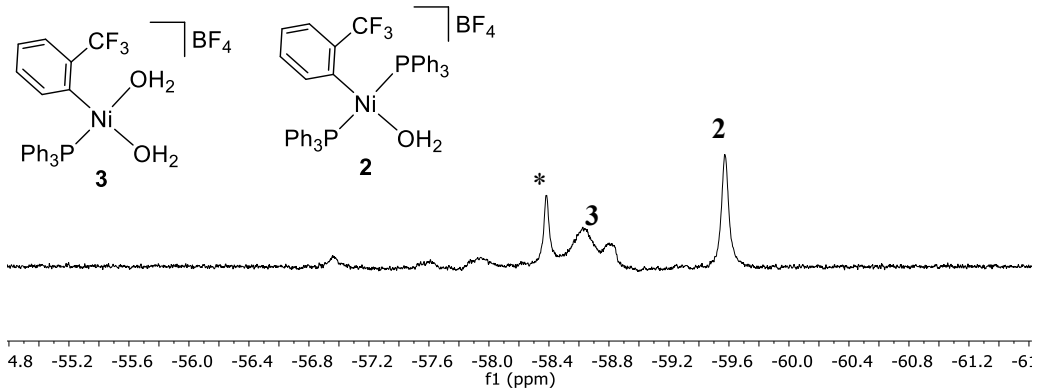

Figure S18. ^{19}F NMR (376.498 MHz, 298 K, CD_2Cl_2) of the organometallic species generated *in situ* from complex **1** and $AgBF_4$ in CH_2Cl_2/toluene (mol ratio $AgBF_4$:**1** = 1.25:1).*unidentified complex.

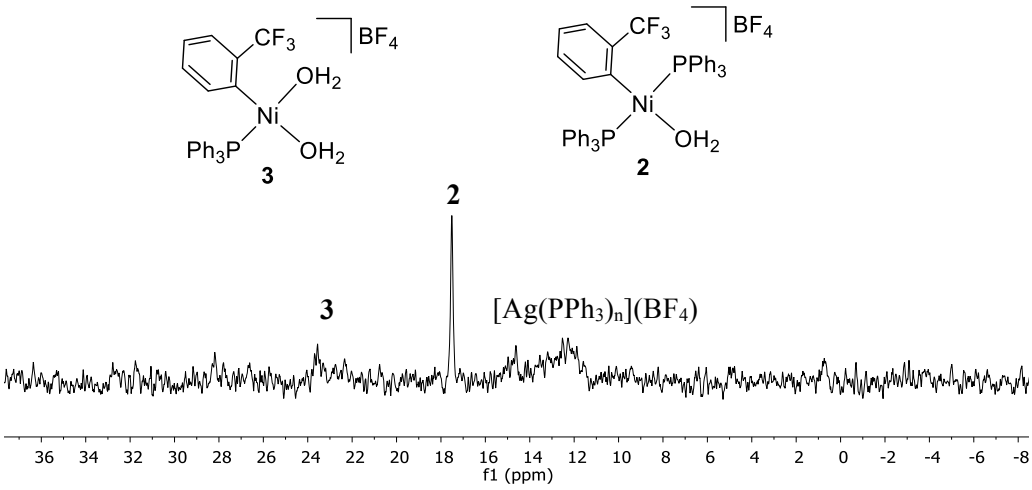

Figure S19. ^{31}P NMR (202.31 MHz, 298 K, CD_2Cl_2) of the organometallic species generated *in situ* from complex **1** and $AgBF_4$ in CH_2Cl_2/toluene (mol ratio $AgBF_4$:**1** = 1.25:1).

1.4.2- Formation *in situ* of complex **3** and $[Ag(PPh_3)_2](BF_4)$ starting from **2** and $AgBF_4$

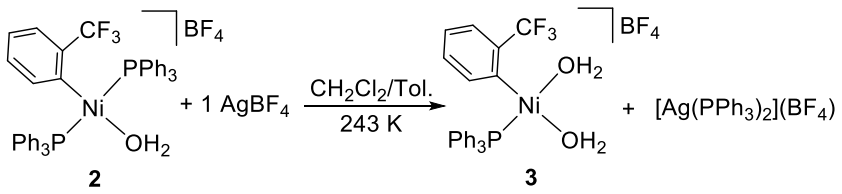

In an oven-dried vial, $AgBF_4$ (5.7 mg, 0.0293 mmol) was placed under N_2. The solid was dissolved in 2 mL of toluene and the solution was cooled in an acetone bath at 243 K for 10 min to ensure a constant temperature. In another vial complex **2** (24.4 mg, 0.0293 mmol) was dissolved in 2 mL of CH_2Cl_2 and cooled at 243 K for 10 min. The cooled yellow solution of **2** was added to the solution of $AgBF_4$ and it was stirred for 10 min. After this time, the solution was evaporated to dryness. The residue was redissolved in dry and cooled CD_2Cl_2. The mixture was checked by NMR spectroscopy.

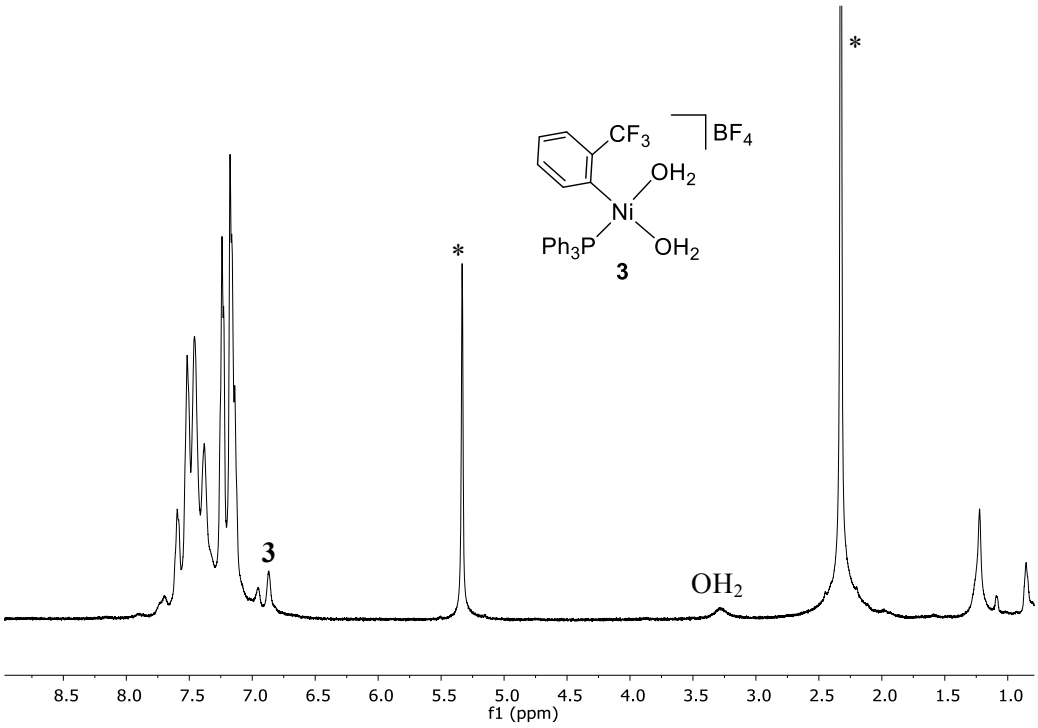

Figure S20. ^{1}H NMR (499.73 MHz, 243 K, CD_2Cl_2) of complex **3** generated *in situ* from **2** and $AgBF_4$ in a mixture of CH_2Cl_2/toluene (mol ratio **2**:$AgBF_4$ = 1:1). *Signal corresponding to CH_2Cl_2 and toluene.

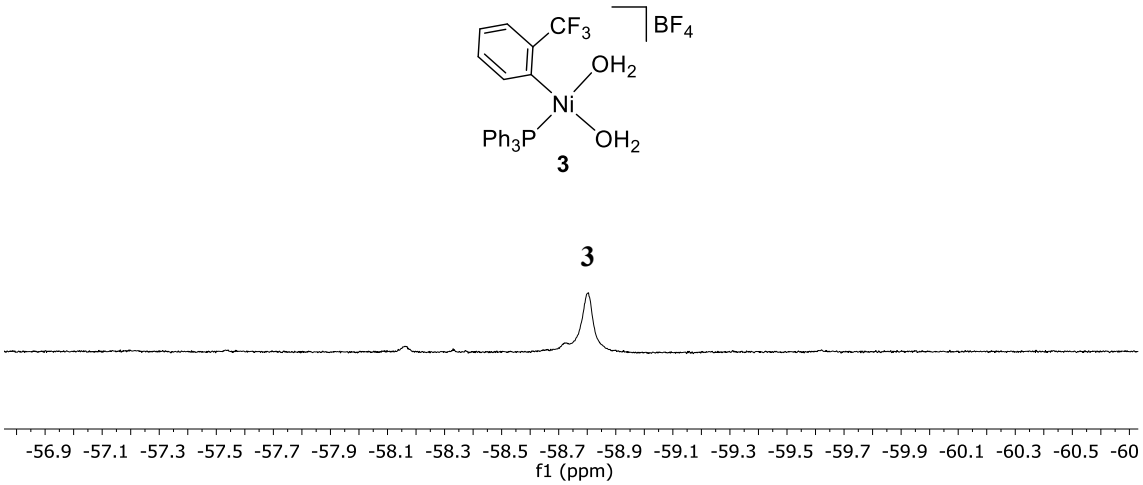

Figure S21. ^{19}F NMR (376.498 MHz, 243 K, CD_2Cl_2) of complex **3** generated *in situ* from **2** and $AgBF_4$ in a mixture of CH_2Cl_2/toluene (mol ratio **2**:$AgBF_4$ = 1:1).

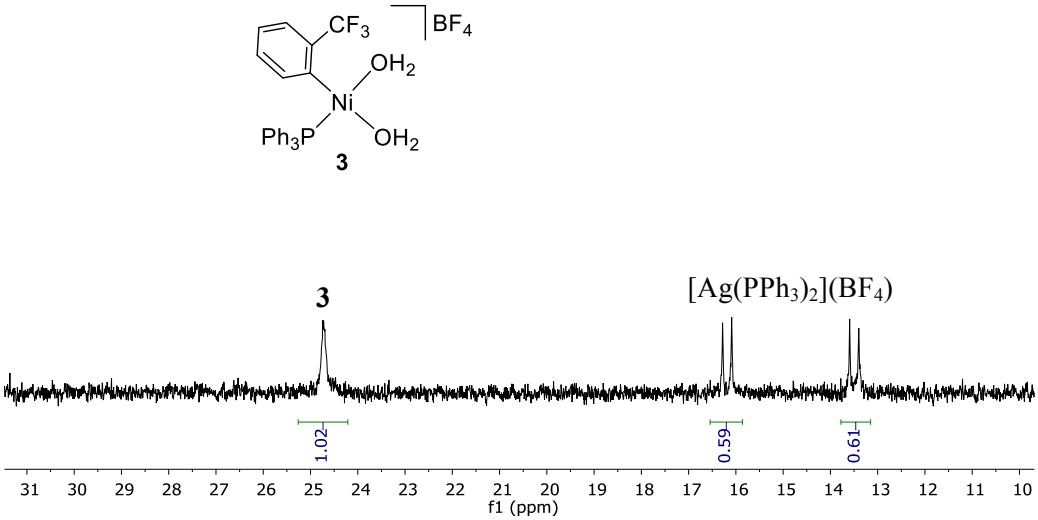

Figure S22. ^{31}P NMR (202.31 MHz, 243 K, CD_2Cl_2) of complex **3** generated *in situ* from **2** and $AgBF_4$ in a mixture of CH_2Cl_2/toluene (mol ratio **2**:$AgBF_4$ = 1:1).

1.4.3- Formation *in situ* of complex **3** starting from **4** and $HBF_{4(aq)}$

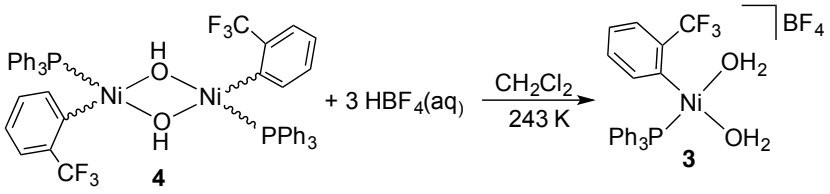

In a Schlenk tube complex **4** (20 mg, 0.0207 mmol) was dissolved in 2 mL of CH_2Cl_2. The solution was cooled in an acetone bath at 243 K for 10 min until constant temperature. HBF_4 (aq) (8 μL, 0.0633 mmol; 48 wt. %) was added to the mixture and the orange solution was stirred for 10 min at 243 K. After this time, the orange solution was evaporated to dryness and the residue was redissolved in 0.6 mL of dry and cooled CD_2Cl_2. The mixture was analyzed by NMR spectroscopy.

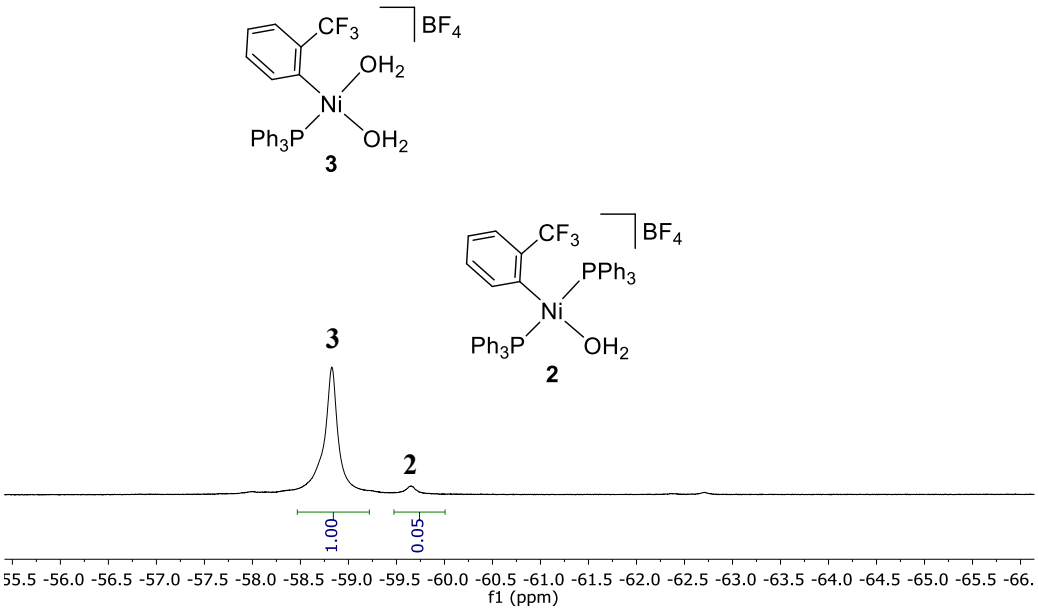

Figure S23. ^{19}F NMR (376.498 MHz, 243 K, CD_2Cl_2) of complex **3** generated *in situ* from **4** and $HBF_{4(aq)}$ in a mixture of CH_2Cl_2.

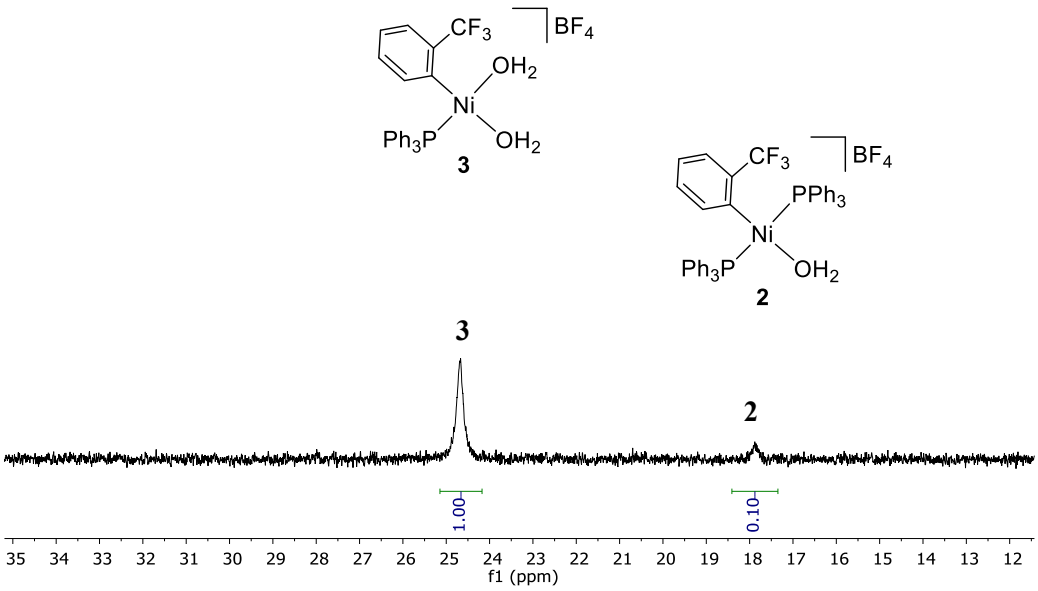

Figure S24. ^{31}P NMR (202.31 MHz, 243 K, CD_2Cl_2) of complex **3** generated *in situ* from **4** and $HBF_{4(aq)}$ in a mixture of CH_2Cl_2.

1.4.4- Formation *in situ* of complex **5** from a mixture of **1** and $AgBF_4$ in acetone

In an oven-dried vial $AgBF_4$ (8 mg, 0.0408 mmol) was dissolved in 3 mL of dry acetone under N_2. The solution was cooled to 243 K for 10 min until constant temperature. Complex **1** (20 mg, 0.0247 mmol) was added to the mixture and instantly a white solid (AgBr) appeared. The suspension was stirred for 15 min at 243 K. The white solid was removed employing a 0.2 μm PTFE filter and the orange solution was transferred to an oven dried and cooled Schlenk tube. The solution was evaporated to dryness. The residue was redissolved in 0.6 mL of $CDCl_3$ and the solution was checked by NMR spectroscopy. The mixture contained **5** as well as $[Ag(PPh_3)_2](BF_4)$ in a molar ratio 1:0.5 (Figures S70-S73).

5: ^{1}H NMR (499.73 MHz, δ, $CDCl_3$, 243 K): 7.88 (d, 1H, $^1J_{H-H}$ = 6.9 Hz, H^6), 7.5-7.12 (m, PPh_3), 6.9-6.7 (m, 3H, H^5, H^4, H^3), 5.05 (bs, 1H, OH), 3.22 (d, 1H, $^1J_{H-H}$ = 19.7 Hz, H^{10}), 2.73 (d, 1H, $^1J_{H-H}$ = 19.7 Hz, $H^{10'}$), 1.75 (s, 3H, H^9), 1.65 (s, 3H, CH_3) 1.29 (s, 3H, CH_3). $^{13}C\{^1H\}$ (125.758 MHz, δ, $CDCl_3$, 233 K): 222.2 (C^8), 137.07 (C^6), 133.9, 129.7, 127.7 (PPh_3), 128.5, 126.7, 124.1 (C^5, C^4, C^3), 71.6 (C^{11}), 51.35 (C^{10}), 32.13 (C^9), 27.8 (CH_3), 27.17 (CH_3).^{19}F NMR (470.17 MHz, δ, $CDCl_3$, 243 K): -58.1 (d, J_{P-F} = 6 Hz, CF_3), -150.2 (BF_4). $^{31}P\{^1H\}$ NMR (202.31 MHz, δ, $CDCl_3$, 243 K): 25.4 (bs, 1P). $[Ag(PPh_3)_2](BF_4)$: $^{31}P\{^1H\}$ NMR (202.31 MHz, δ, $CDCl_3$, 243 K): 13 (dd, $J_{Ag^{109}-P}$ = 584 Hz; $J_{Ag^{107}-P}$ = 510 Hz).

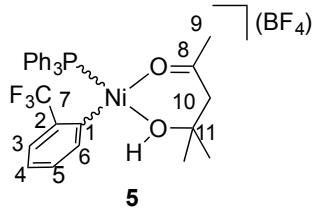

5

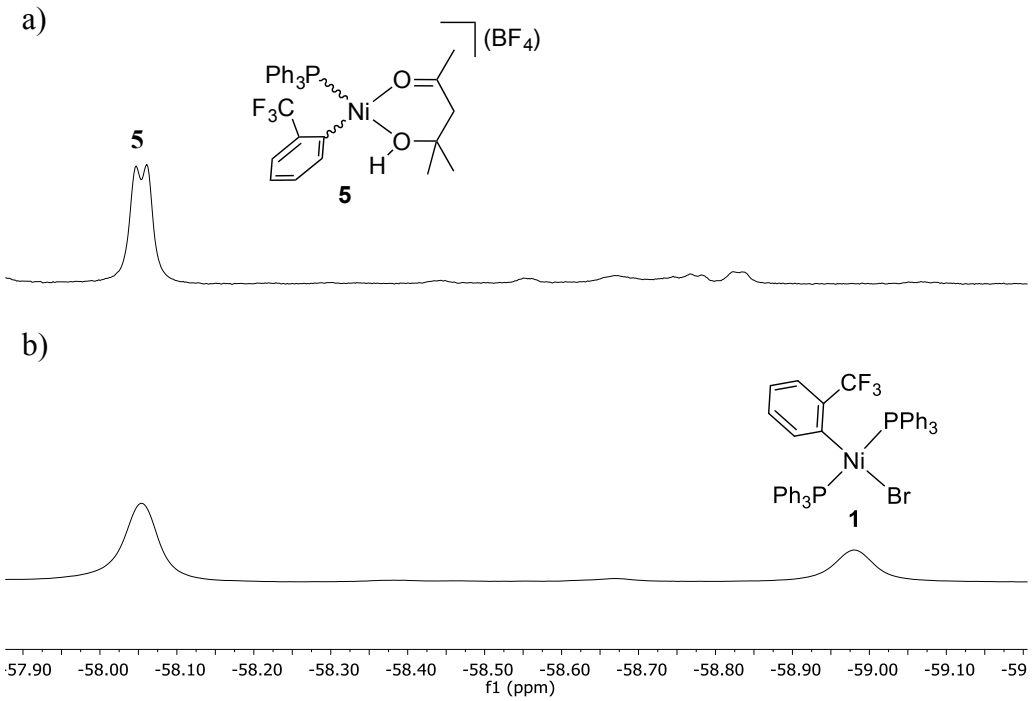

Figure S25. Comparative ^{19}F NMR (376.498 MHz, 243 K, $CDCl_3$) of the organometallic species generated *in situ* from complex **1** and different amounts of $AgBF_4$ in acetone: a) mol ratio $AgBF_4$:**1** = 1.5:1; b) mol ratio $AgBF_4$:**1** = 1:1.

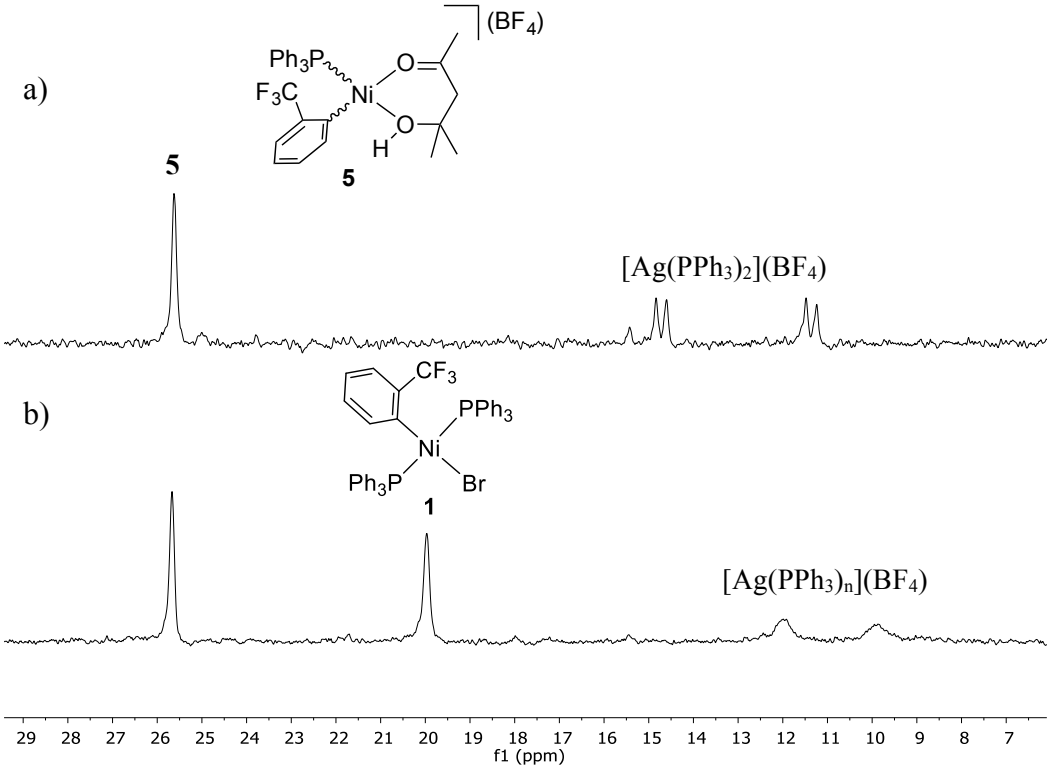

Figure S26. Comparative ^{31}P NMR (202.31 MHz, 243 K, $CDCl_3$) of the organometallic species generated *in situ* from complex **1** and different amounts of $AgBF_4$ in acetone: a) mol ratio $AgBF_4$:**1** = 1.5:1; b) mol ratio $AgBF_4$:**1** = 1:1.

1.4.5- Formation of complex **5** by reaction of **1**/HBF_4·Et_2O/$MeCOCH_2C(OH)Me_2$

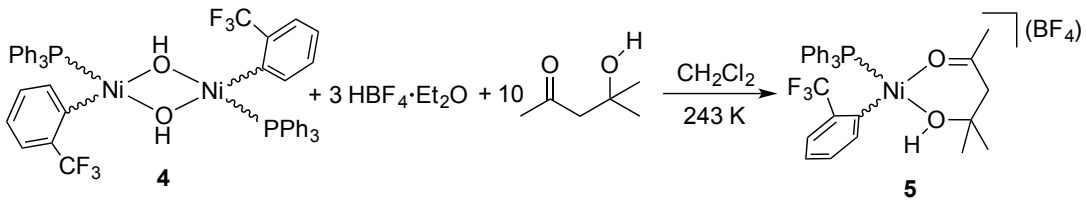

In a Schlenk tube, complex **4** (20 mg, 0.0213 mmol) was dissolved in 3 mL of dry CH_2Cl_2 under N_2. The solution was cooled in an acetone bath at 243 K for 10 min until constant temperature. The ligand $MeCOCH_2C(OH)Me_2$ (27 μL, 0.216 mmol) and HBF_4·Et_2O (9 μL, 0.066 mmol) were added. The orange solution was stirred at 243 K for 10 min. After this time, the solution was evaporated to dryness and the orange residue was redissolved in 0.6 mL of dry $CDCl_3$ at 243 K. The solution was checked by NMR spectroscopy showing the formation of **5** as major species and free ligand (Figures S27-S29).

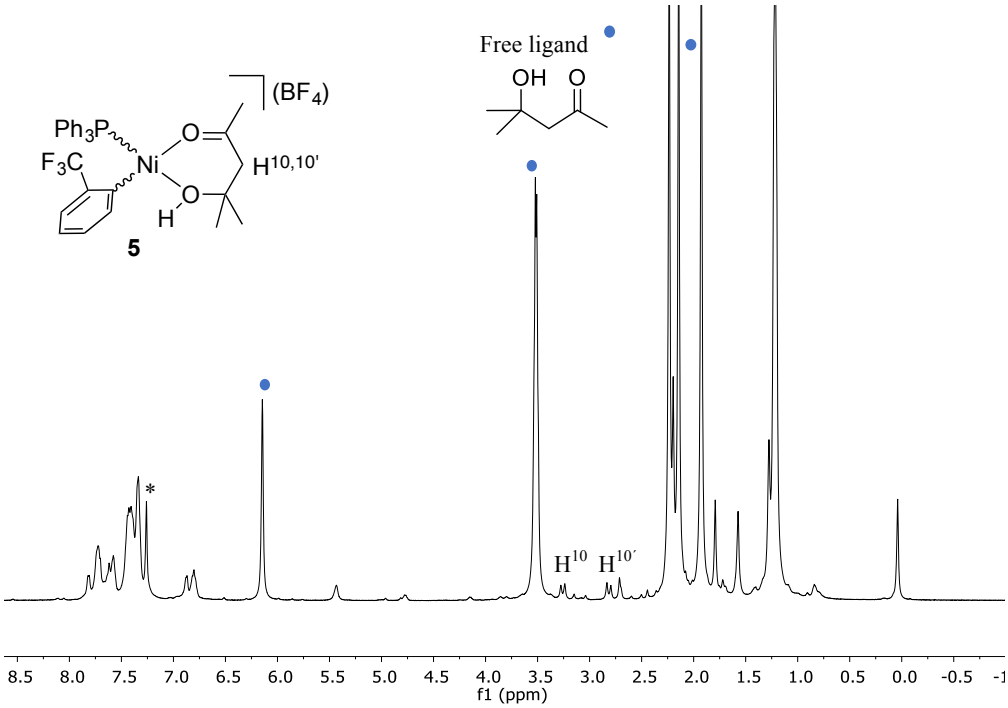

Figure S27. ^1H NMR spectra (499.73 MHz, 243 K, $CDCl_3$) of the reaction mixture of the hydroxo dimer **5**, HBF_4·Et_2O and the ligand $MeCOCH_2C(OH)Me_2$ (in excess).*$CHCl_3$

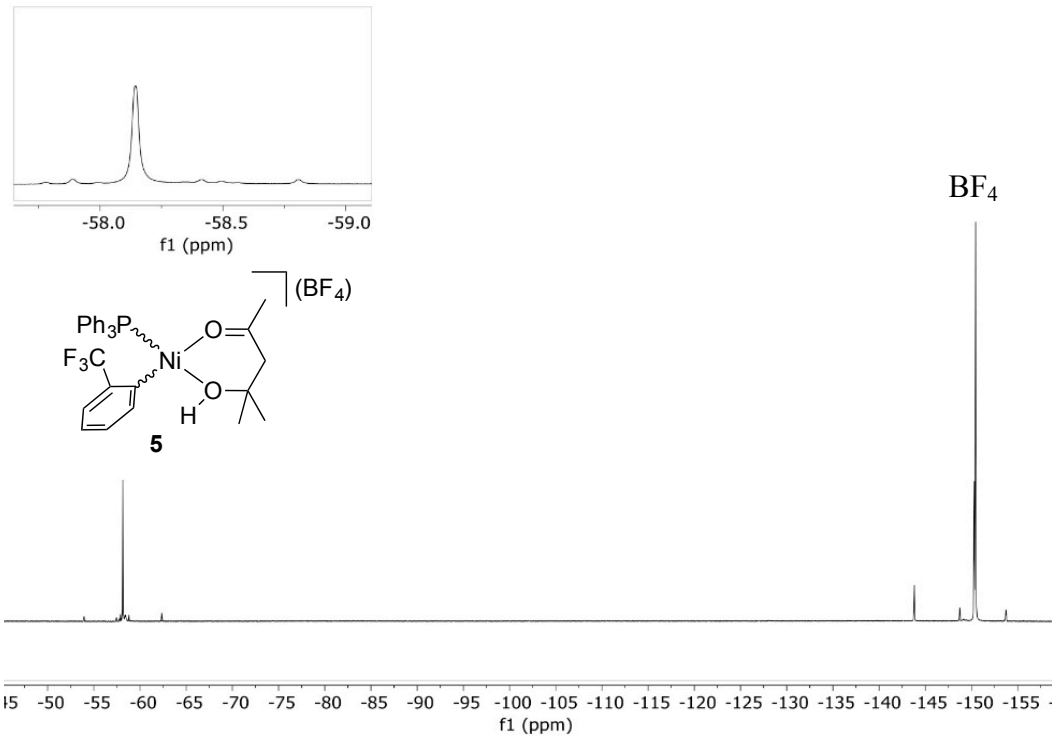

Figure S28. ^{19}F NMR spectra (376.498 MHz, 243 K, $CDCl_3$) of the reaction mixture of the hydroxo dimer **5**, $HBF_4 \cdot Et_2O$ and the ligand $MeCOCH_2C(OH)Me_2$.

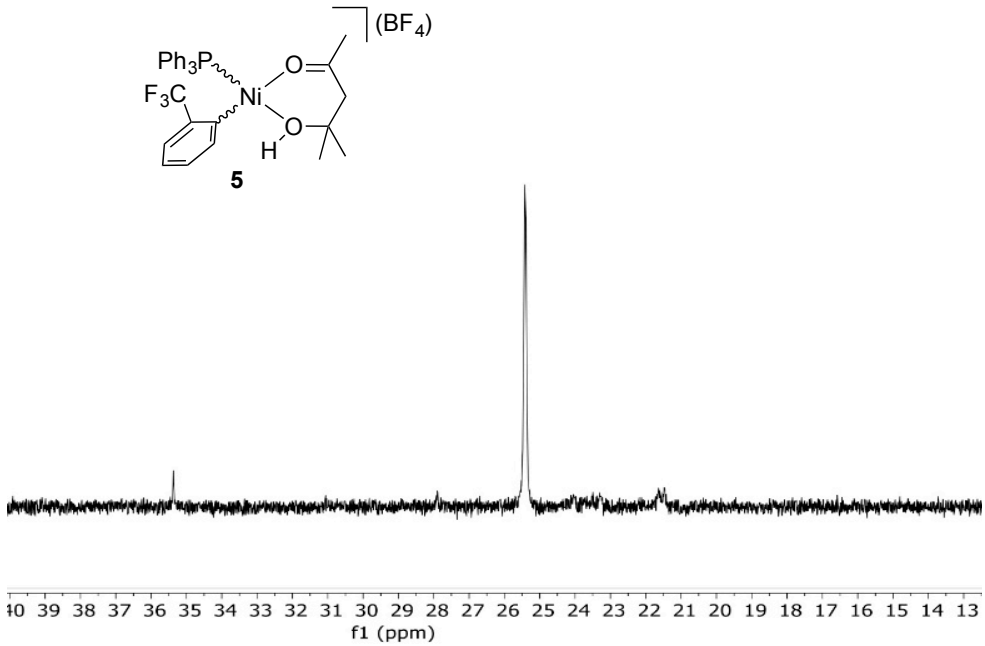

Figure S29. ^{31}P NMR spectra (202.31 MHz, 243 K, $CDCl_3$) of the reaction mixture of the hydroxo dimer **5**, $HBF_4 \cdot Et_2O$ and the ligand $MeCOCH_2C(OH)Me_2$.

1.5- Study of the formation *in situ* of organometallic species starting from complexes **7**, **8** and **10**

1.5.1- Effect of the amount of $AgBF_4$ in the formation of palladium cationic species in a mixture of CH_2Cl_2/toluene

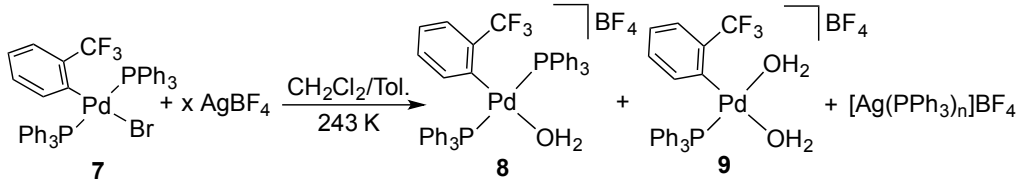

A general procedure for the following experiments is described (mol ratio **7**:$AgBF_4$ = 1:2.5). In an oven-dried vial $AgBF_4$ (9.1 mg, 0.0467 mmol) was dissolved in 2 mL of dry toluene under N_2. The solution was cooled to 243 K for 10 min until constant temperature. Complex **7** (16 mg, 0.0187 mmol) and 1 mL of cooled CH_2Cl_2 were added. Instantly, a white solid (AgBr) appeared and the suspension was stirred for 15 min at 243. The solid was removed employing a 0.2 μm PTFE filter and the solution was transferred to a cooled Schlenk tube. The solution was evaporated to dryness. The residue was redissolved in 0.6 mL of dry and cooled CD_2Cl_2 and checked by NMR spectroscopy.

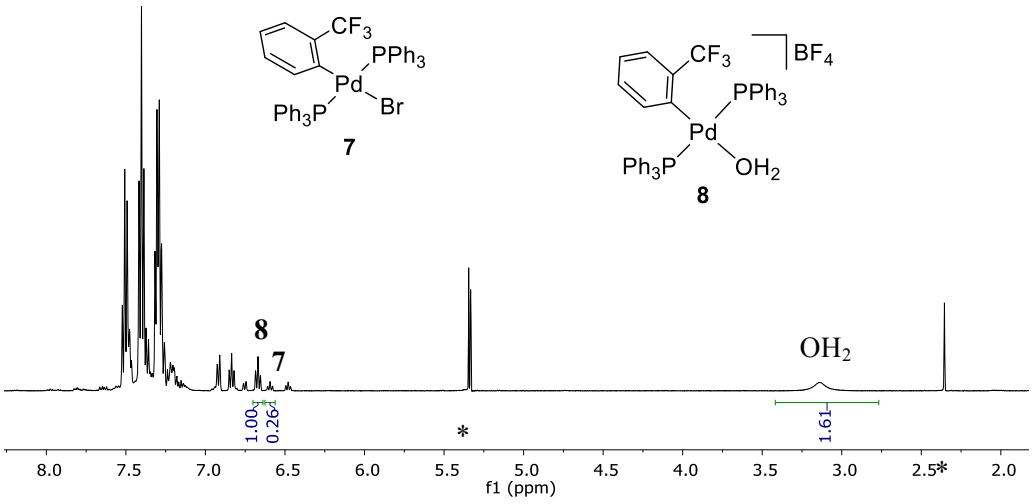

Figure S30. ^1H NMR (499.73 MHz, 243 K, CD_2Cl_2) of the organometallic species generated *in situ* from complex **7** and $AgBF_4$ in CH_2Cl_2/toluene (mol ratio $AgBF_4$:**7** = 1:1). *Signal corresponding to CH_2Cl_2 and toluene.

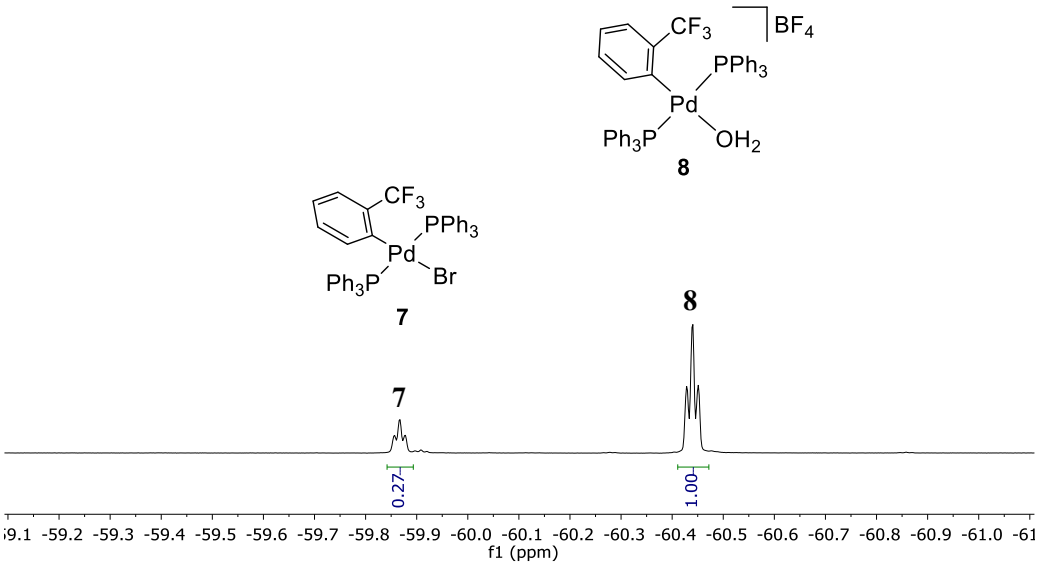

Figure S31. ^{19}F NMR (376.498 MHz, 243 K, CD_2Cl_2) of the organometallic species generated *in situ* from complex **7** and $AgBF_4$ in CH_2Cl_2/toluene (mol ratio $AgBF_4$:**7** = 1:1). Mol % **7** = 21.3; mol % **8** = 78.7).

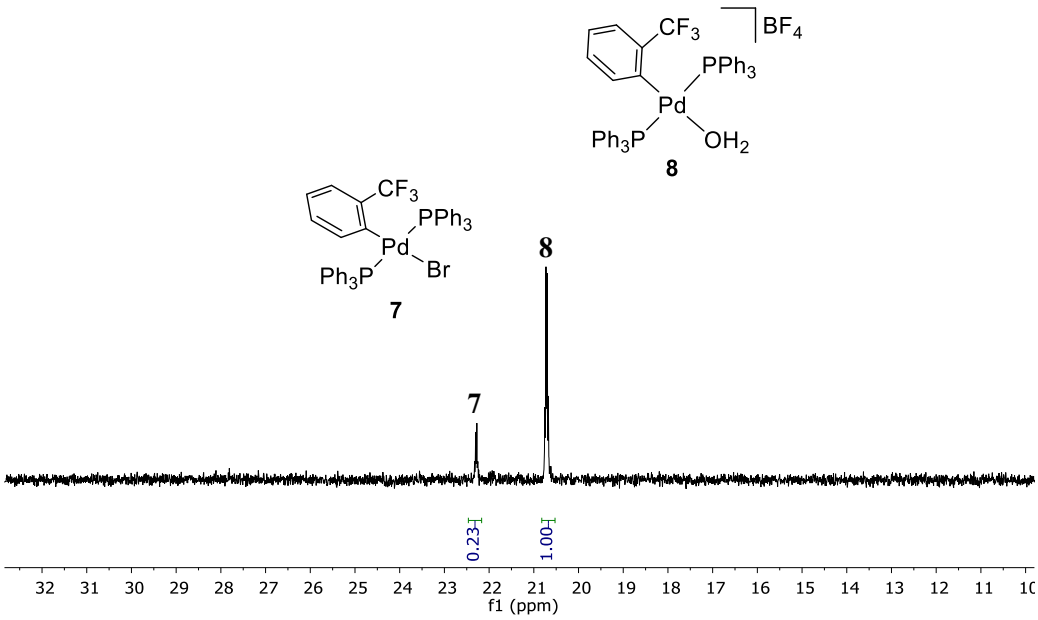

Figure S32. ^{31}P NMR (202.31 MHz, 243 K, CD_2Cl_2) of the organometallic species generated *in situ* from complex **7** and $AgBF_4$ in CH_2Cl_2/toluene (mol ratio $AgBF_4$:**7** = 1:1).

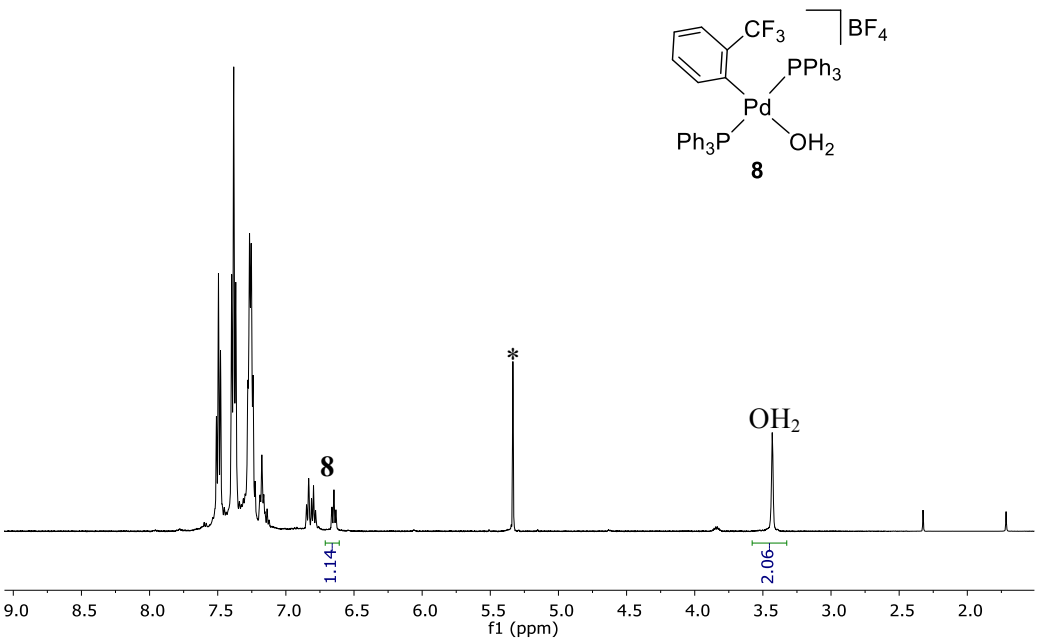

Figure S33. ^{1}H NMR (499.73 MHz, 243 K, CD_2Cl_2) of the organometallic species generated *in situ* from complex **7** and $AgBF_4$ in CH_2Cl_2/toluene (mol ratio $AgBF_4$:**7** = 1.25:1). *Signal corresponding to CH_2Cl_2.

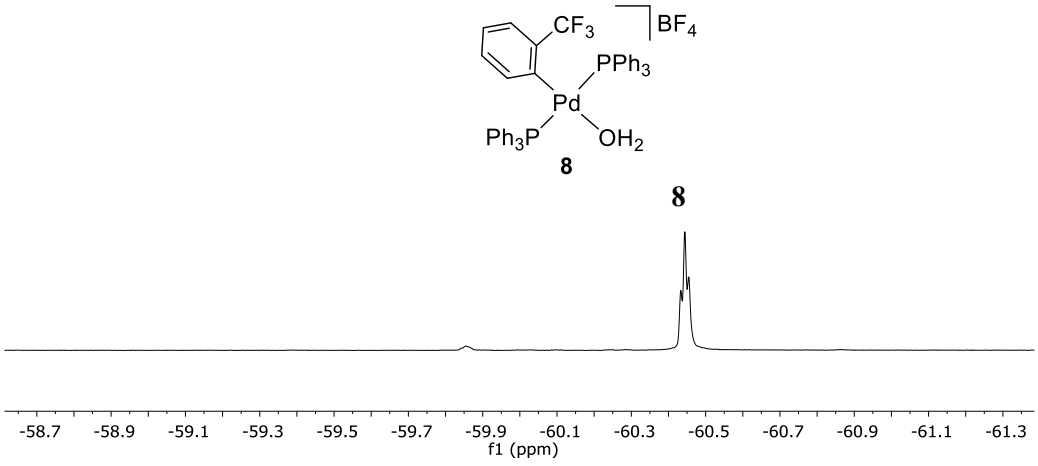

Figure S34. ^{19}F NMR (376.498 MHz, 243 K, CD_2Cl_2) of the organometallic species generated *in situ* from complex **7** and $AgBF_4$ in CH_2Cl_2/toluene (mol ratio $AgBF_4$:**7** = 1.25:1).

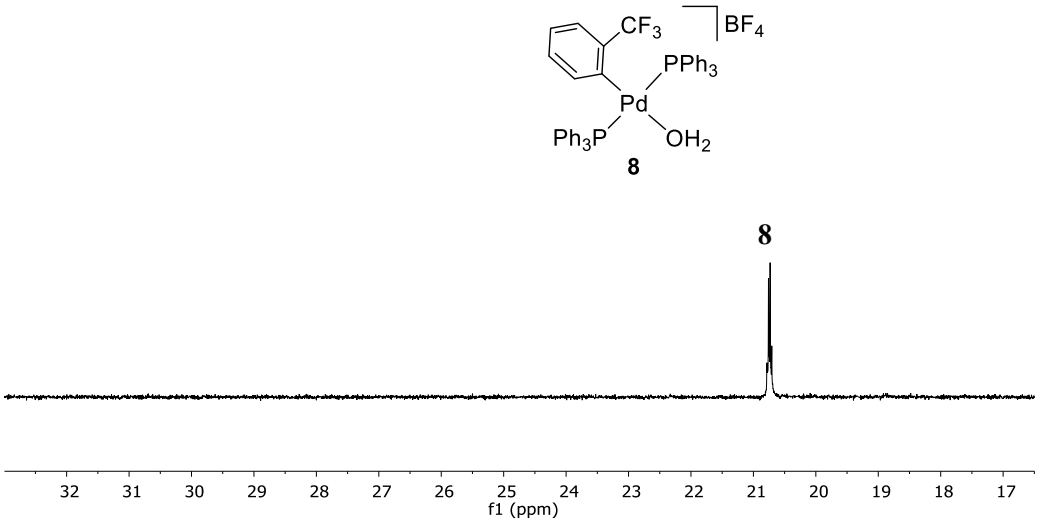

Figure S35. ^{31}P NMR (202.31 MHz, 243 K, CD_2Cl_2) of the organometallic species generated *in situ* from complex **7** and $AgBF_4$ in CH_2Cl_2/toluene (mol ratio $AgBF_4$:**7** = 1.25:1).

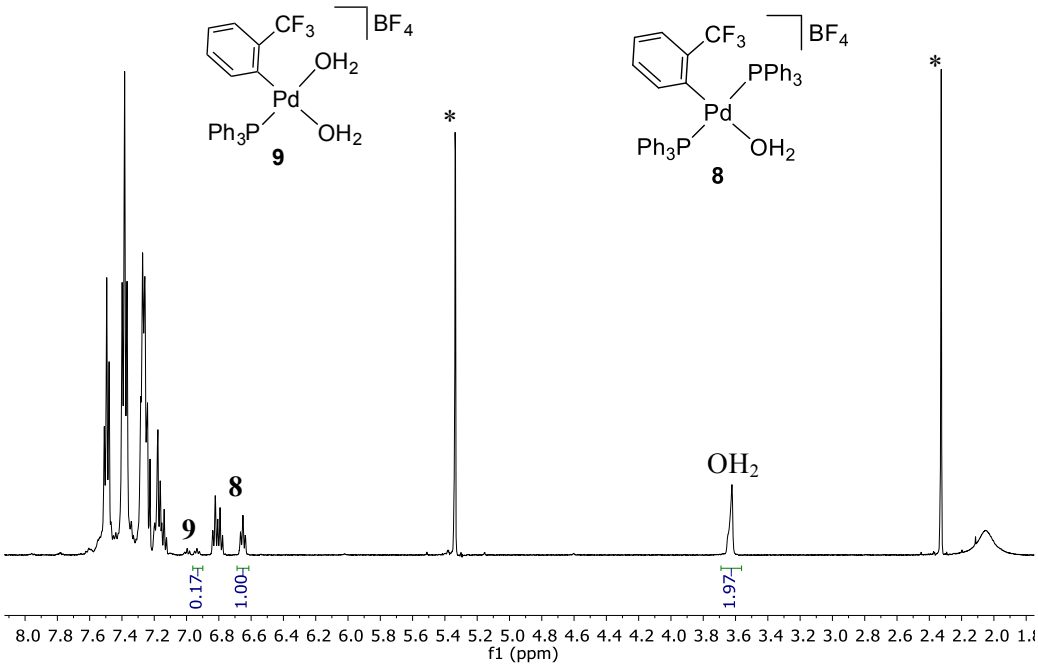

Figure S36. ^{1}H NMR (499.73 MHz, 243 K, CD_2Cl_2) of the organometallic species generated *in situ* from complex **7** and $AgBF_4$ in CH_2Cl_2/toluene (mol ratio $AgBF_4$:**7** = 2.5:1). *Signal corresponding to CH_2Cl_2 and toluene.

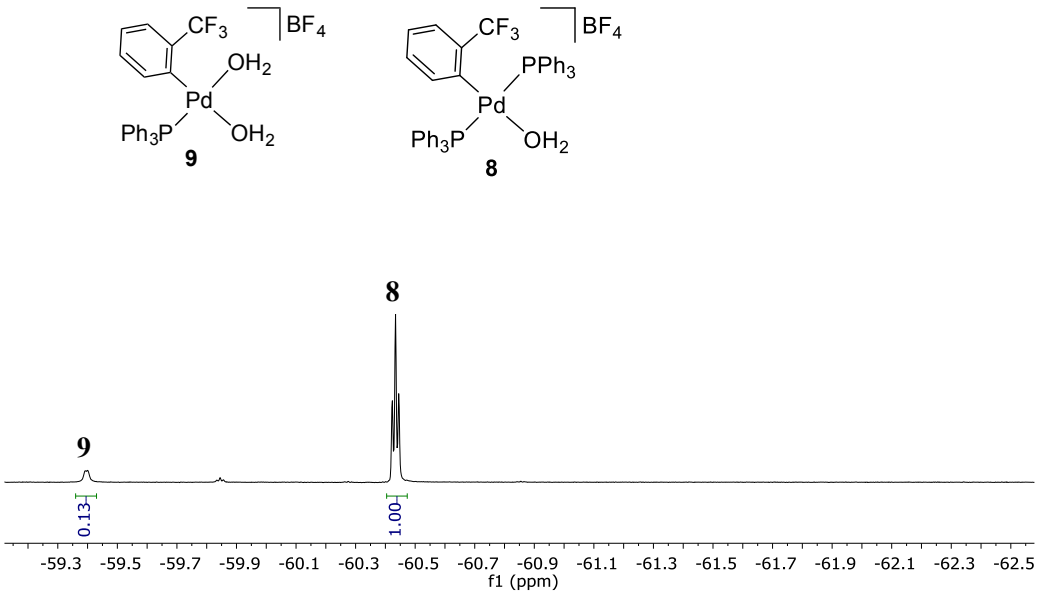

Figure S37. ^{19}F NMR (376.498 MHz, 243 K, CD_2Cl_2) of the organometallic species generated *in situ* from complex **7** and $AgBF_4$ in CH_2Cl_2/toluene (mol ratio $AgBF_4$:**7** = 2.5:1). Mol % **8** = 88.5; mol % **9** = 11.5).

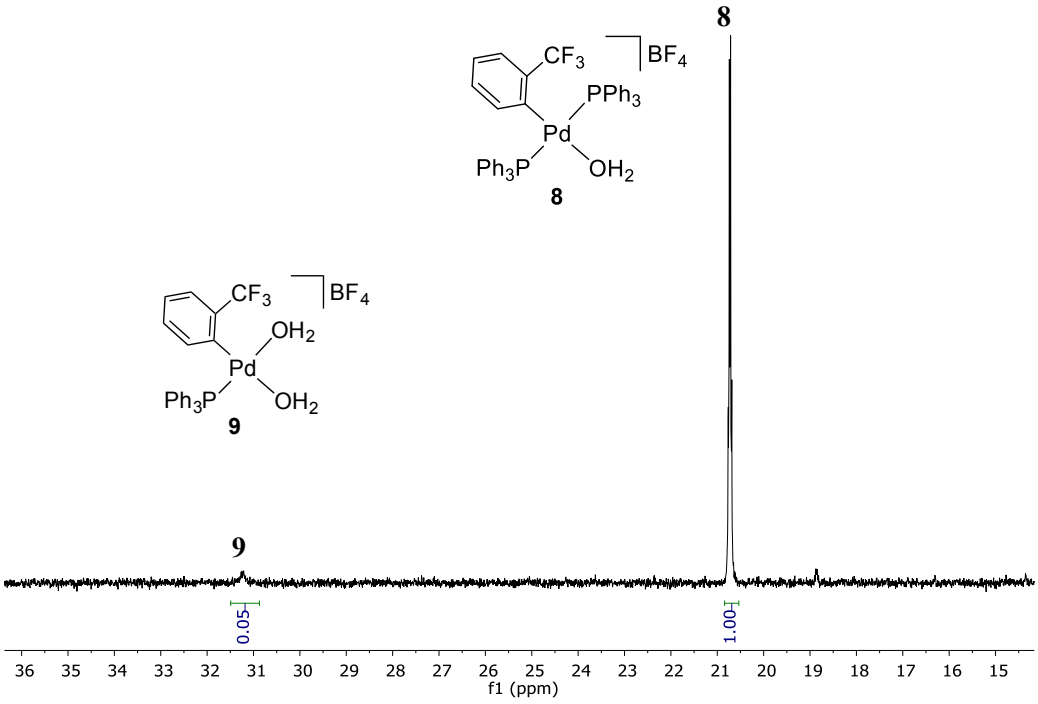

Figure S38. ^{31}P NMR (202.31 MHz, 243 K, CD_2Cl_2) of the organometallic species generated *in situ* from complex **7** and $AgBF_4$ in CH_2Cl_2/toluene (mol ratio $AgBF_4$:**7** = 2.5:1).

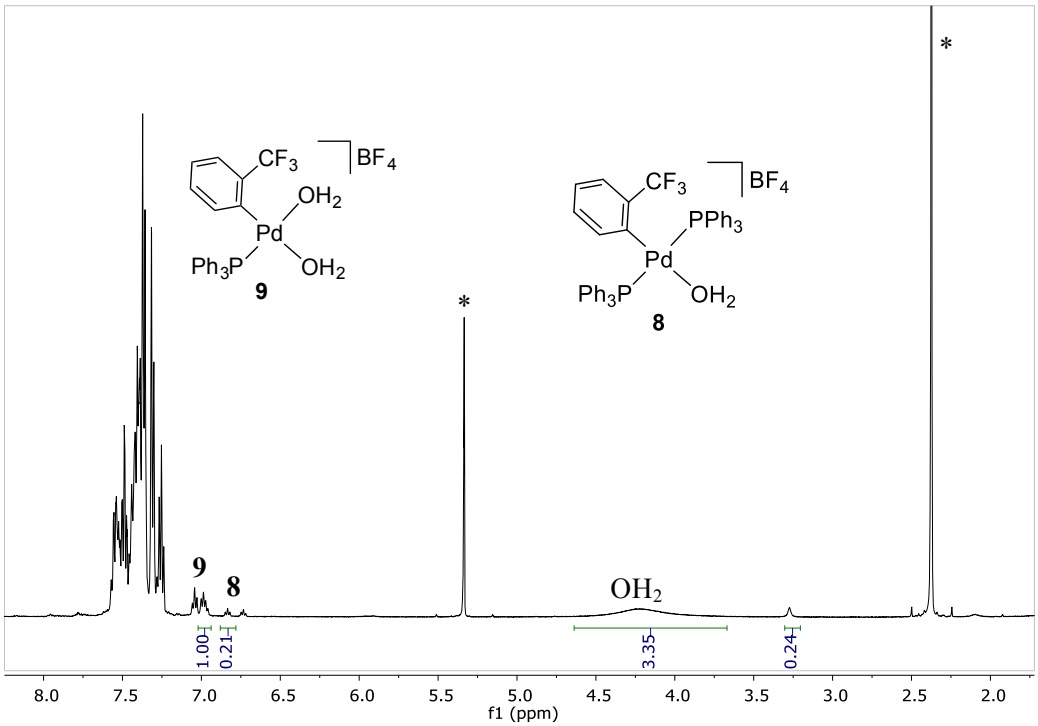

Figure S39. ^{1}H NMR (499.73 MHz, 243 K, CD_2Cl_2) of the organometallic species generated *in situ* from complex **7** and $AgBF_4$ in CH_2Cl_2/toluene (mol ratio $AgBF_4$:**7** = 10:1). *Signal corresponding to CH_2Cl_2 and toluene.

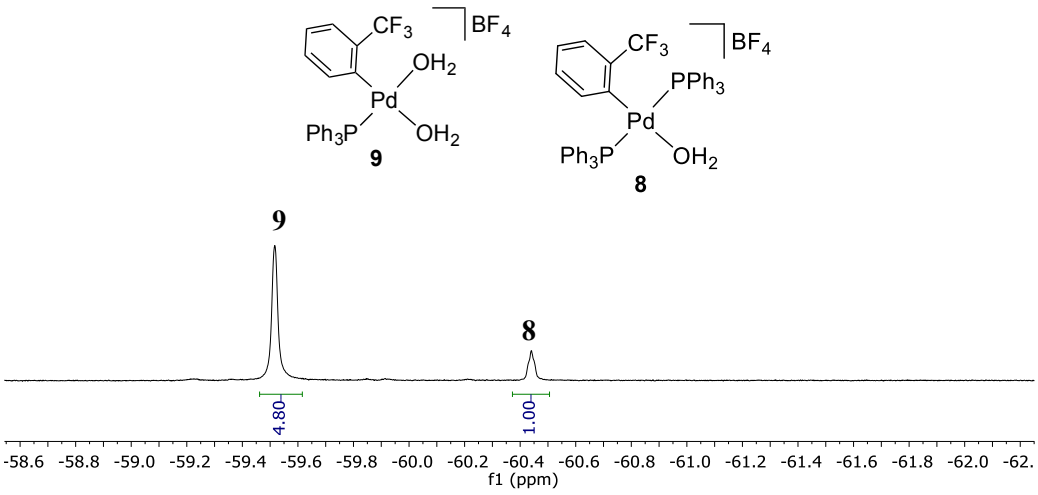

Figure S40. ^{19}F NMR (376.498 MHz, 243 K, CD_2Cl_2) of the organometallic species generated *in situ* from complex **7** and $AgBF_4$ in CH_2Cl_2/toluene (mol ratio $AgBF_4$:**7** = 10:1). Mol % **8** = 17.3; mol % **9** = 82.7).

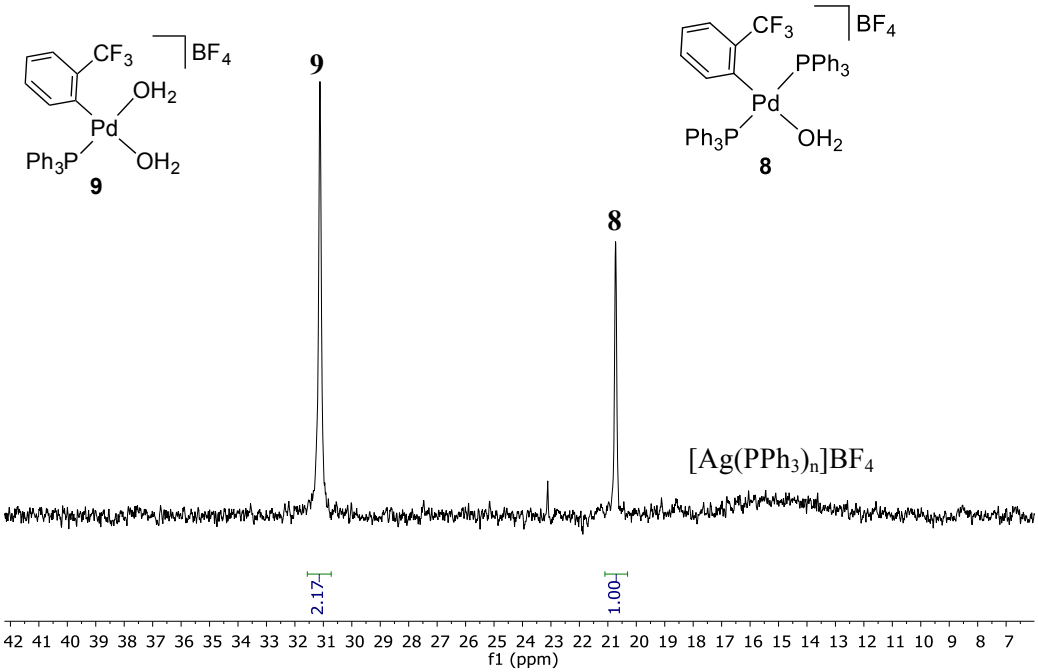

Figure S41. ^{31}P NMR (202.31 MHz, 243 K, CD_2Cl_2) of the organometallic species generated *in situ* from complex **7** and $AgBF_4$ in CH_2Cl_2/toluene (mol ratio $AgBF_4$:**7** = 10:1).

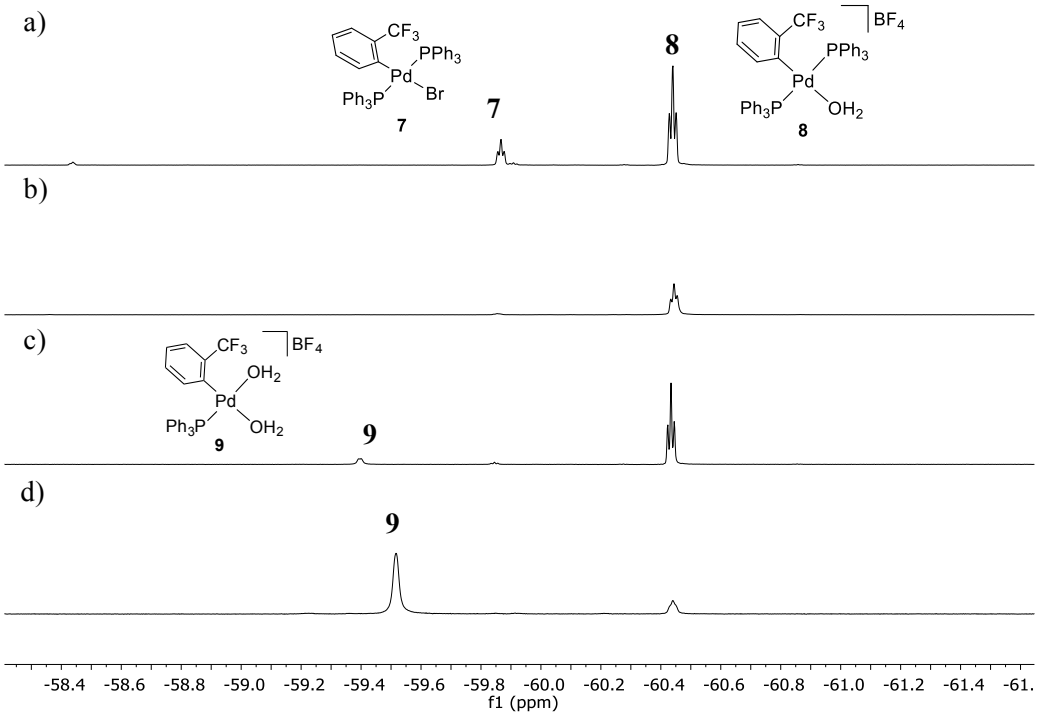

Figure S42. Comparative ^{19}F NMR (376.498 MHz, 243 K, CD_2Cl_2) spectra of the organometallic species generated *in situ* from complex **7** and different amounts of $AgBF_4$ in CH_2Cl_2/toluene: a) mol ratio $AgBF_4$:**7** = 1:1; b) mol ratio $AgBF_4$:**7** = 1.25:1; c) mol ratio $AgBF_4$:**7** = 2.25:1; d) mol ratio $AgBF_4$:**7** = 10:1.

To compare the species generated *in situ* at room temperature, we performed the abstraction of the bromide in complex **7** with 10 equiv. of $AgBF_4$ in CH_2Cl_2/toluene following the procedure mentioned above. The NMR spectra (Figures S43-S45) showed the formation of a similar mixture of **8** and **9** to that detected at low temperature (Figures S39-S41). We decided to perform all experiments at low temperature to avoid the decomposition of the diaquo complex **9** that is unstable at room temperature.

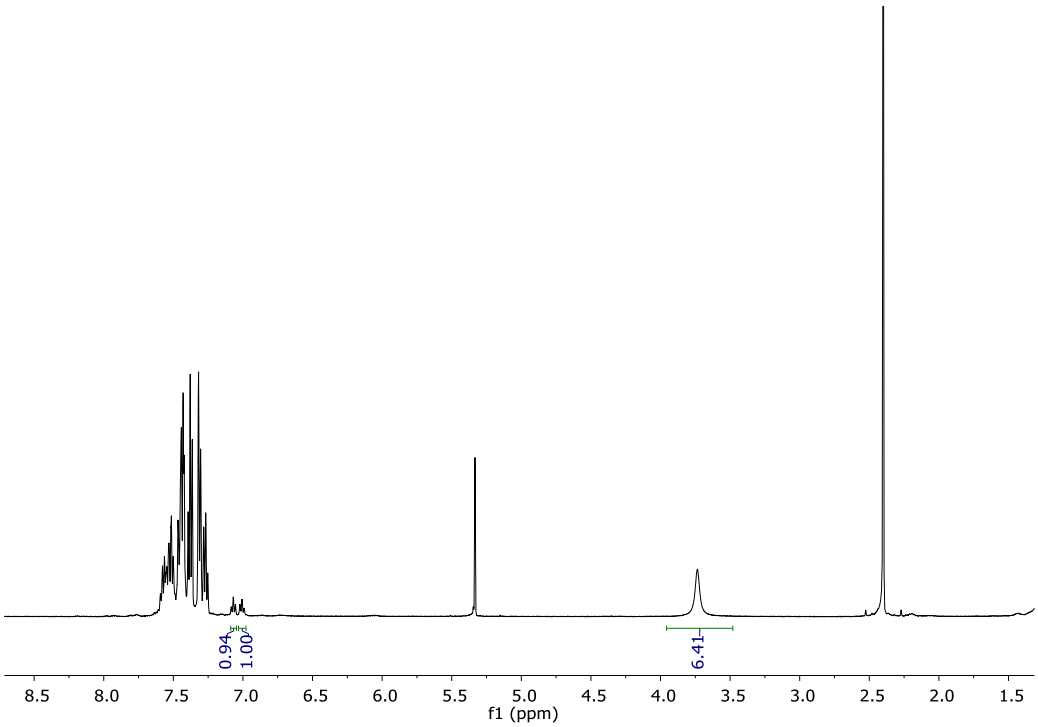

Figure S43. ^1H NMR (499.73 MHz, 298 K, CD_2Cl_2) of the organometallic species generated *in situ* from complex **7** and $AgBF_4$ in CH_2Cl_2/toluene (mol ratio $AgBF_4$:**7** = 10:1). *Signal corresponding to CH_2Cl_2 and toluene.

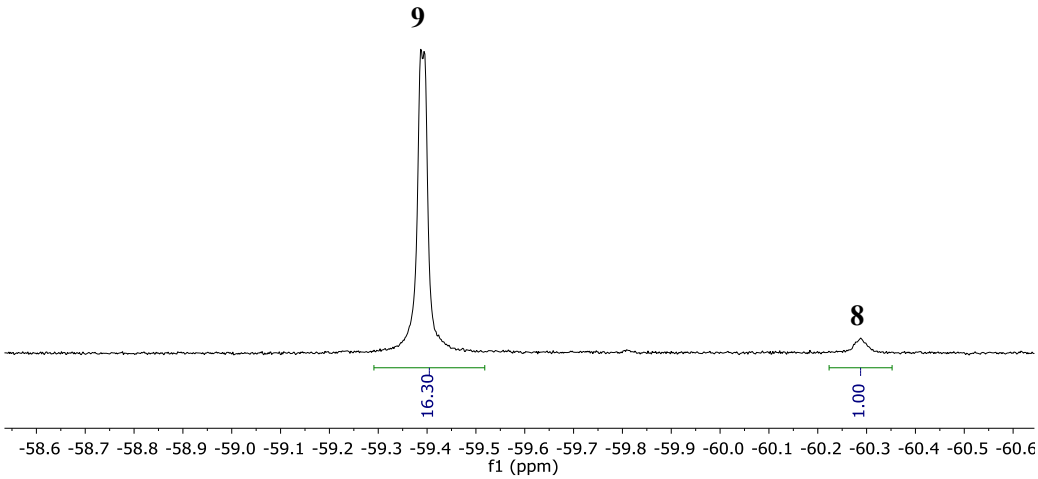

Figure S44. ^{19}F NMR (376.498 MHz, 298 K, CD_2Cl_2) of the organometallic species generated *in situ* from complex **7** and $AgBF_4$ in CH_2Cl_2/toluene (mol ratio $AgBF_4$:**7** = 10:1). Mol % **8** = 5.7; mol % **9** = 94.3).

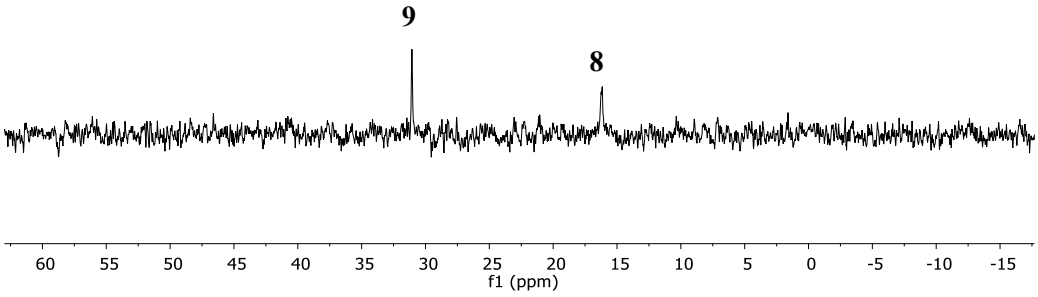

Figure S45. ^{31}P NMR (202.31 MHz, 298 K, CD_2Cl_2) of the organometallic species generated *in situ* from complex **7** and $AgBF_4$ in CH_2Cl_2/toluene (mol ratio $AgBF_4$:**7** = 10:1).

1.5.2- Formation *in situ* of a mixture of complexes **8**, **9** and $[Ag(PPh_3)_n]BF_4$ starting from **8** and $AgBF_4$

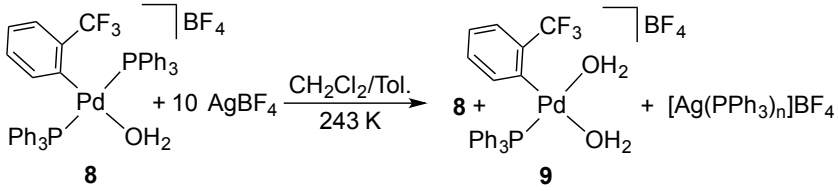

In an oven-dried vial, $AgBF_4$ (19.68 mg, 0.101 mmol) was placed under N_2. The solid was dissolved in 4 mL of dry toluene and the solution was cooled in an acetone bath at 243 K for 10 min to ensure a constant temperature. Complex **8** (8.9 mg, 0.01 mmol) and 2 mL of dry CH_2Cl_2 were added. The solution was stirred for 15 min at 243 K. After this time, the solution was evaporated to dryness. The residue was redissolved in 0.6 mL of dry and cooled CD_2Cl_2 and the mixture was checked by NMR spectroscopy.

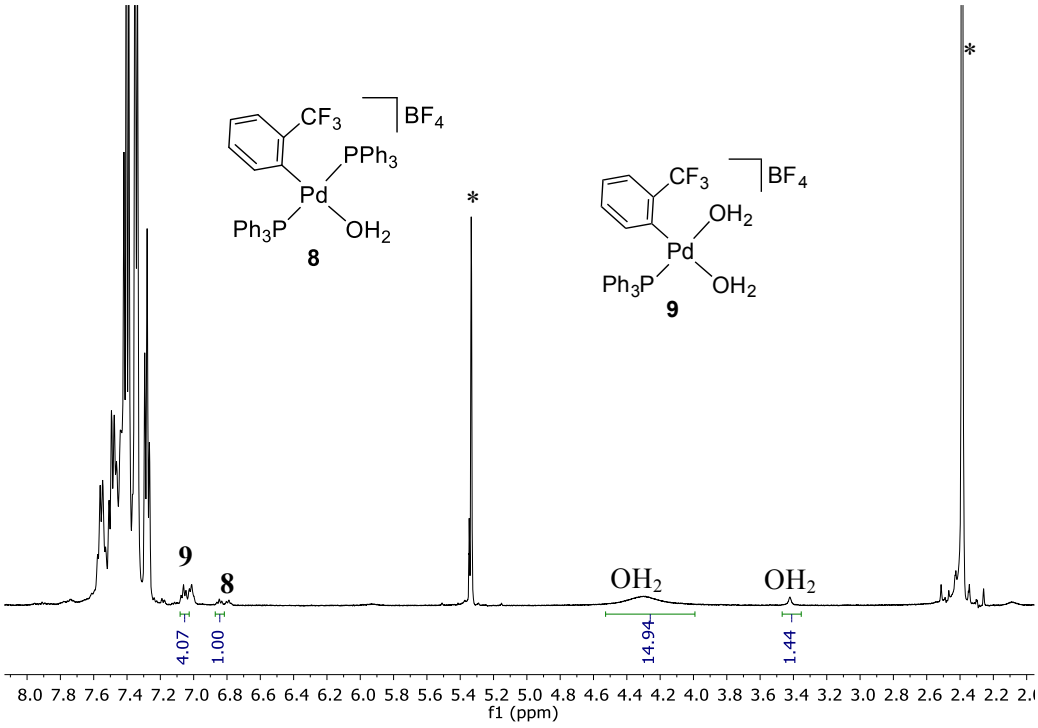

Figure S46. ^1H NMR (499.73 MHz, 243 K, CD_2Cl_2) of the organometallic species generated *in situ* from **8** and $AgBF_4$ in a mixture of CH_2Cl_2/toluene (mol ratio **8**:$AgBF_4$ = 1:10). *Signal corresponding to CH_2Cl_2 and toluene.

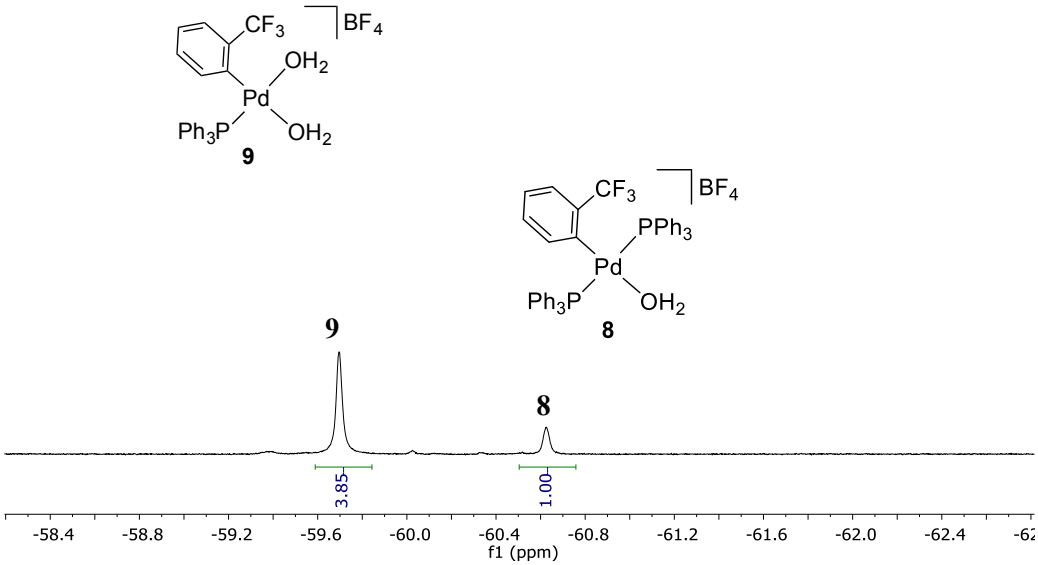

Figure S47. ^{19}F NMR (376.498 MHz, 243 K, CD_2Cl_2) of the organometallic species generated *in situ* from **8** and $AgBF_4$ in a mixture of CH_2Cl_2/toluene (mol ratio **8**:$AgBF_4$ = 1:10; % mol **8** = 20.6; % mol **9** = 79.4).

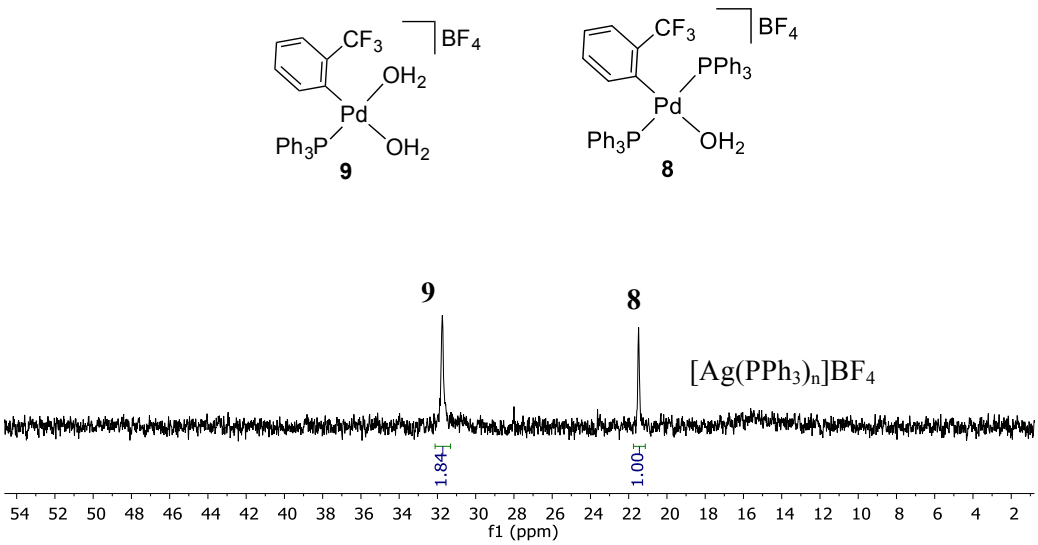

Figure S48. ^{31}P NMR (202.31 MHz, 243 K, CD_2Cl_2) of the organometallic species generated *in situ* from **8** and $AgBF_4$ in a mixture of CH_2Cl_2/toluene (mol ratio **8**:$AgBF_4$ = 1:10).

1.5.3- Formation *in situ* of complex **9** starting from **10** and $HBF_{4(aq)}$

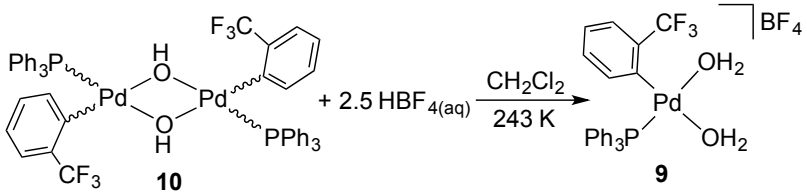

In a Schlenk tube complex **10** (20 mg, 0.0188 mmol) was dissolved in 2 mL of CH_2Cl_2. The solution was cooled in an acetone bath at 243 K for 10 min until constant temperature. $HBF_{4(aq)}$ was added (6 μL, 0.0459 mmol; 48 wt. %) to the mixture and the yellow solution was stirred for 15 min at 243 K. After this time, the orange solution was evaporated to dryness and the residue was redissolved in 0.6 mL of dry CD_2Cl_2 at low temperature. The mixture was analyzed by NMR spectroscopy. ^{1}H NMR (499.73 MHz, δ, 243 K, CD_2Cl_2): 7.48 (m, 3H, H_{para} PPh_3), 7.35 (m, 13H, H_{meta}, H_{ortho} PPh_3, H^6), 7.15 (d, 1H, J = 7.8 Hz, H^3), 6.96 (t, 1H, J = 7.8 Hz, H^4), 6.88 (t, 1H, J = 7.8 Hz, H^5), 3.7 (bs, 4H, OH_2). $^{13}C\{^{1}H\}$ (125.758 MHz, δ, 243 K, CD_2Cl_2): 141.3 (C^1), 135.5 (d, $^{3}J_{C\text{-}P}$ = 6.5 Hz, C^6), 133.4 (q, $^{2}J_{C\text{-}F}$ = 28 Hz, C^2), 134, 128.9 (C_{meta}, C_{ortho} Ph PPh_3), 127.2 (vt, $J_{C\text{-}P}$ = 56 Hz, C^{ipso} PPh_3), 131.6 (C_{para} Ph PPh_3), 130.3 (C^5), 124 (q, $^{1}J_{C\text{-}F}$ = 273 Hz, C^7), 127.1 (C^3), 124.7 (C^4). ^{19}F NMR (470.17 MHz, δ, 243 K, CD_2Cl_2): -59.41 (d, $J_{P\text{-}F}$ = 3.5 Hz, CF_3), -149.04 (BF_4^-). $^{31}P\{^{1}H\}$ (202.31 MHz, δ, 243 K, CD_2Cl_2): 31.3 (Figures S86-S89).

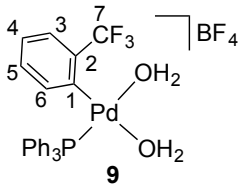

1.5.4- Abstraction of bromide in complex **7** with $AgBF_4$ in acetone

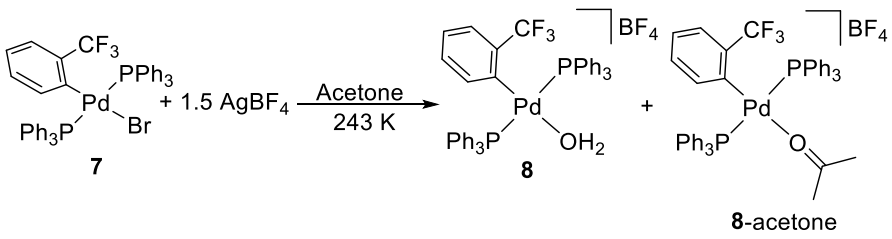

In an oven-dried vial $AgBF_4$ (9.1 mg, 0.0467 mmol) was dissolved in 3 mL of dry acetone under N_2. The solution was cooled to 243 K for 10 min until constant temperature and complex **7** (26.6 mg, 0.0311 mmol) was added. Instantly, a white solid (AgBr) appeared and the suspension was stirred for 15 min at 243 K. The solid was removed employing a 0.2 μm PTFE filter and the solution was transferred to a cooled Schlenk tube. The solution was evaporated to dryness. The residue was dissolved in 0.6 mL of dry and cooled CD_2Cl_2 and it was checked by NMR spectroscopy.

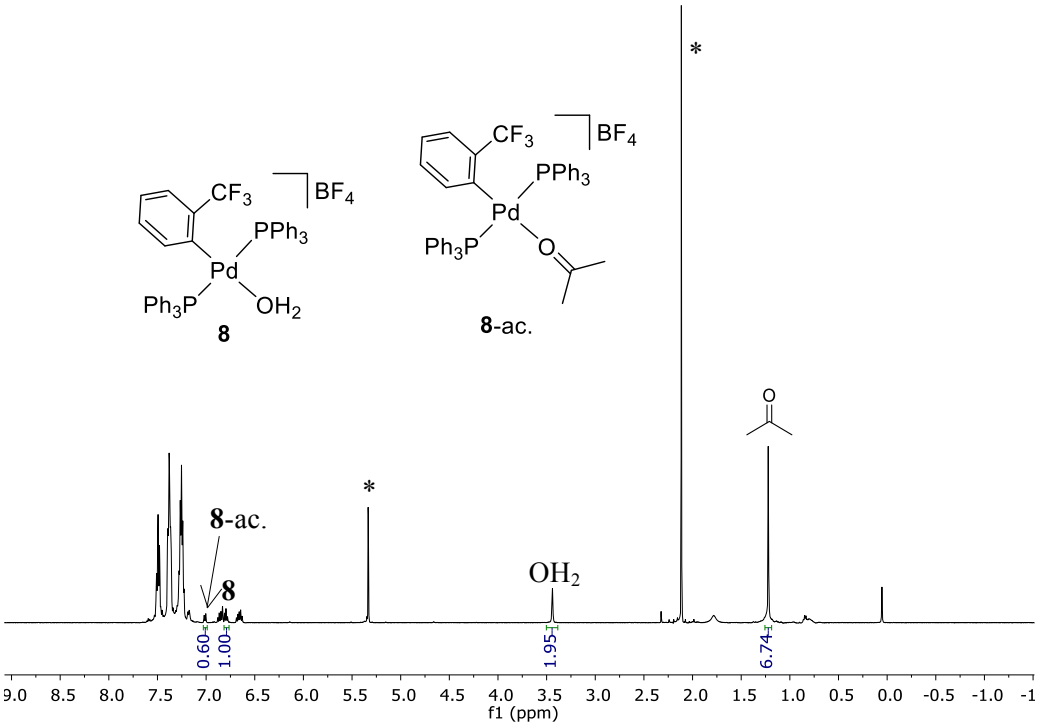

Figure S49. ^1H NMR (499.73 MHz, 243 K, CD_2Cl_2) of the organometallic species generated *in situ* from complex **7** and $AgBF_4$ in acetone (mol ratio $AgBF_4$:**7** = 1.5:1). *Signal corresponding to CH_2Cl_2 and free acetone.

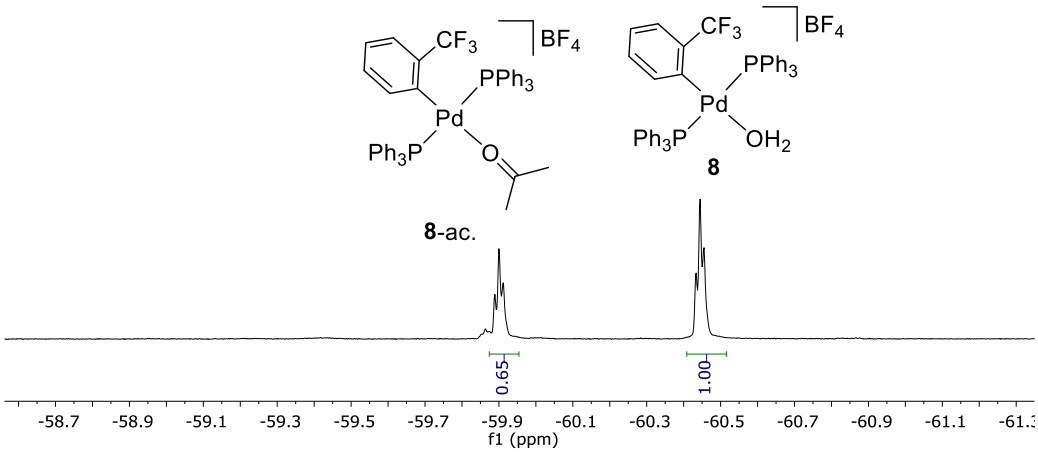

Figure S50. ^{19}F NMR (376.498 MHz, 243 K, CD_2Cl_2) of the organometallic species generated *in situ* from complex **7** and $AgBF_4$ in acetone (mol ratio $AgBF_4$:**7** = 1.5:1). Mol % **8** = 60%; mol % **8**-ac = 40%).

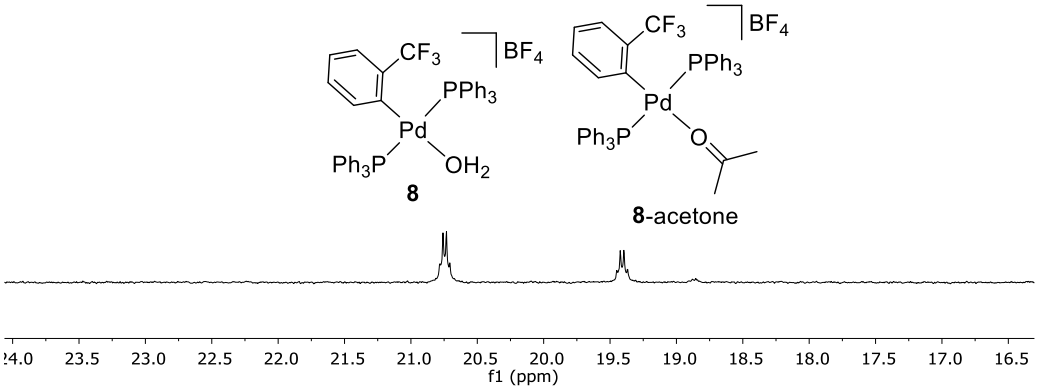

Figure S51. ^{31}P NMR (202.31 MHz, 243 K, CD_2Cl_2) of the organometallic species generated *in situ* from complex **7** and $AgBF_4$ in acetone (mol ratio $AgBF_4$:**7** = 1.5:1).

No signals for the self-condensation product of the acetone ($MeCOCH_2C(OH)Me_2$) were detected in the ^1H NMR, as we distinguished previously for complex **1**. The two complexes detected are assigned to complex **8** and a derivative of complex **8** where the molecule of water is substituted by a molecule of acetone (**8**-ac.). The formation of this similar mixture is confirmed dissolving complex **8** in 2 mL of dry acetone. After the evaporation of the acetone, the residue was redissolved in 0.6 mL of dry CD_2Cl_2 and the mixture was analyzed by NMR spectroscopy at 243 K giving the same mixture (Figures S52-S53).

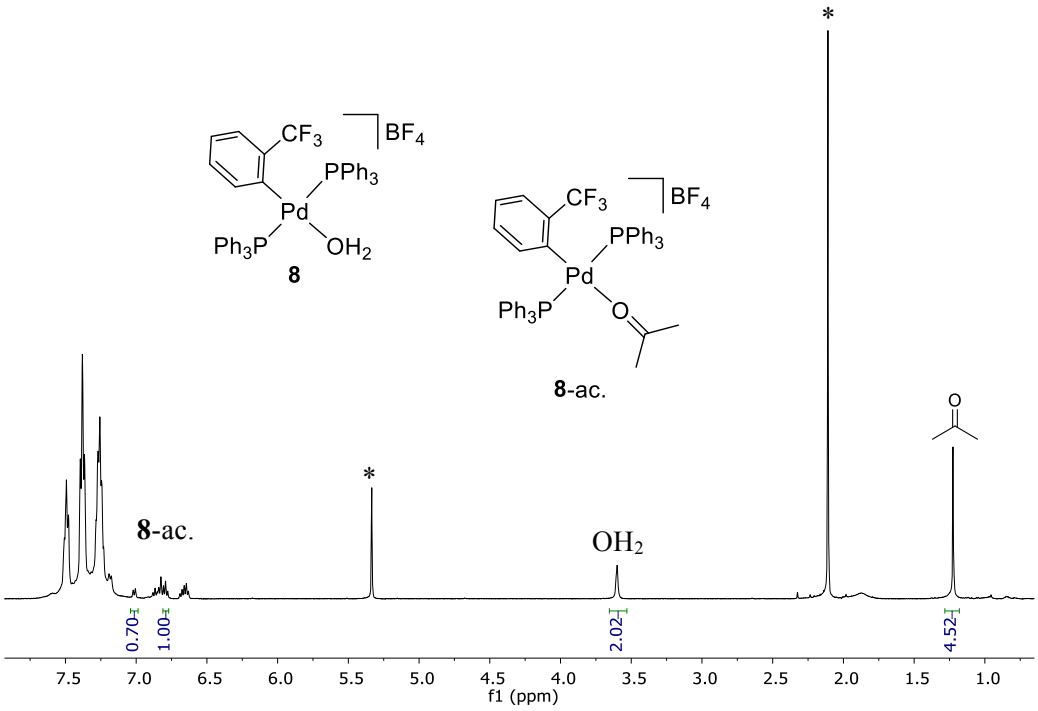

Figure S52. ^1H NMR (499.73 MHz, 243 K, CD_2Cl_2) of the organometallic species formed by dissolving **8** in dry acetone. *Signal corresponding to CH_2Cl_2 and free acetone.

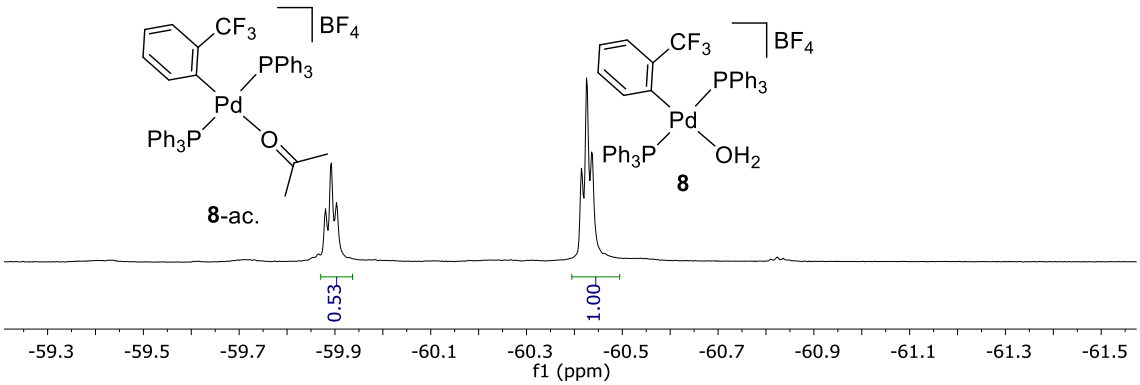

Figure S53. ^{19}F NMR (376.498 MHz, 243 K, CD_2Cl_2) of the organometallic species formed by dissolving **8** in dry acetone (mol % **8** = 65%; mol % **8**-ac = 35%).

1.6- General procedure for the polymerization experiments with norbornene

1.6.1. VA-polymerization of NB with a mixture of complex **1** and $AgBF_4$ (mol ratio $AgBF_4$: **1** = 1.25:1) prepared in CH_2Cl_2/toluene.

In an oven-dried vial $AgBF_4$ (0.035 mmol, 6.8 mg) was dissolved in 2 mL of dry toluene under N_2. Complex **1** (0.0281 mmol, 22.7 mg) dissolved in 1 mL of dry CH_2Cl_2 was added. Instantly, a white solid (AgBr) appeared and the suspension was stirred for 10 min at room temperature. The white solid was removed employing a 0.2 μm PTFE filter and the yellow solution was transferred to a Schlenk tube. The solution was evaporated to dryness and the residue was redissolved in 6.5 mL of dry CH_2Cl_2 and then a solution of NB in CH_2Cl_2 was added (0.55 mL, 2.107 mmol; 3.8 M, $[NB]_0$ = 0.3 M). A white solid appeared and the suspension was stirred for 24 h at 25 ºC. MeOH (10 mL) was added to the suspension inducing the complete precipitation of the polymer and the suspension was stirred for 30 min at room temperature. The white solid was filtered off, washed with MeOH (2 x 10 mL) and Et_2O (5 mL) and air-dried (0.18 g, 91 % yield).[7] ^1H NMR (499.73 MHz, δ, $CDCl_3$): 2.5-2 (b, H^1, H^4), 2-0.61 (b, H^7, H^6, H^5, H^3, H^2). $^{13}C\{^1H\}$ NMR (125.67 MHz, δ, $CDCl_3$): 55-50 (C^3, C^2), 48-38 (C^4, C^1), 37-35 (C^7), 32.5-28 (C^6, C^5). ^{19}F NMR (470.17 MHz, δ, $CDCl_3$): -58 (VA-PNB-(*o*-CF_3-C_6H_4).*
The polymer is insoluble and its molecular weight could not be determined.
* The presence of a fluorine signal indicates that the polymerization initiates by insertion of norbornene into the Ni-Ar bond.

1.6.2. Test polymerization of norbornene with the mixture $AgBF_4$/2PPh_3

In an oven-dried vial was placed the $AgBF_4$ (4.1 mg, 0.021 mmol). The solid was suspended in 4 mL of dry CH_2Cl_2 and PPh_3 (11 mg, 0.042 mmol) was added. After 5 min ofstirring, a colorless solution was formed. Subsequently, a solution of NB in CH_2Cl_2 was added (0.57 mL, 1.575 mmol; 3.8 M, $[NB]_o$ = 0.34 M). The solution was stirred for 24 h at 25 ºC. After this time, 10 mL of MeOH were added but no solid (polymer) appeared in the solution. The solution was evaporated to dryness and the residue was checked by NMR spectroscopy in $CDCl_3$. Neither oligomers nor dimers were detected in the residue.

1.6.3. VA-polymerization of NB with a mixture of complex **1** and $AgBF_4$ (mol ratio $AgBF_4$: **1** = 1.5:1) prepared in acetone.

In an oven-dried vial $AgBF_4$ (8 mg, 0.0408 mmol) was dissolved in 3 mL of dry acetone under N_2. The solution was cooled to 243 K for 10 min until constant temperature. Complex **1** (0.0247 mmol, 20 mg) was added to the mixture and instantly a white solid (AgBr) appeared. The suspension was stirred for 15 min at 243 K. The white solid was removed employing a 0.2 μm PTFE filter and the orange solution was transferred to an previously cooled Schlenk tube. The solution was evaporated to dryness and the residue was redissolved in 5.6 mL of dry CH_2Cl_2. Then, a solution of norbornene was added (0.48 mL, 1.85 mmol; 3.8 M, $[NB]_0$ = 0.3 M). The solution was stirred for 24 h at 25 ºC. MeOH (10 mL) was added to the suspension inducing the complete precipitation of the polymer and the suspension was stirred 30 min at room temperature. The white solid was filtered off and washed with MeOH (2 x 10 mL) and Et_2O (5 mL) and air-dried (0.1 g, 57.4% yield).[8] Ratio NB_{VA}/NB_{RO} = 7.5/1. M_w = 4200 Da; Đ = 1.3. ^{1}H NMR (499.73 MHz, δ, $CDCl_3$): 5.86-5.18 (b, $H^{3RO.int}$, $H^{3RO.term}$, $H^{2RO.int}$, $H^{2RO.term}$), 4.79, 4.68 ($H^{7RO.term}$), 3.28 (H^{3VA}), 2.5-1.55 (b, $H^{6RO.int}$, $H^{5RO.int}$, $H^{5RO.term}$, $H^{4RO.int}$, $H^{4RO.term}$, H^{4VA}, $H^{3'VA}$, H^{2VA}, H^{1VA}, $H^{1RO.int}$, $H^{1RO.term}$), 1.55-0.55 (b, H^{7VA}, H^{6VA}, H^{5VA}, $H^{7RO.int}$). ^{13}C{^{1}H} NMR (125.67 MHz, δ, $CDCl_3$): 152-148 ($C^{6RO.term}$), 134.6-126.6 ($C^{3RO.int}$, $C^{3RO.term}$, $C^{2RO.int}$, $C^{2RO.term}$), 108.2 ($C^{7RO.term}$), 54.3-36.8 ($C^{6RO.int}$, C^{4VA}, C^{3VA}, $C^{3'VA}$, C^{2VA}, C^{1VA}, $C^{1RO.int}$, $C^{1RO.term}$), 36.6-28.7 ($C^{7RO.int}$, C^{7VA}, C^{6VA}, C^{5VA}, $C^{5RO.term}$, $C^{4RO.term}$), 25.4-21 ($C^{5RO.int}$, $C^{4RO.int}$). ^{19}F NMR (499.73 MHz, δ, $CDCl_3$): -58 (VA/RO-PNB-(*o*-CF_3-C_6H_4).*

* The presence of a fluorine signal indicates that the polymerization initiates by insertion of norbornene into the Ni-Ar bond.

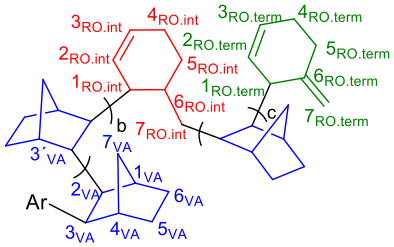

VA/RO-PNB

Ar = *o*-CF_3-C_6H_4

1.6.4. VA-polymerization of NB with complex **6**

Catalyst **6** (0.020 g, 0.0286 mmol) was dissolved in 6.8 mL of dry CH_2Cl_2 under N_2. Immediately, a solution of norbornene in CH_2Cl_2 (0.55 mL, 2.1 mmol; 3.8 M, $[NB]_0$ = 0.3 M) was added. The yellow solution was stirred for 24 h at 25 ºC. After this time, 20 mL of MeOH was added but no solid (polymer) appeared. The solution was evaporated to dryness and the yellow residue was dissolved in 1 mL of $CHCl_3$. A preparative TLC in silica gel using Et_2O as eluent was performed. The component with Rf ≈ 0.6 was extracted with 15 mL of CH_2Cl_2. The suspension was filtered off and the solution was evaporated to dryness. The residue was checked by NMR spectroscopy in $CDCl_3$. The spectroscopy data matches those of the dimer represented below and reported previously.[8,9]

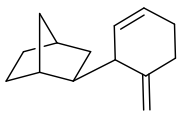

11

2. Data for X-Ray molecular structure determinations.

Crystals suitable for X-ray analyses were obtained by slow vapor-diffusion of pentane to a solution of complexes **2** and *cis-anti*-**4** in CH_2Cl_2, and complex **6** in $CHCl_3$ at 238 K. The crystals were mounted on the tip of glass fibers. X-ray measurements were made using an Agilent Supernova diffractometer with an Atlas CCD area detector. Data collection was performed with Mo Kα radiation (0.71073 Å). Data integration and empirical absorption correction was carried out using the CrysAlisPro program package.[10] The structures were solved by direct methods and refined by full-matrix least squares against F^2 with SHELX,[11] in OLEX2.[12] Non-hydrogen atoms were refined anisotropically and hydrogen atoms were constrained to ideal geometries and refined with fixed isotropic displacement parameters. Refinement proceeded smoothly to give the residuals shown in Table S1.

The crystal structures have been deposited in the CCDC database: CCDC 2220622-2220624.

Table S1. Crystal data and structure refinement parameters for complexes **2**, **4** and **6**.

Complex	**2**	*cis-anti*-**4**	**6**
Empirical formula	$C_{43}H_{36}BF_7NiOP_2$	$C_{50}H_{40}F_6Ni_2O_2P_2$	$C_{32}H_{30}BF_7NiOPS$
Formula weight	833.18	966.18	682.09
Temperature/K	298	298	298
Crystal system	monoclinic	triclinic	orthorhombic
Space group	P21/n	P-1	Pbcn
a/Å	14.9997(11)	13.0312(11)	16.7171(6)
b/Å	16.0731(9)	13.1540(13)	14.3676(6)
c/Å	17.9157(8)	14.7181(6)	37.0248(11)
α/°	90	81.840(5)	90
β/°	95.104(5)	86.385(5)	90
γ/°	90	63.640(9)	90
Volume/$Å^3$	4302.2(4)	2237.7(3)	8892.7(5)
Z	4	2	11
$\rho_{calc}g/cm^3$	1.286	1.377	1.401
μ/mm^{-1}	0.586	0.975	0.935
F(000)	1712	916	3808
Crystal size/mm^3	0.365 × 0.275 × 0.123	0.248 × 0.151 × 0.079	0.524 × 0.524 × 0.319
Radiation	Mo Kα (λ = 0.71073)	Mo Kα (λ = 0.71073)	Mo Kα (λ = 0.71073)
2Θ range for data collection/°	6.604 to 59.062	6.592 to 59.332	6.534 to 59.616

Index ranges	-17 ≤ h ≤ 19, -16 ≤ k ≤ 21, -24 ≤ l ≤ 18	-18 ≤ h ≤ 16, -13 ≤ k ≤ 16, -14 ≤ l ≤ 18	-15 ≤ h ≤ 22, -17 ≤ k ≤ 10, -50 ≤ l ≤ 35
Reflections collected	19444	19757	24643
Independent reflections	9976 [Rint = 0.0471, Rsigma = 0.1005]	10477 [Rint = 0.0501, Rsigma = 0.1094]	10307 [Rint = 0.0376, Rsigma = 0.0589]
Data/restraints/parameters	9976/1/553	10477/0/567	10307/0/473
Goodness-of-fit on F^2	1.028	1.036	1.033
Final R indexes [I>=2σ (I)]	R1 = 0.0833, wR2 = 0.1833	R1 = 0.0766, wR2 = 0.1771	R1 = 0.0896, wR2 = 0.2418
Final R indexes [all data]	R1 = 0.1724, wR2 = 0.2250	R1 = 0.1539, wR2 = 0.2273	R1 = 0.1476, wR2 = 0.2851
Largest diff. peak/hole / e $Å^{-3}$	0.868/-0.401	0.658/-0.415	0.681/-0.690

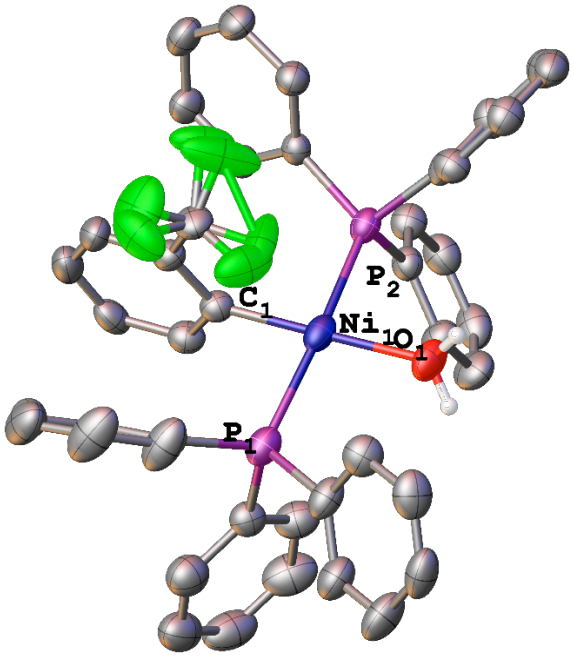

Figure S54. Molecular structure of complex **2** (ORTEP 30% probability ellipsoids). Hydrogen atoms and BF_4^- were omitted for clarity.

Table S2. Selected bond distances (Å) and angles (º) for complex **2**.

Ni1-P1	2.3231(19)	P1-Ni1-P2	169.18(6)
Ni1-P2	2.3687(17)	O1-Ni1-P1	95.31(14)
Ni1-O1	1.987(4)	C1-Ni1-P1	85.62(16)
Ni1-C1	1.881(5)		

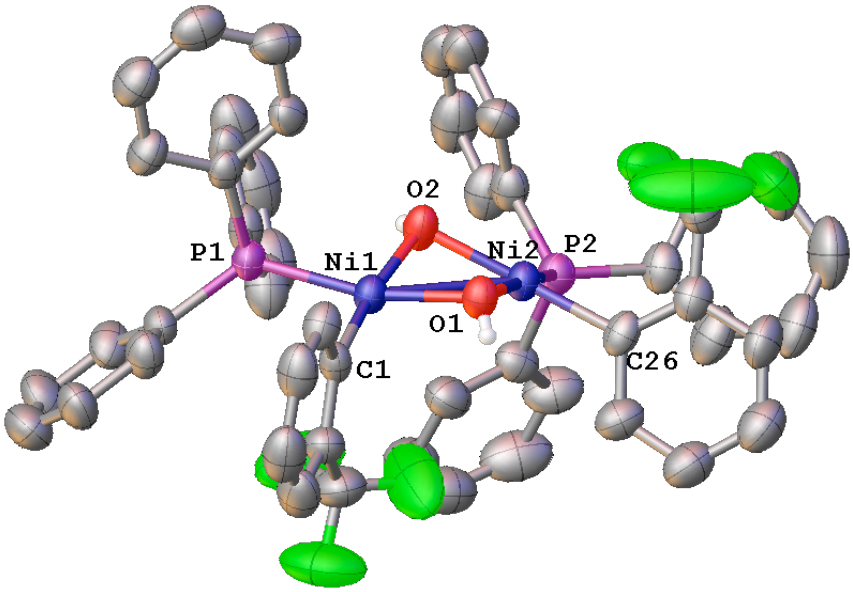

Figure S55. Molecular structure of complex 4 (ORTEP 30% probability ellipsoids). Hydrogen atoms (except those for the OH groups) were omitted for clarity.

Table S3. Selected bond distances (Å) and angles (º) for complex **4**.

Ni1-P1	2.1478(16)	P1-Ni1-O2	95.18(14)
Ni1-C1	1.894(5)	P1-Ni1-C1	92.63(16)
Ni1-O1	1.885(4)	C1-Ni1-O1	94.2(2)
Ni1-O2	1.909(4)	Ni1-O2-Ni2	94.2(2)
Ni2-P2	2.1489(16)	Ni1-O1-Ni2	92.23(19)
Ni2-C26	1.898(5)	P2-Ni2-O2	98.00(15)
Ni2-O1	1.879(4)	P2-Ni2-C26	91.25(16)
Ni2-O2	1.917(4)	C26-Ni2-O1	93.2(2)

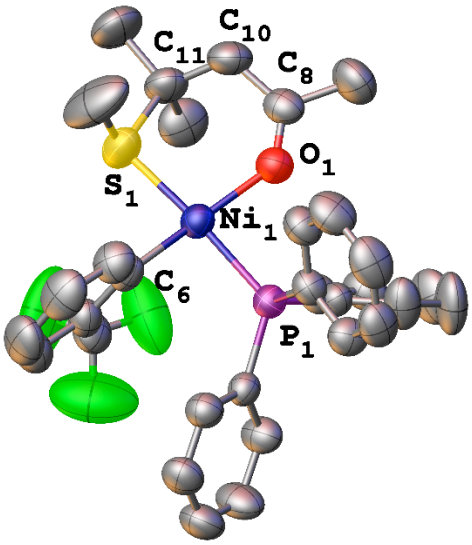

Figure S56. Molecular structure of complex **6** (ORTEP 30% probability ellipsoids). Hydrogen atoms and BF_4^- were omitted for clarity.

Table S4. Selected bond distances (Å) and angles (º) for complex **6**.

Ni1-S1	2.2041(17)	O1-Ni1-P1	87.47(12)
Ni1-O1	1.944(4)	S1-Ni1-C1	87.99(16)
Ni1-C1	1.891(5)	C1-Ni1-P1	90.16(16)
O1-C8	1.226(7)	S1-Ni1-O1	95.22(12)
S1-C11	1.842(6)		
C8-C10	1.468(9)		
C10-C11	1.537(10)		

3. *Selected NMR spectra of nickel(II) complexes*

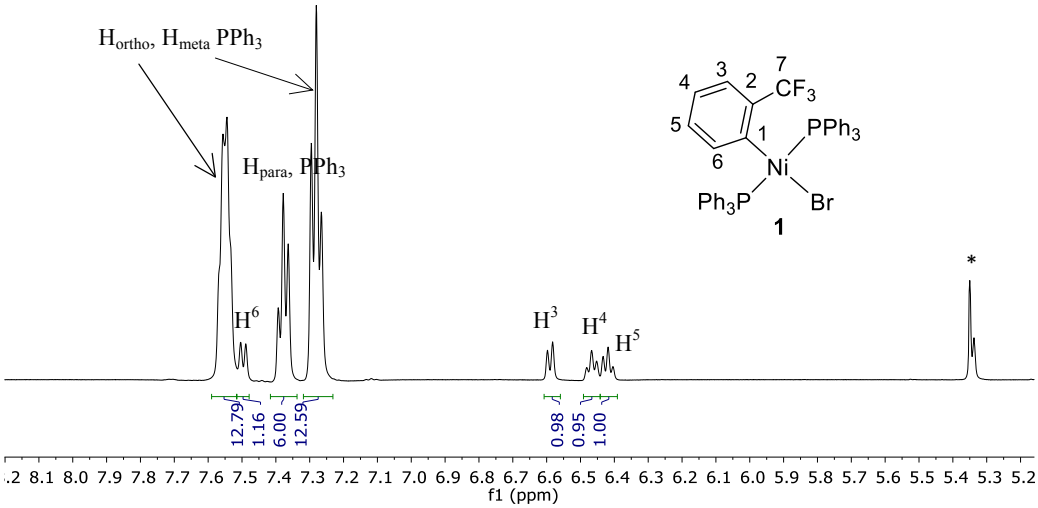

Figure S57. ^{1}H NMR (499.73 MHz, CD_2Cl_2) of complex [Ni(*o*-CF_3-C_6H_4)Br(PPh_3)$_2$] (**1**) at 298 K. *Signal corresponding to the solvent.

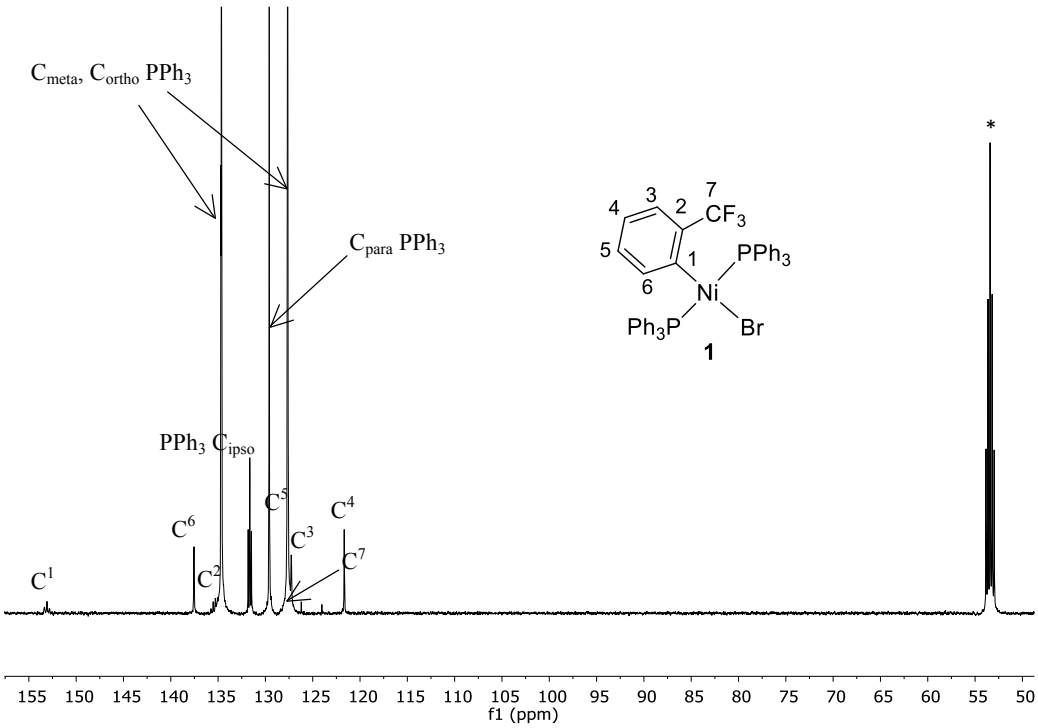

Figure S58. $^{13}C\{^1H\}$ NMR (125.67 MHz, CD_2Cl_2) of complex [Ni(*o*-CF_3-C_6H_4)Br(PPh_3)$_2$] (**1**) at 298 K. *Signal corresponding to the solvent.

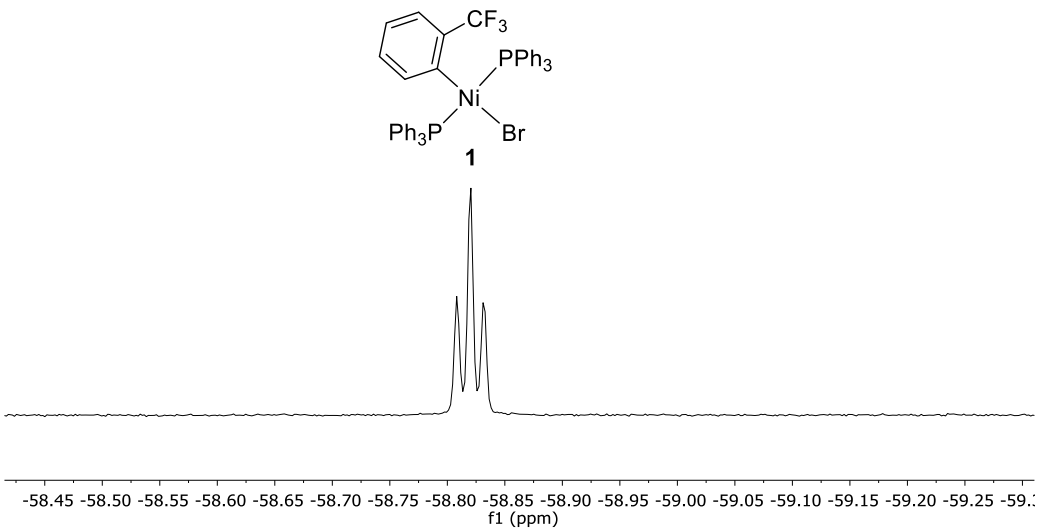

Figure S59. ^{19}F NMR (470.17 MHz, $CDCl_3$) of complex [Ni(*o*-CF_3-C_6H_4)Br(PPh_3)$_2$] (**1**) at 298 K.

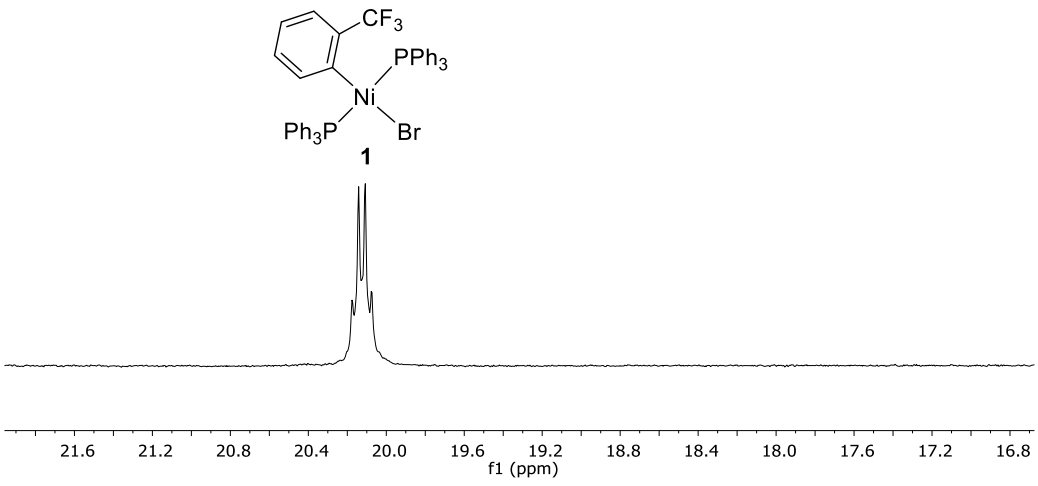

Figure S60. $^{31}P\{^1H\}$ NMR (202.31 MHz, $CDCl_3$) of complex [Ni(*o*-CF_3-C_6H_4)Br(PPh_3)$_2$] (**1**) at 298 K.

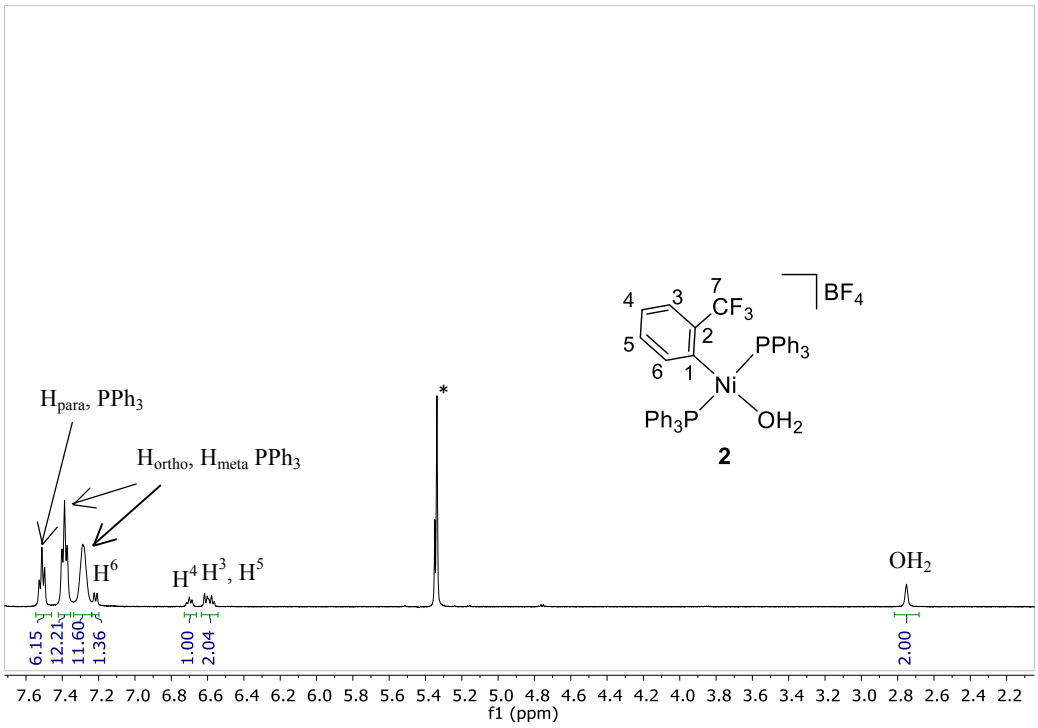

Figure S61. ^{1}H NMR (499.73 MHz, CD_2Cl_2) of complex [Ni(*o*-CF_3-C_6H_4)(OH_2)(PPh_3)$_2$](BF_4) (**2**) at 243 K.*Signal corresponding to the solvent.

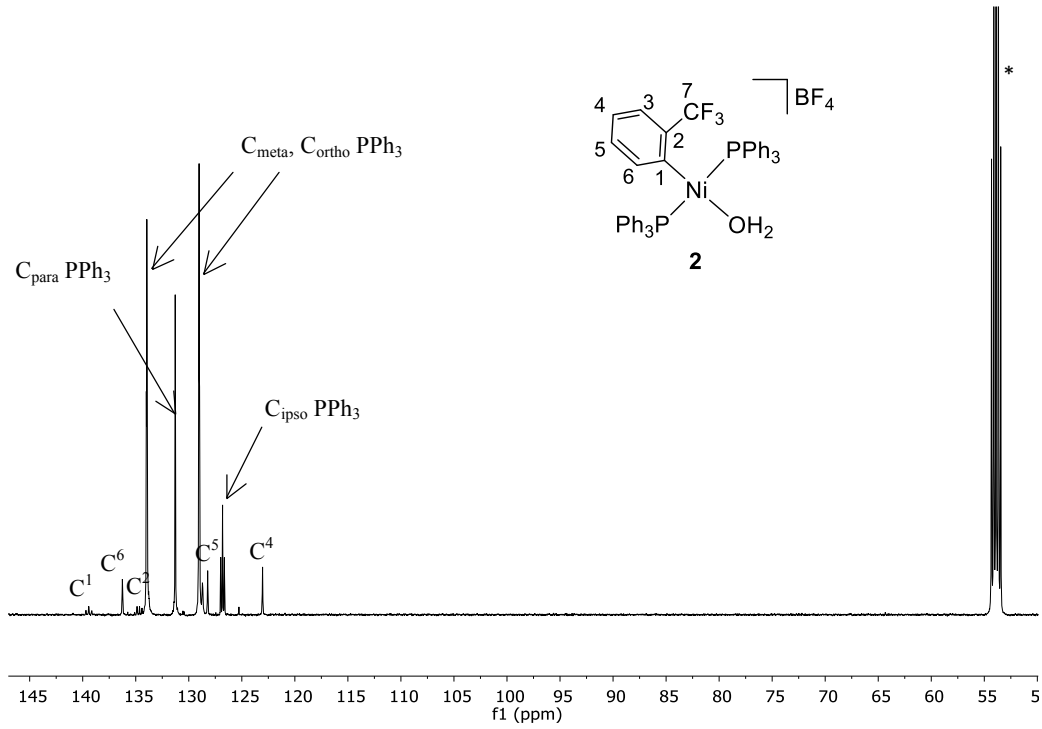

Figure S62. $^{13}C\{^1H\}$ NMR (125.67 MHz, CD_2Cl_2) of complex [Ni(*o*-CF_3-C_6H_4)(OH_2)(PPh_3)$_2$](BF_4) (**2**) at 243 K. *Signal corresponding to the solvent.

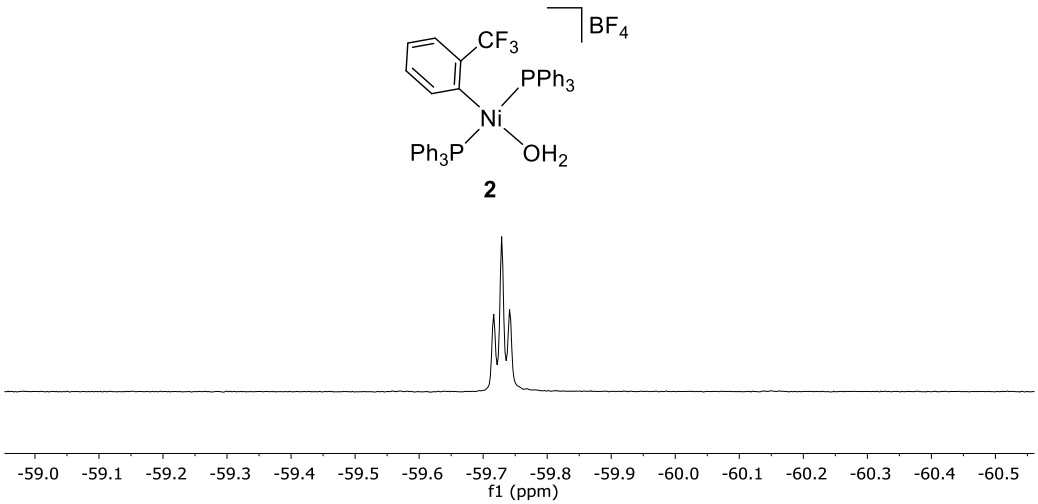

Figure S63. ^{19}F NMR (470.17 MHz, 243 K, CD_2Cl_2) of complex [Ni(*o*-CF_3-C_6H_4)(OH_2)(PPh_3)$_2$](BF_4) (**2**) at 243 K. Signal of BF_4 (-150.7) was omitted for clarity.

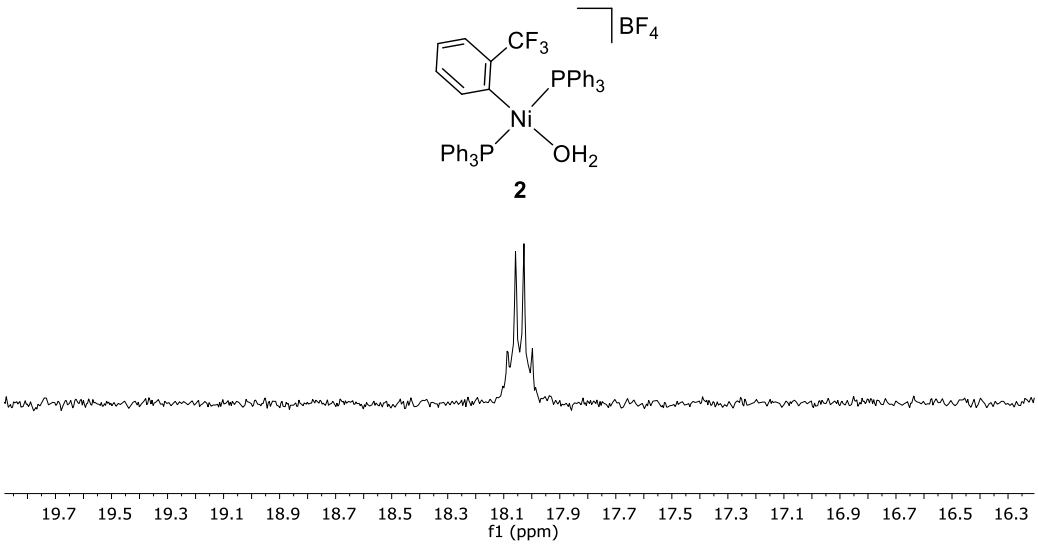

Figure S64. $^{31}P\{^1H\}$ NMR (202.31 MHz, dry CD_2Cl_2) of complex [Ni(*o*-CF_3-C_6H_4)(OH_2)(PPh_3)$_2$](BF_4) (**2**) at 243 K.

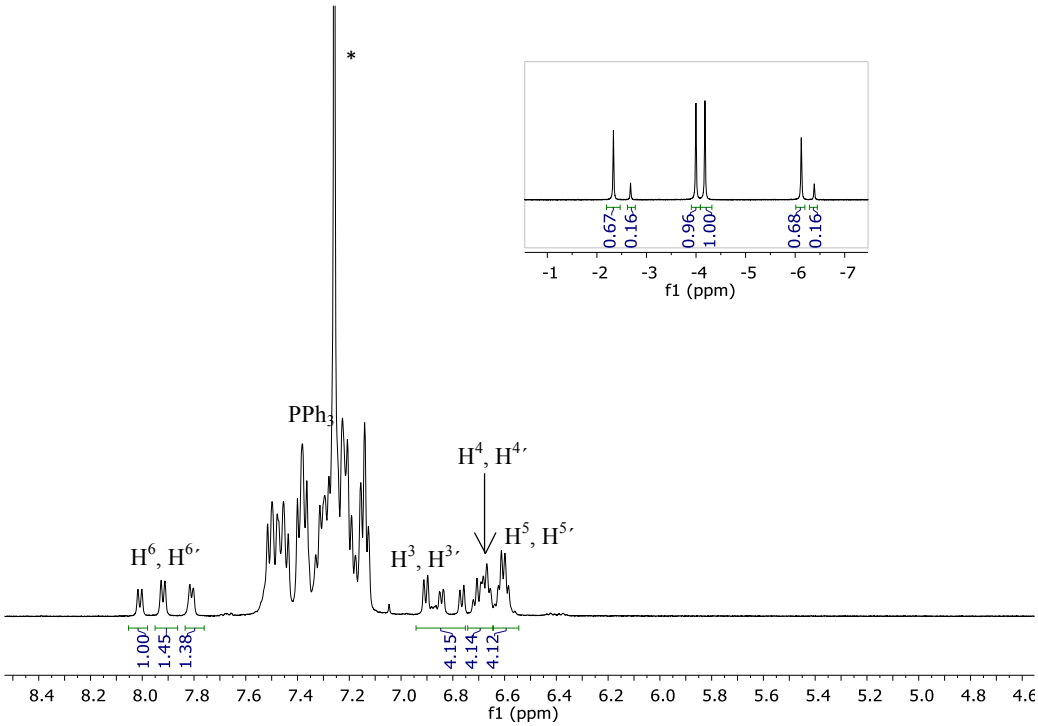

Figure S65. ^{1}H NMR (499.73 MHz, dry $CDCl_3$) for complex $[Ni(o\text{-}CF_3\text{-}C_6H_4)(\mu\text{-}OH)(PPh_3)]_2$ (**4**, mixture of isomers) at 298 K.* Signal corresponding to the solvent.

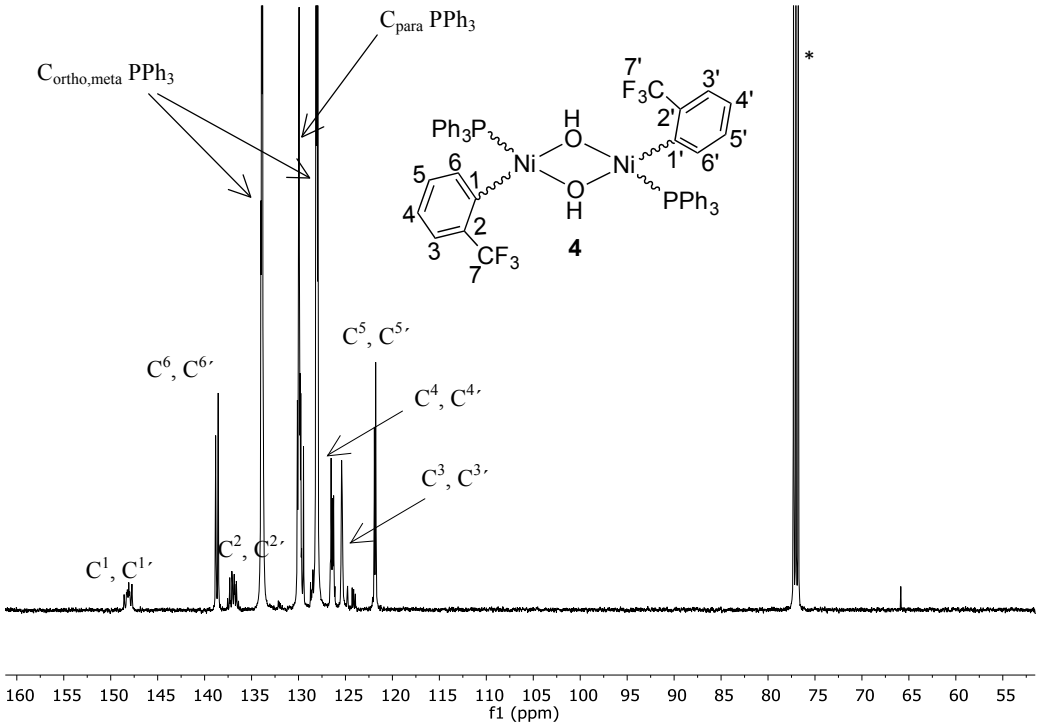

Figure S66. $^{13}C\{^{1}H\}$ NMR (125.67 MHz, dry $CDCl_3$) of complex $[Ni(o\text{-}CF_3\text{-}C_6H_4)(\mu\text{-}OH)(PPh_3)]_2$ (**4**, mixture of isomers) at 298 K.*Signal corresponding to the solvent.

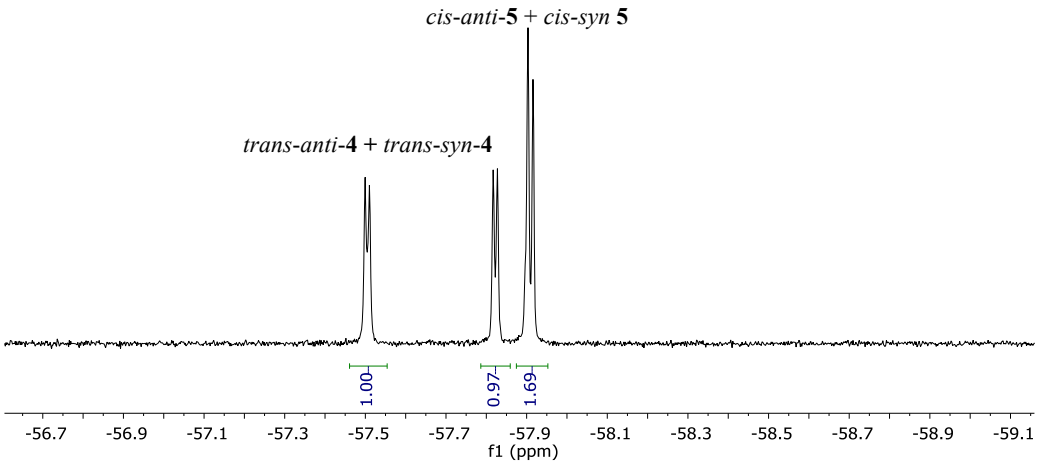

Figure S67. ^{19}F NMR (470.17 MHz, dry $CDCl_3$) of complex [Ni(*o*-CF_3-C_6H_4)(μ-OH)(PPh_3)]$_2$ (**4**, mixture of isomers) at 298 K.

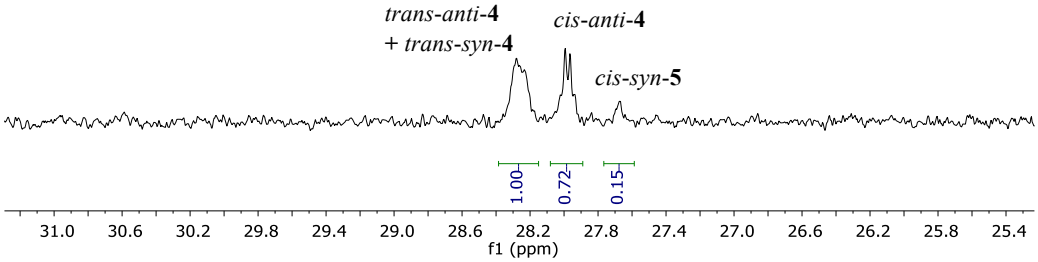

Figure S68. $^{31}P\{^1H\}$ NMR (202.31 MHz, dry $CDCl_3$) of complex [Ni(*o*-CF_3-C_6H_4)(μ-OH)(PPh_3)]$_2$ (**4**, mixture of isomers) at 298 K.

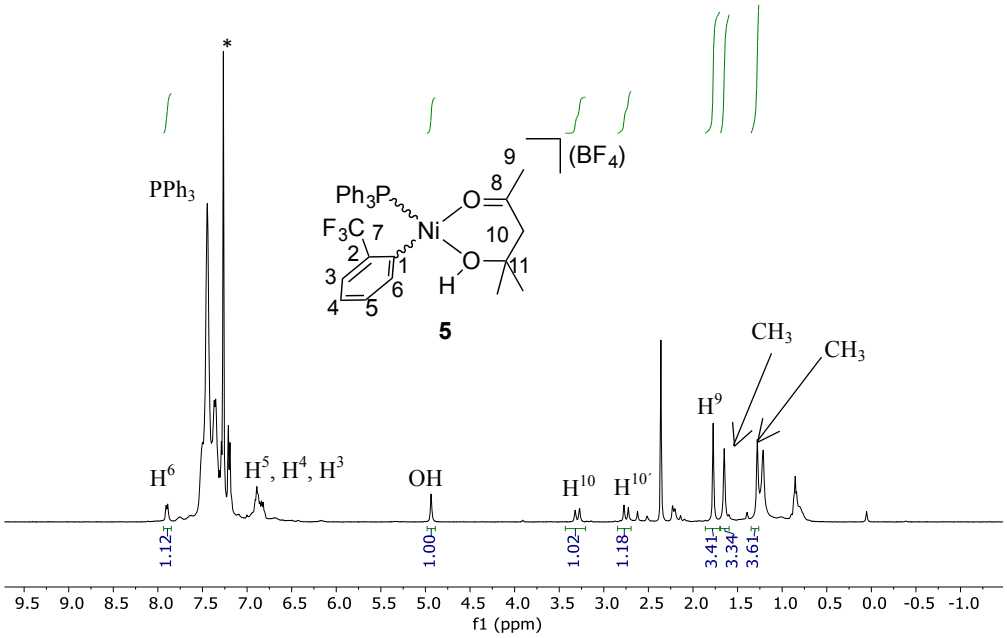

Figure S69. ^{1}H NMR (499.73 MHz, $CDCl_3$) of complex [Ni(*o*-CF_3-C_6H_4)(κ^2-O, O-MeC(O)CH_2C(OH)Me_2)-(PPh_3)](BF_4) (**5**) generated in situ from complex **1** and $AgBF_4$ at 243 K.*Signal corresponding to the solvent.

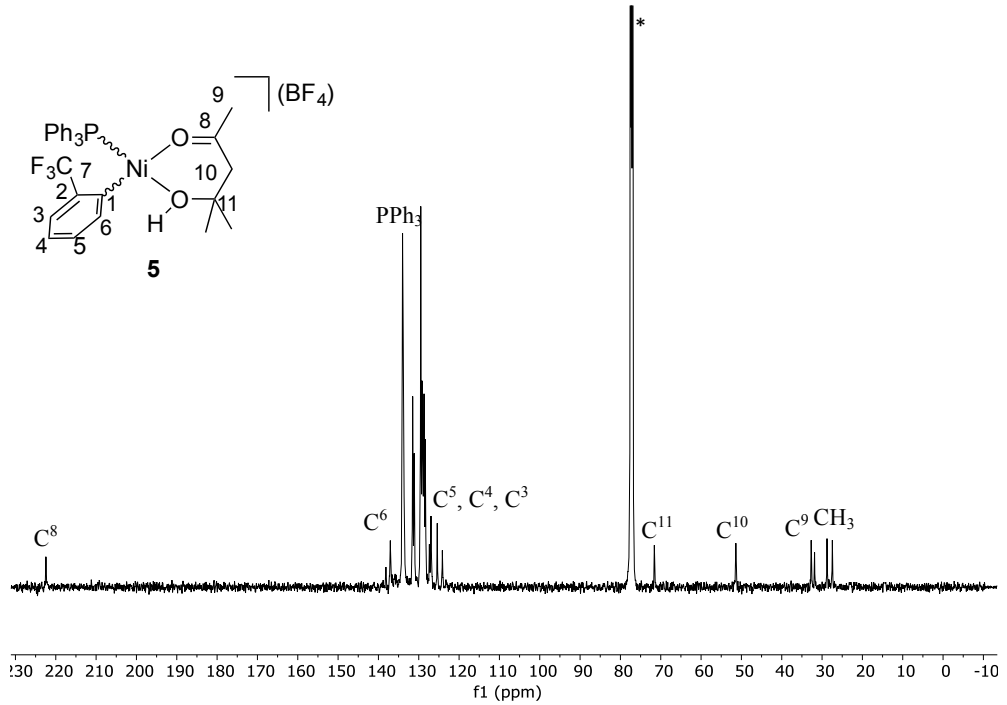

Figure S70 $^{13}C\{^{1}H\}$ NMR (125.67 MHz, $CDCl_3$) of complex [Ni(*o*-CF_3-C_6H_4)(κ^2-O, O-MeC(O)CH_2C(OH)Me_2)-(PPh_3)](BF_4) (**5**) generated in situ from complex **1** and $AgBF_4$ at 243 K. *Signal corresponding to the solvent.

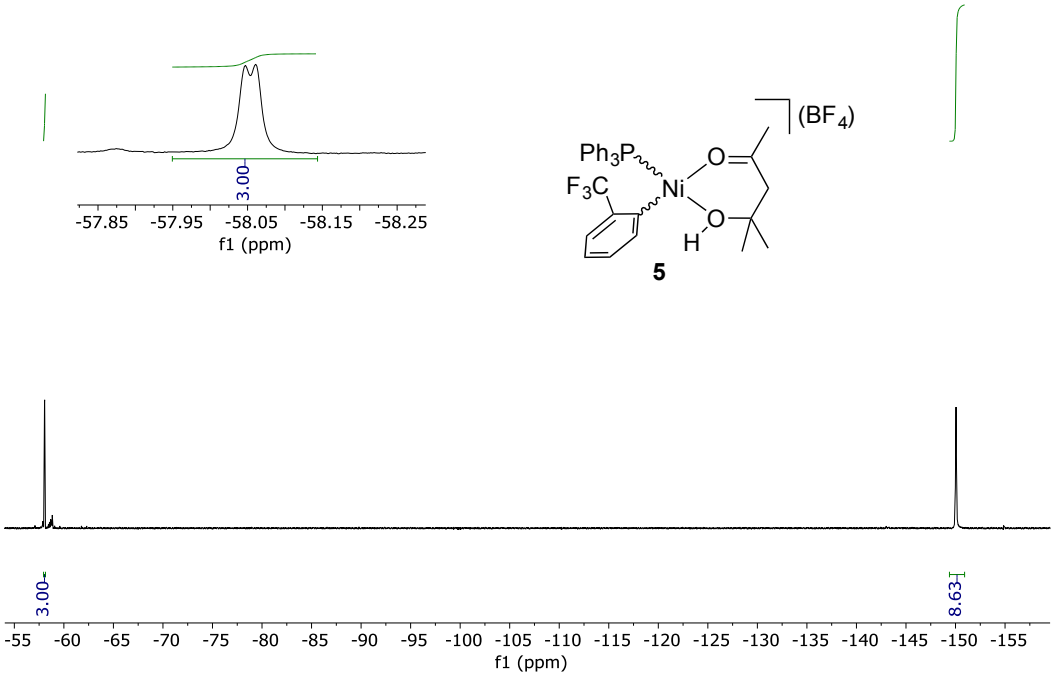

Figure S71. ^{19}F NMR (470.17 MHz, 243 K, $CDCl_3$) of complex[Ni(*o*-CF_3-C_6H_4)(κ^2-O, O-MeC(O)CH_2C(OH)Me_2)-(PPh_3)](BF_4) (**5**) generated in situ from complex **1** and $AgBF_4$ at 243 K.

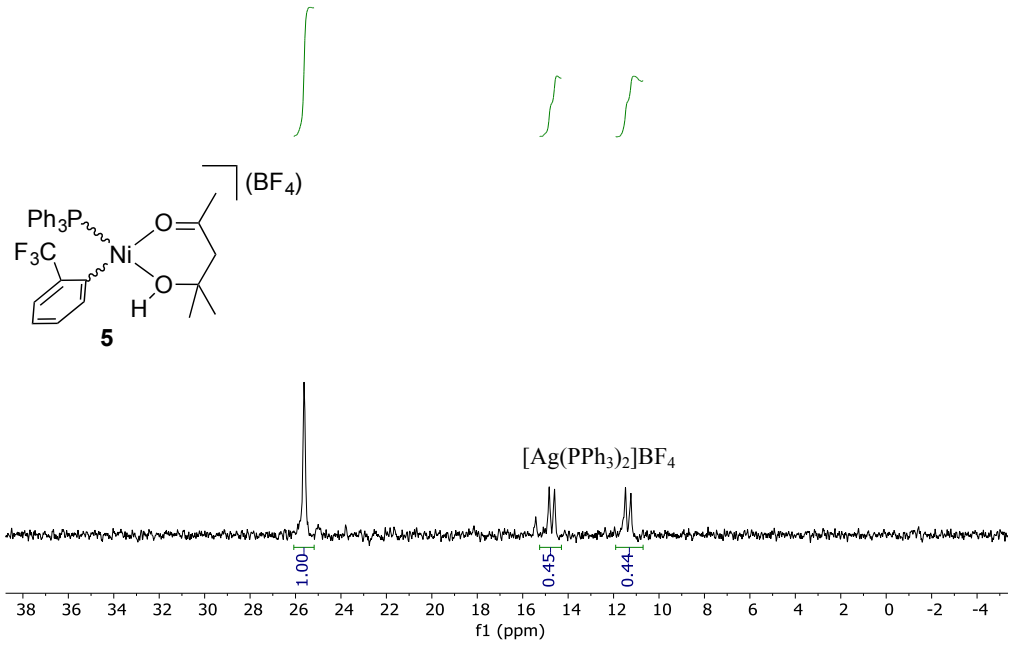

Figure S72. $^{31}P\{^1H\}$ NMR (202.31 MHz, $CDCl_3$) of complex [Ni(*o*-CF_3-C_6H_4)(κ^2-O, O-MeC(O)CH_2C(OH)Me_2)-(PPh_3)](BF_4) (**5**) generated in situ from complex **1** and $AgBF_4$ at 243 K.

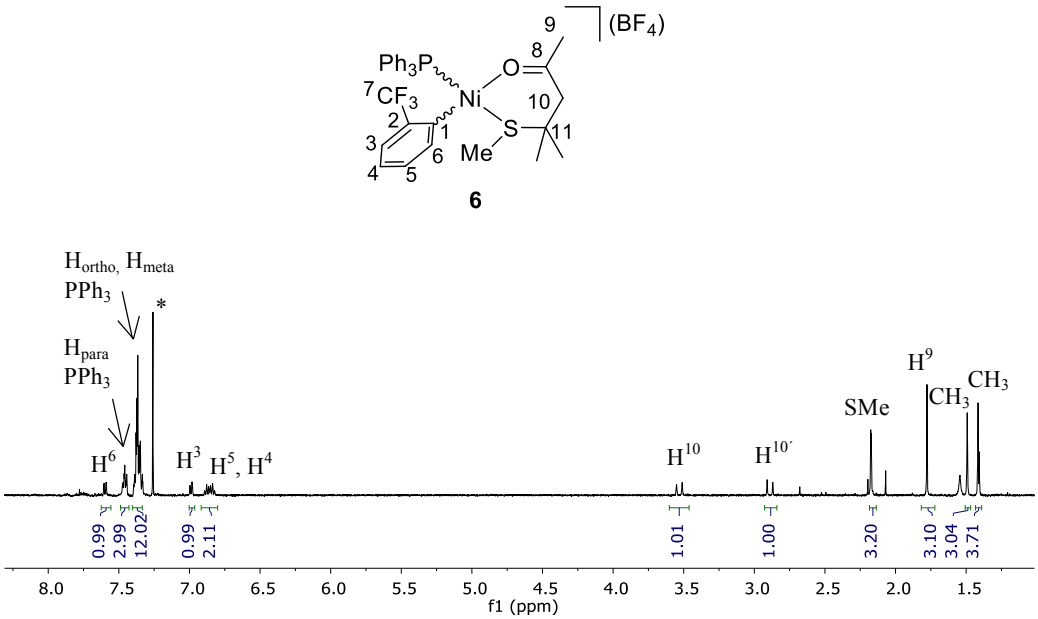

Figure S73. ^{1}H NMR (499.73 MHz, $CDCl_3$) of complex [Ni(-o-CF_3-C_6H_4)(κ^2-O, S-MeC(O)CH_2C(SMe)Me_2)(PPh_3)](BF_4) (**6**) at 298 K.*Signal corresponding to the solvent.

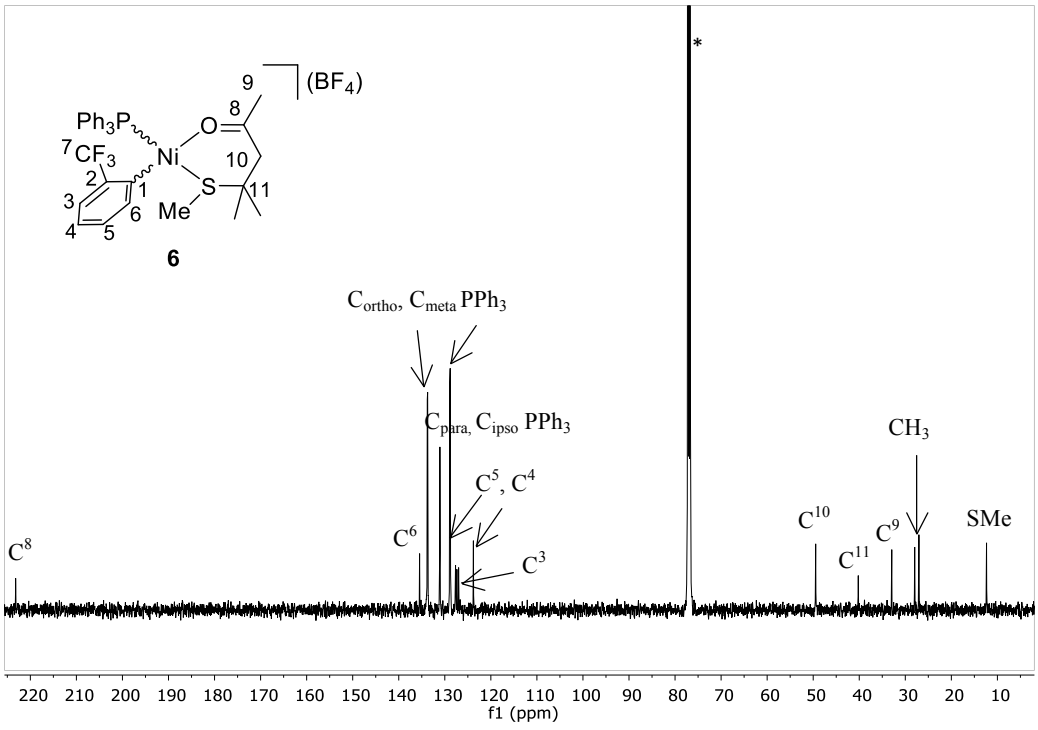

Figure S74. $^{13}C\{^{1}H\}$ NMR (125.67 MHz, $CDCl_3$) of complex [Ni(*o*-CF_3-C_6H_4)(κ^2-O, S-MeC(O)CH_2C(SMe)Me_2)(PPh_3)](BF_4) (**6**) at 298 K.*Signal corresponding to the solvent.

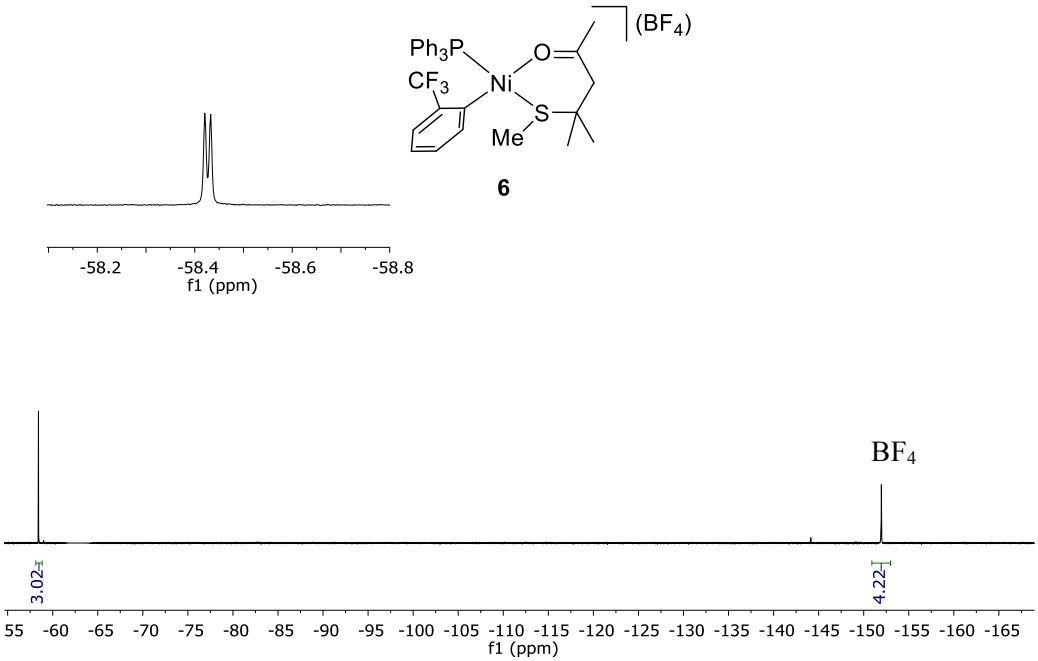

Figure S75. ^{19}F NMR (470.17 MHz, $CDCl_3$) of complex [Ni(*o*-CF_3-C_6H_4)(κ^2-O, S-MeC(O)CH_2C(SMe)Me_2)(PPh_3)](BF_4) (**6**) at 298 K.

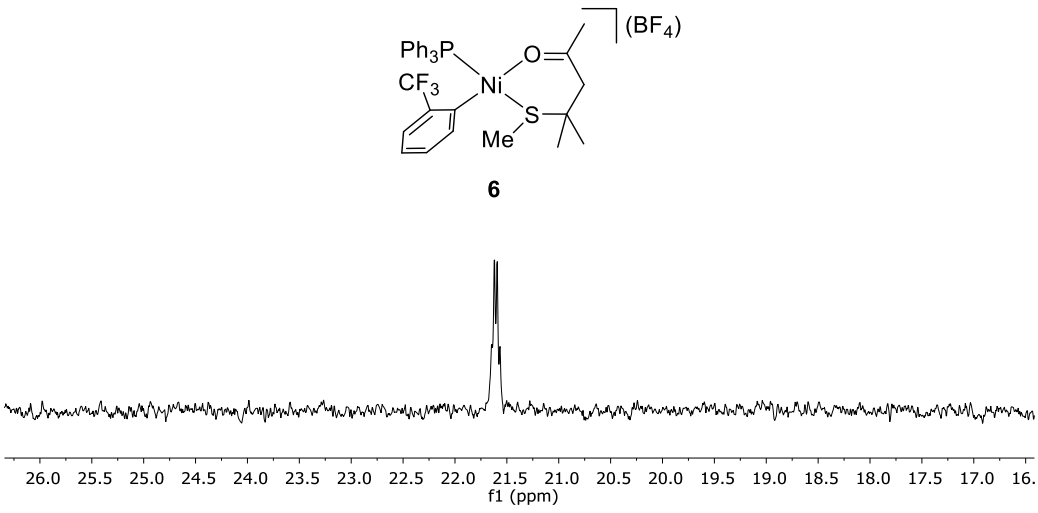

Figure S76. $^{31}P\{^1H\}$ NMR (202.31 MHz, $CDCl_3$) of complex [Ni(*o*-CF_3-C_6H_4)(κ^2-O, S-MeC(O)CH_2C(SMe)Me_2)(PPh_3)](BF_4) (**6**) at 298 K.

4. Selected NMR spectra of palladium(II) complexes

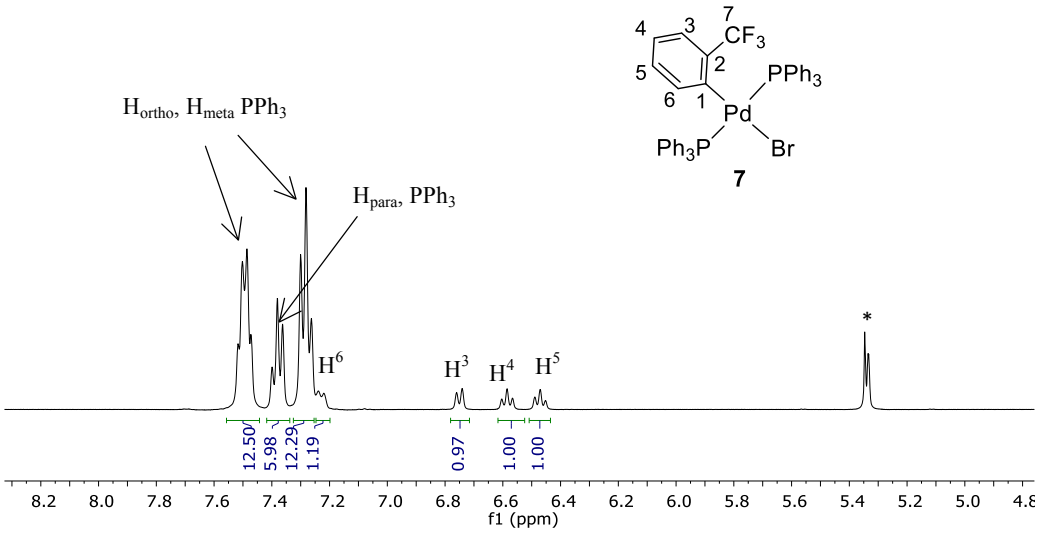

Figure S77. ^{1}H NMR (499.73 MHz, CD_2Cl_2) of complex [Pd(*o*-CF_3-C_6H_4)Br(PPh_3)$_2$] (**7**) at 298 K. *Signal corresponding to the solvent.

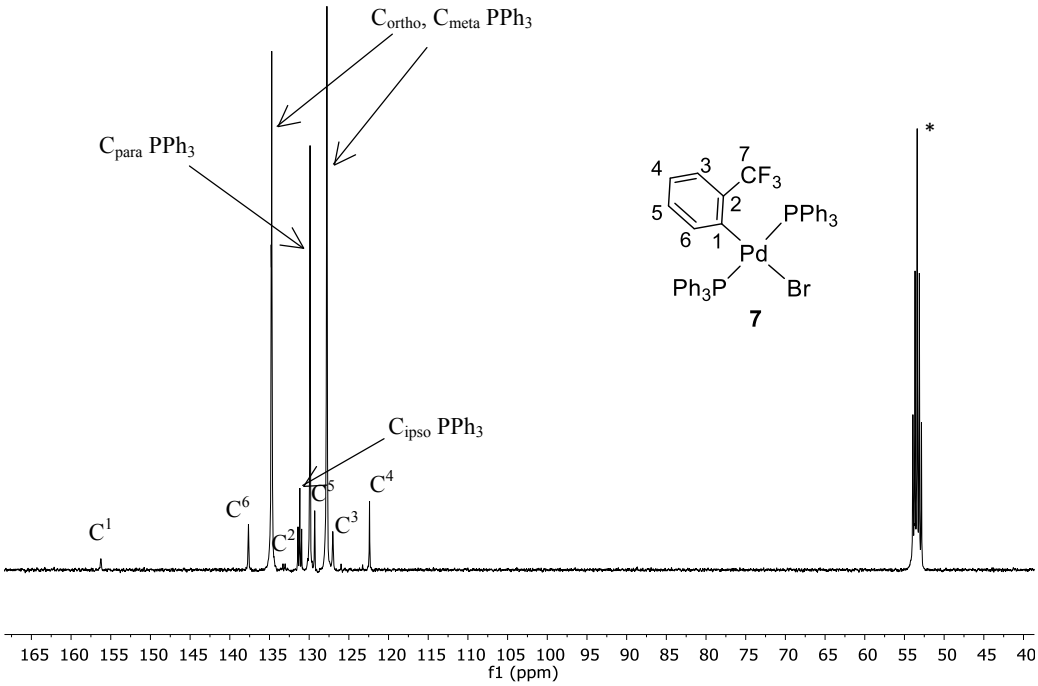

Figure S78. $^{13}C\{^1H\}$ NMR (125.67 MHz, CD_2Cl_2) of complex [Pd(*o*-CF_3-C_6H_4)Br(PPh_3)$_2$] (**7**) at 298 K. *Signal corresponding to the solvent.

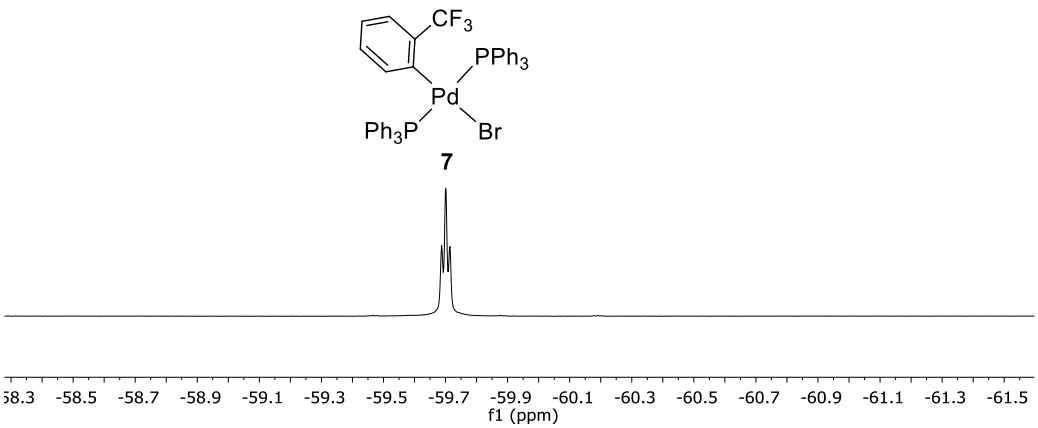

Figure S79. ^{19}F NMR (470.17 MHz, CD_2Cl_2) of complex [Pd(*o*-CF_3-C_6H_4)Br(PPh_3)$_2$] (**7**) at 298 K.

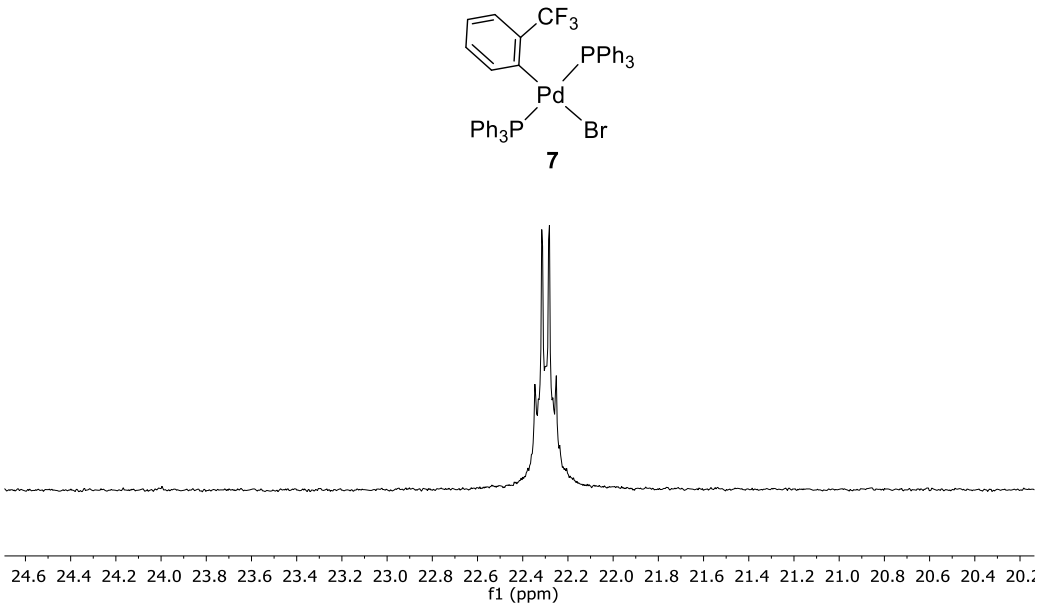

Figure S80. $^{31}P\{^1H\}$ NMR (202.31 MHz, CD_2Cl_2) of complex [Pd(*o*-CF_3-C_6H_4)Br(PPh_3)$_2$] (**7**) at 298 K.

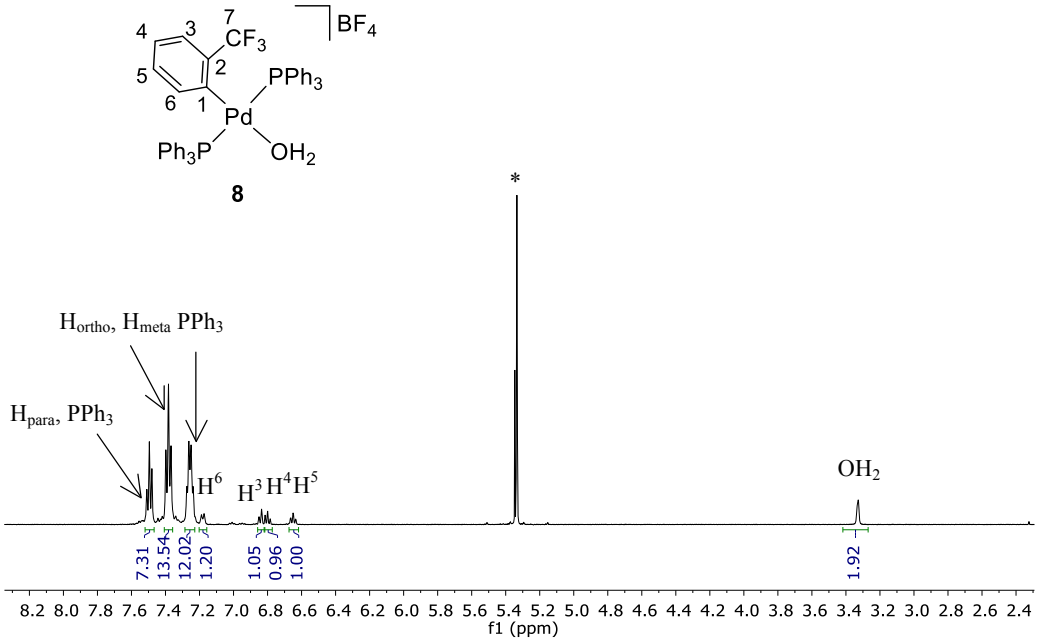

Figure S81. ^{1}H NMR (499.73 MHz, CD_2Cl_2) of complex [Pd(*o*-CF_3-C_6H_4)(OH_2)(PPh_3)$_2$] (**8**) at 243 K. *Signal corresponding to the solvent.

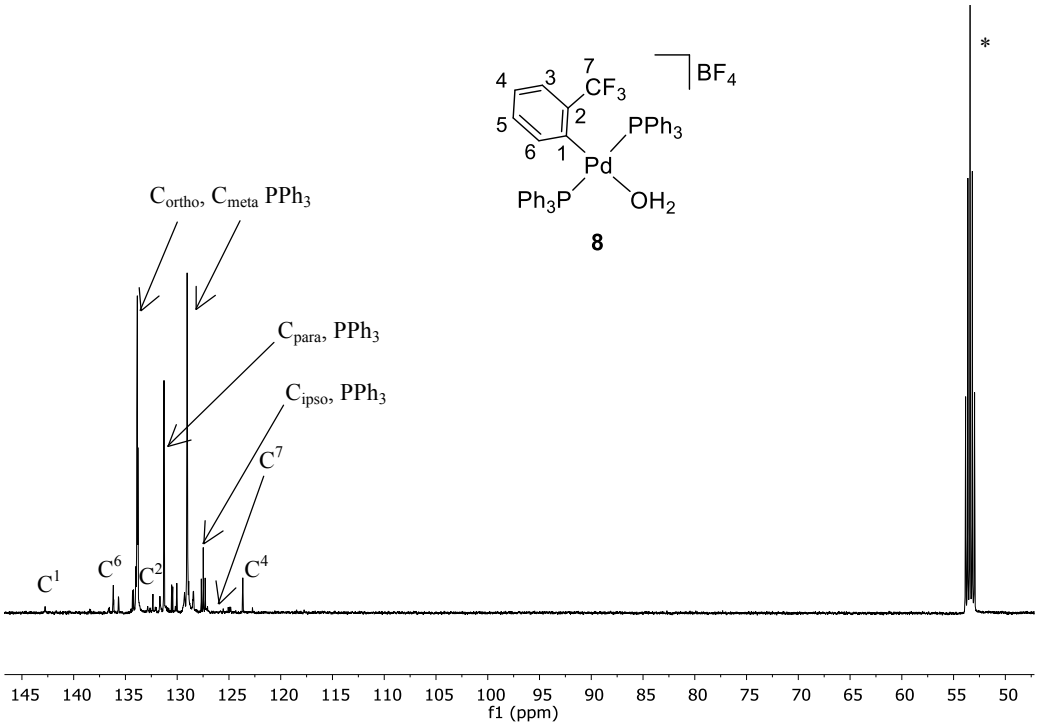

Figure S82. $^{13}C\{^{1}H\}$ NMR (125.67 MHz, CD_2Cl_2) of complex [Pd(*o*-CF_3-C_6H_4)(OH_2)(PPh_3)$_2$] (**8**) at 243 K. *Signal corresponding to the solvent.

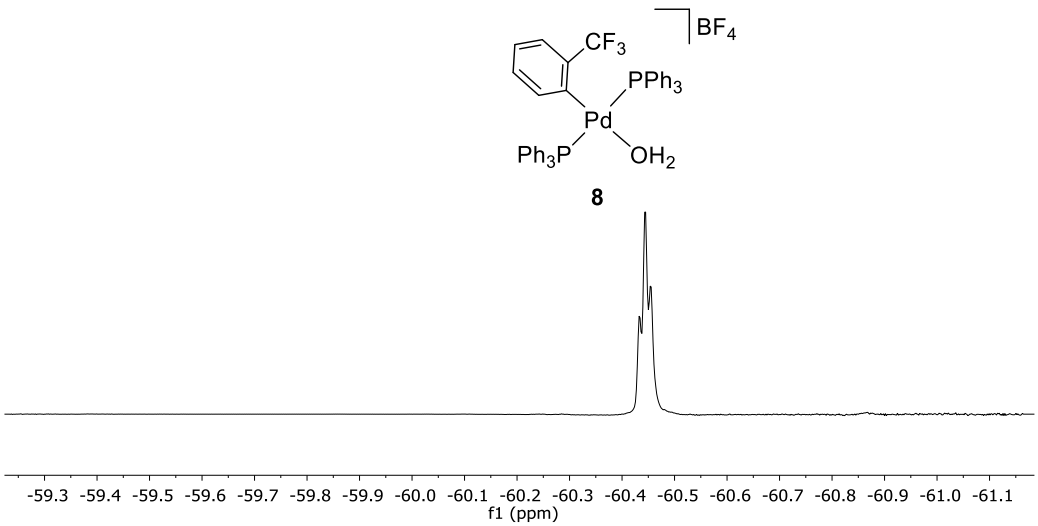

Figure S83. ^{19}F NMR (470.17 MHz, CD_2Cl_2) of complex [Pd(*o*-CF_3-C_6H_4)(OH_2)(PPh_3)$_2$] (**8**) at 243 K.

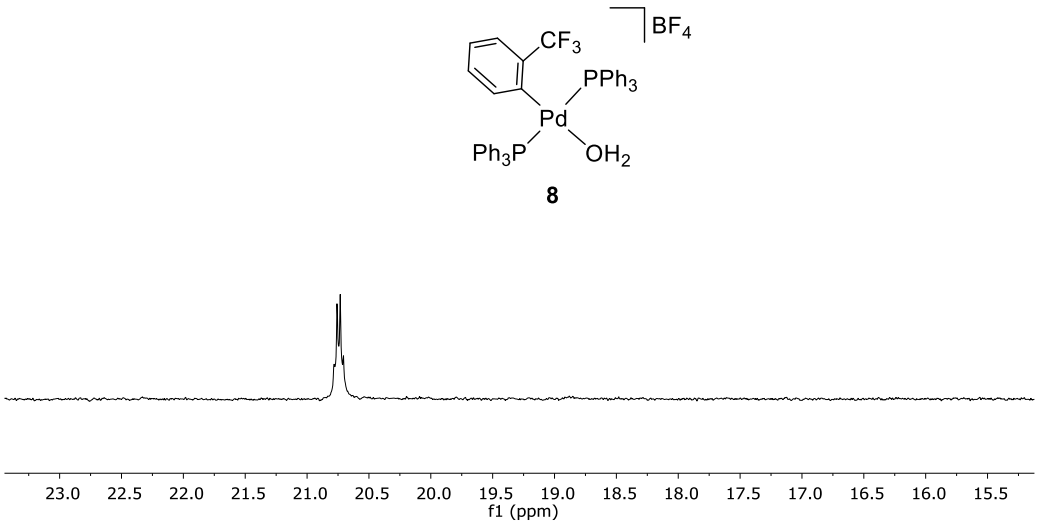

Figure S84. $^{31}P\{^1H\}$ NMR (202.31 MHz, CD_2Cl_2) of complex [Pd(*o*-CF_3-C_6H_4)(OH_2)(PPh_3)$_2$] (**8**) at 243 K.

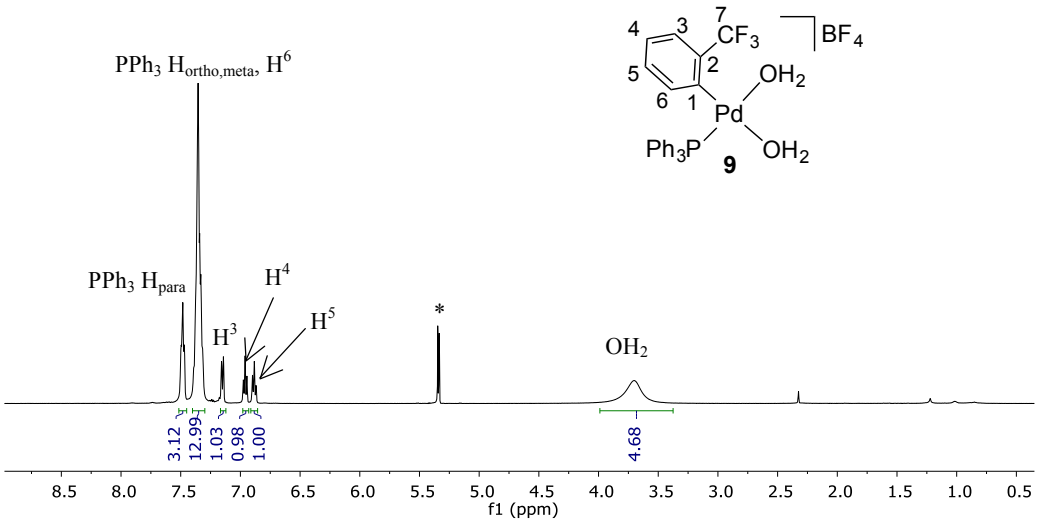

Figure S85. ^{1}H NMR (499.73 MHz, CD_2Cl_2) of complex [Pd(*o*-CF_3-C_6H_4)$(OH_2)_2(PPh_3)$] (**9**) at 243 K. *Signal corresponding to the solvent.

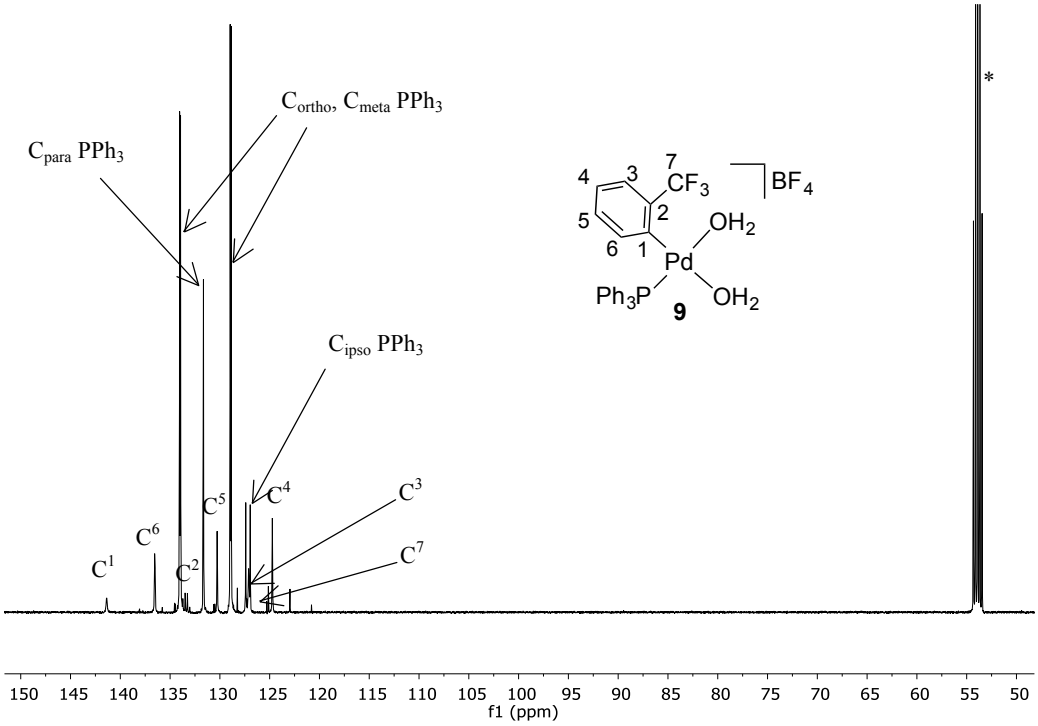

Figure S86. $^{13}C\{^{1}H\}$ NMR (125.67 MHz, CD_2Cl_2) for complex [Pd(*o*-CF_3-C_6H_4)$(OH_2)_2(PPh_3)$] (**9**) at 243 K. *Signal corresponding to the solvent.

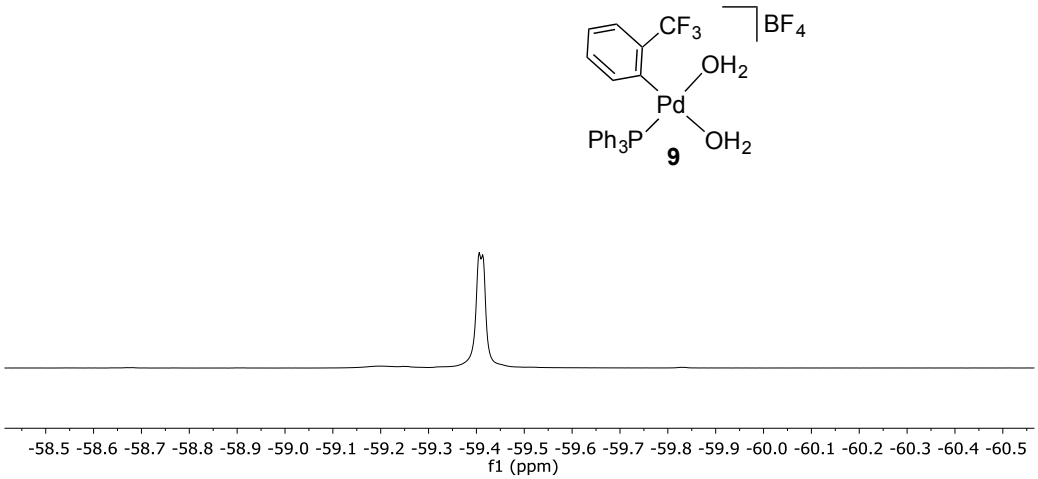

Figure S87. ^{19}F NMR (470.17 MHz, CD_2Cl_2) of complex [Pd(*o*-CF_3-C_6H_4)$(OH_2)_2(PPh_3)$] (**9**) at 243 K. The signal corresponding to BF_4^- (-149.04 ppm) was omitted to clarity.

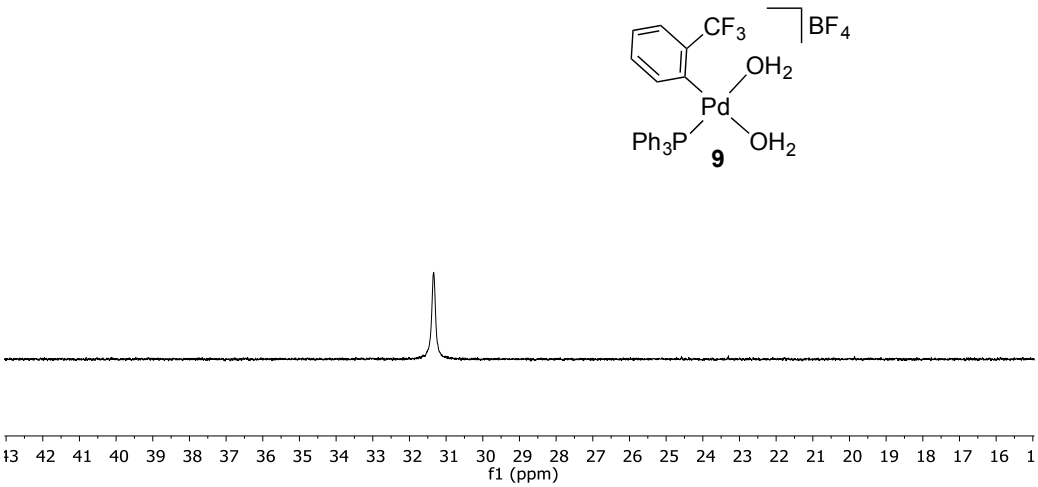

Figure S88. $^{31}P\{^1H\}$ NMR (202.31 MHz, CD_2Cl_2) of complex [Pd(*o*-CF_3-C_6H_4)$(OH_2)_2(PPh_3)$] (**9**) at 243 K.

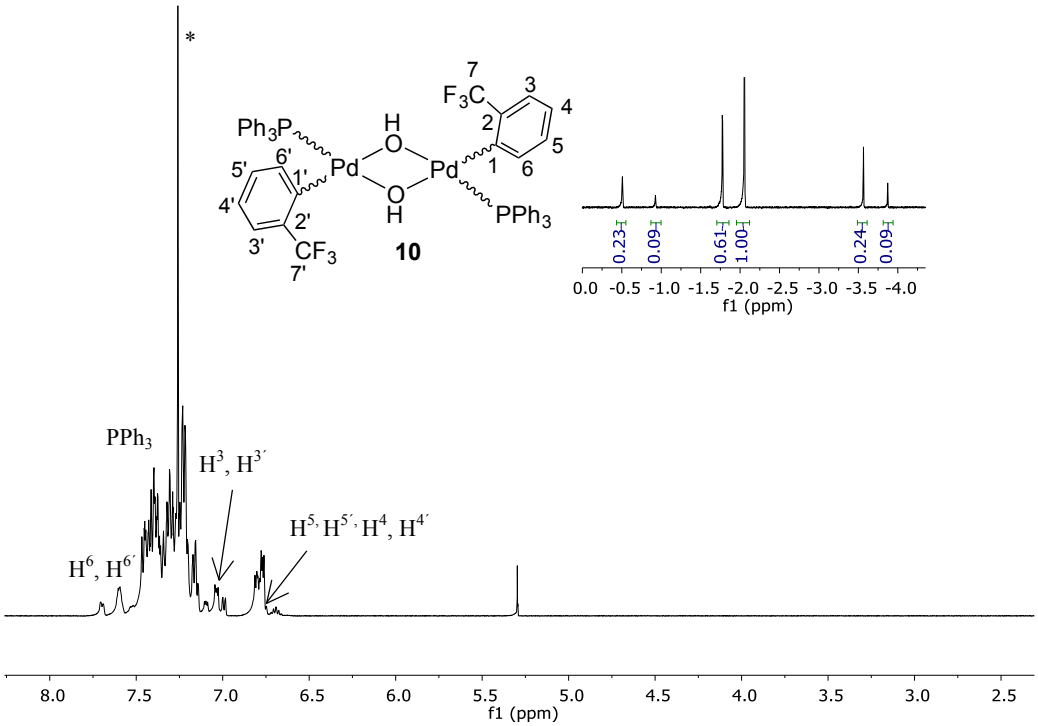

Figure S89. ^{1}H NMR (499.73 MHz, $CDCl_3$) of complex [Pd(*o*-CF_3-C_6H_4)(μ-OH)(PPh_3)]$_2$ (**10**, mixture of isomers) at 298 K. *Signal corresponding to the solvent.

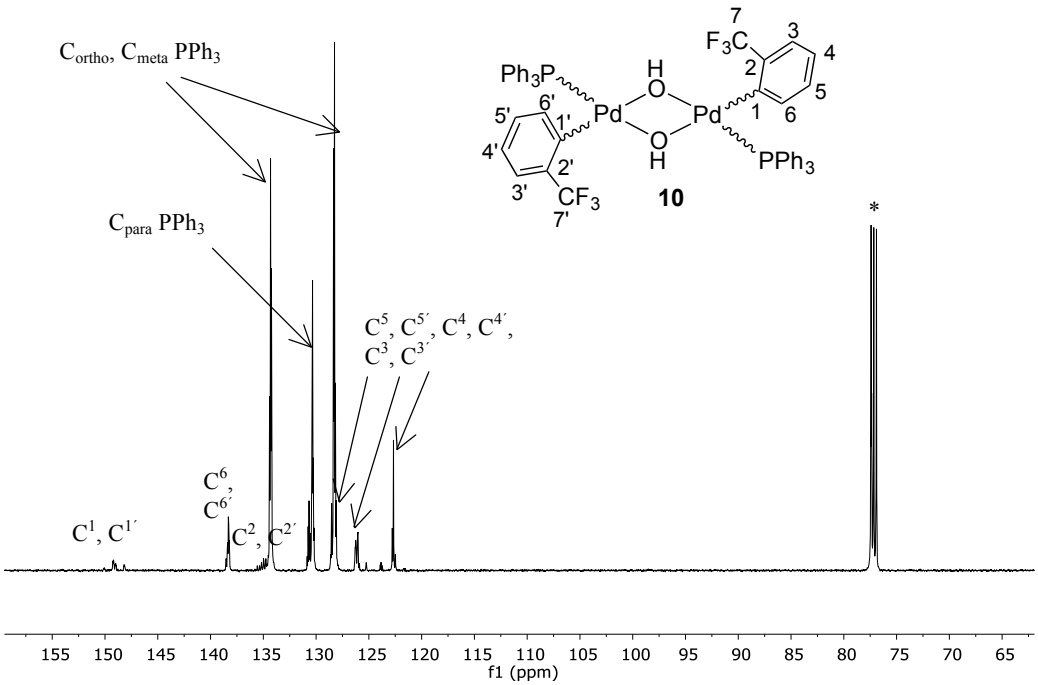

Figure S90. $^{13}C\{^{1}H\}$ NMR (125.67 MHz, $CDCl_3$) of complex [Pd(*o*-CF_3-C_6H_4)(μ-OH)(PPh_3)]$_2$ (**10**, mixture of isomers) at 298 K. *Signal corresponding to the solvent.

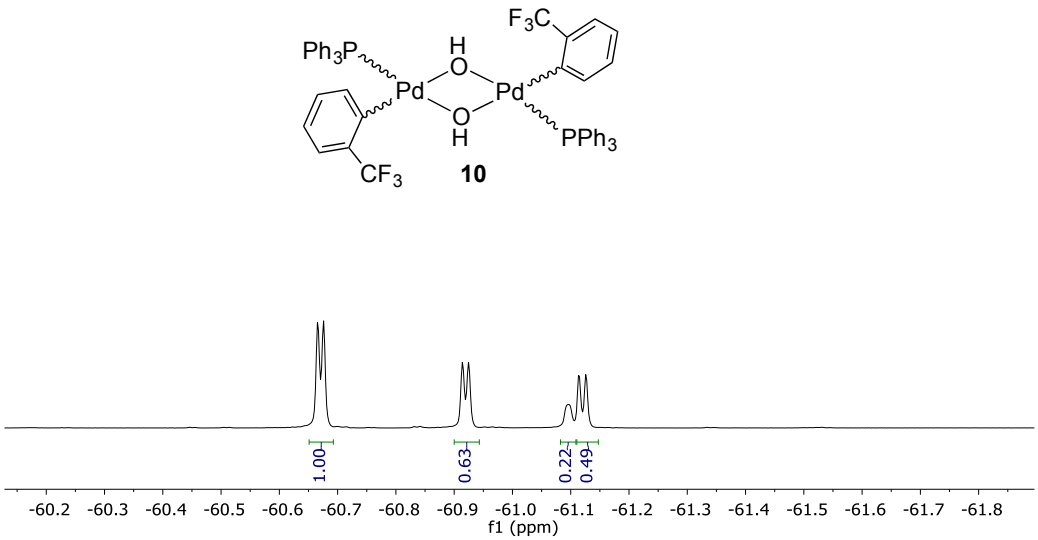

Figure S91. ^{19}F NMR (470.17 MHz, $CDCl_3$) for complex [Pd(*o*-CF_3-C_6H_4)(μ-OH)(PPh_3)]$_2$ (**10**, mixture of isomers) at 298 K.

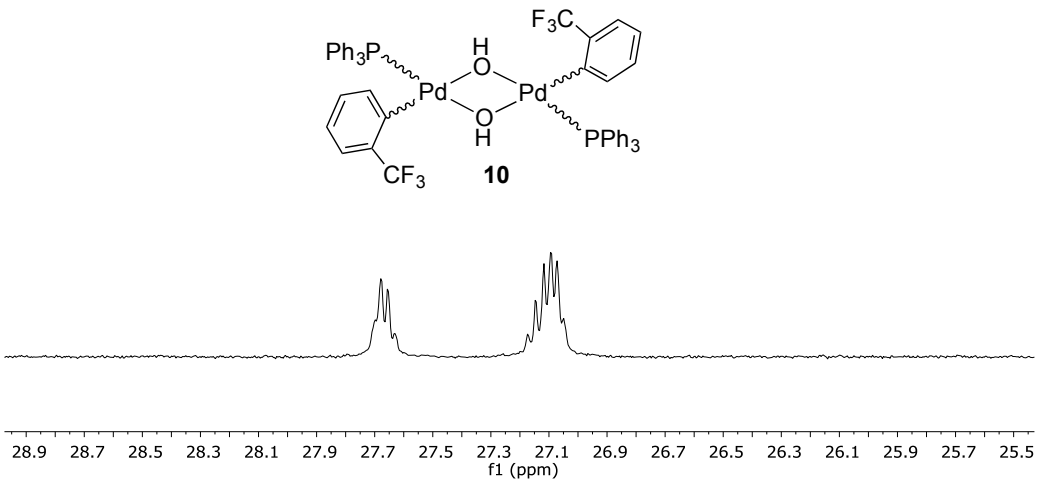

Figure S92. $^{31}P\{^1H\}$ NMR (202.31 MHz, $CDCl_3$) for complex [Pd(*o*-CF_3-C_6H_4)(μ-OH)(PPh_3)]$_2$ (**10**, mixture of isomers) at 298 K.

4. Selected NMR spectra and GPC chromatogram of the polymers

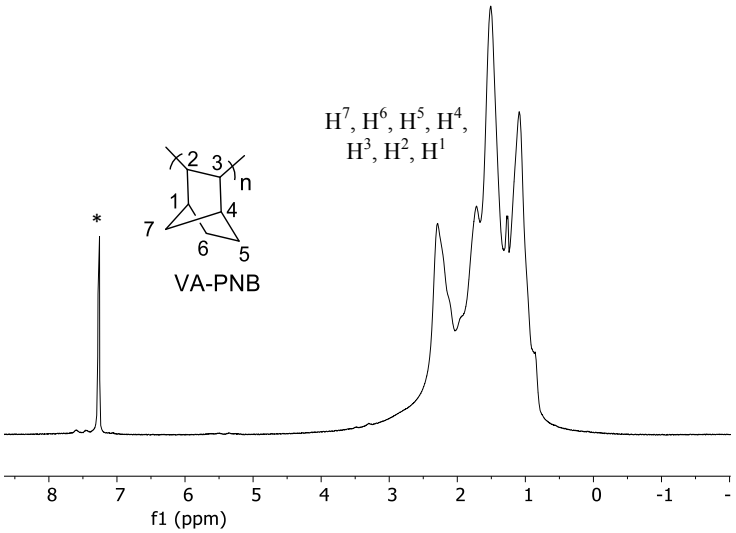

Figure S93. ^{1}H NMR (499.73 MHz, $CDCl_3$) of VA-PNB generated with the catalyst prepared from **1**/$AgBF_4$ in CH_2Cl_2/toluene (ratio NB:**1**/$AgBF_4$ = 75:1:1.25) at 298 K. *Signal corresponding to the solvent.

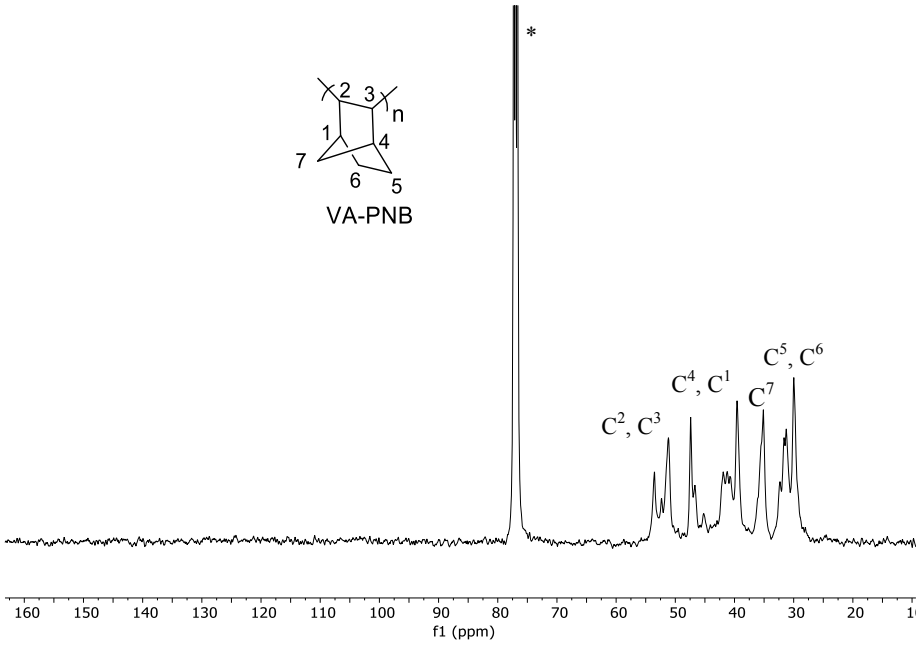

Figure S94. $^{13}C\{^{1}H\}$ NMR (125.67 MHz, $CDCl_3$) for VA-PNB generated with the catalyst prepared from **1**/$AgBF_4$ in CH_2Cl_2/toluene (ratio NB:**1**/$AgBF_4$ = 75:1:1.25) at 298 K. *Signal corresponding to the solvent.

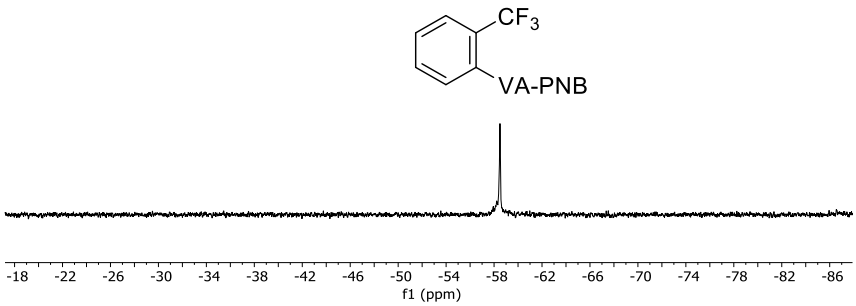

Figure S95. ^{19}F NMR (470.17 MHz, $CDCl_3$) for VA-PNB generated with the catalyst prepared from **1**/$AgBF_4$ in CH_2Cl_2/toluene (ratio NB:**1**/$AgBF_4$ = 75:1:1.25) at 298 K.

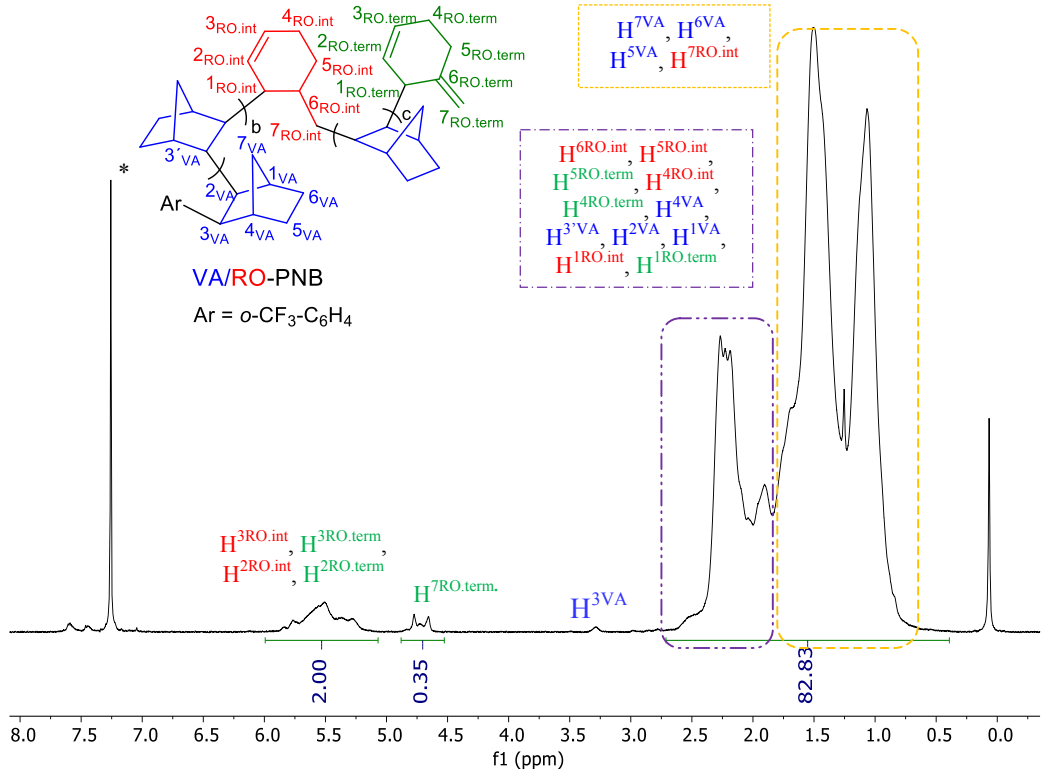

Figure S96. ^{1}H NMR (499.73 MHz, $CDCl_3$) of the polymer VA/RO-PNB generated with the catalyst prepared from **1**/$AgBF_4$ in acetone (ratio NB:**1**/$AgBF_4$ = 75:1:1.5) at 298 K. *Signal corresponding to the solvent.

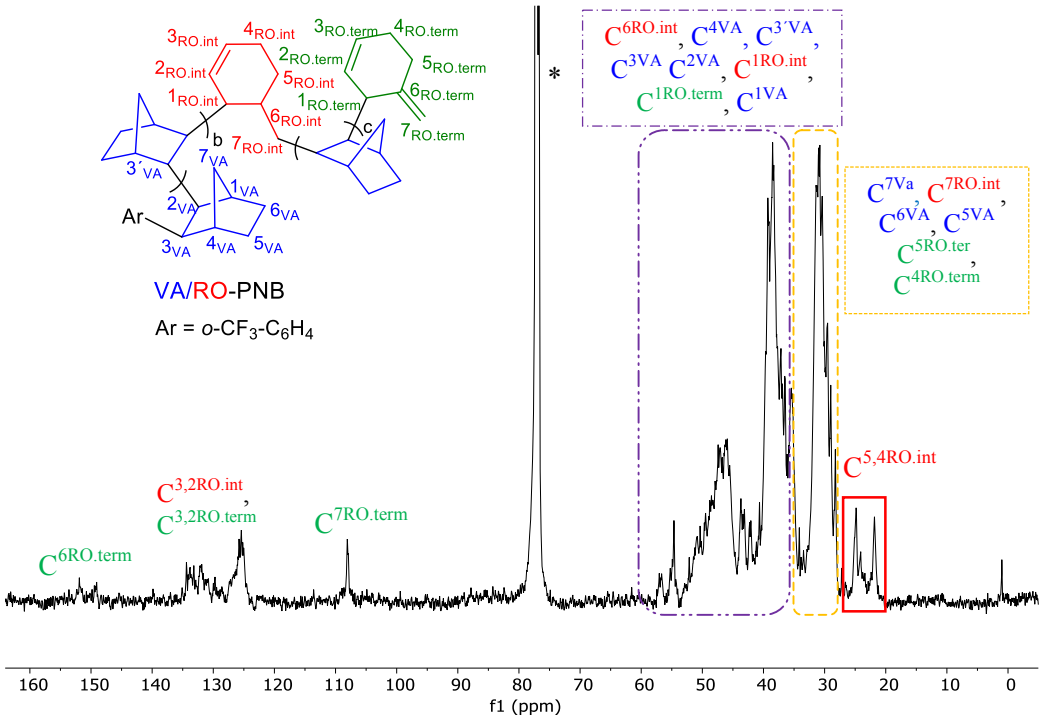

Figure S97. $^{13}C\{^{1}H\}$ NMR (125.67 MHz, $CDCl_3$) of the polymer VA/RO-PNB generated with the catalyst prepared from **1**/$AgBF_4$ in acetone (ratio NB:**1**/$AgBF_4$ = 75:1:1.5) at 298 K. *Signal corresponding to the solvent.

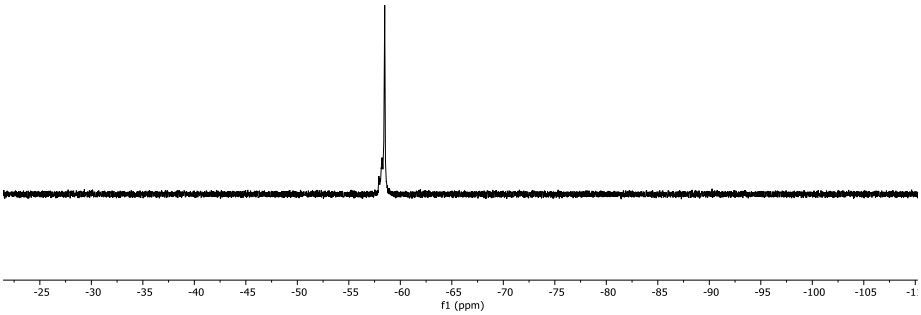

Figure S98. ^{19}F NMR (470.17 MHz, $CDCl_3$) of the polymer VA/RO-PNB generated with the catalyst prepared from **1**/$AgBF_4$ in acetone (ratio NB:**1**/$AgBF_4$ = 75:1:1.5 at 298 K.

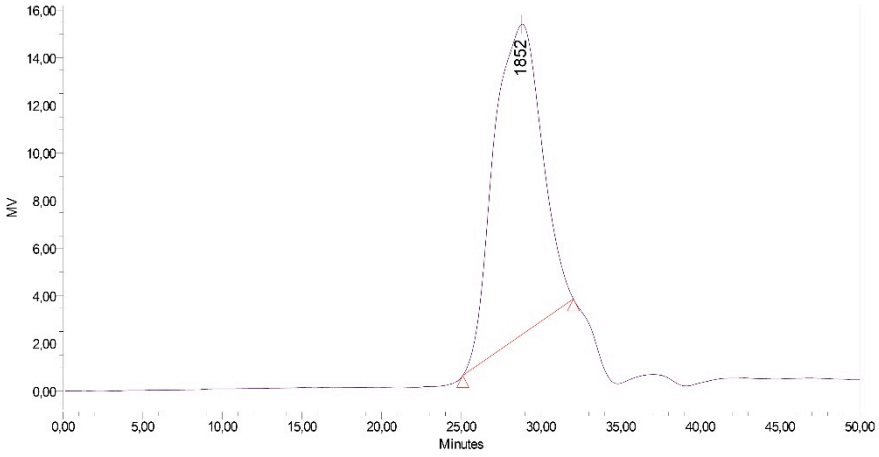

GPC Results

	Dist Name	Elution Volume (ml)	Retention Time (min)	Adjusted RT (min)	Mn	Mw	MP	Mz	Mz+1	Mz/Mw	Mz+1/Mw
1		28,767	28,767	28,767	3168	4200	1852	5692	7396	1,355256	1,761156

Figure S99. GPC chromatogram for VA/RO-PNB synthesized with the catalyst prepared from **1**/$AgBF_4$ in acetone.

6. References

1 a) E. A. Standley, S. J. Smith, P. Müller and T. F. Jamison, *Organometallics* 2014, **33**, 2012-2018; b) M. SennŌ, S. Tsuchiya, M. Hidai and Y. Uchida, *Bull. Chem. Soc. Japan*, 1976, **49**, 1184-1186.

2 D. R. Coulson, L. C. Satek and S. O. Grim, *Inorg. Synth*. 1972, **13**, 121-124.

3 P. Fitton and E. A. Rick, *J. Organomet. Chem.* 1971, **28**, 287-291.

4 a) H. F. Klein and H. K. Karsch, *Chem. Ber.* 1973, **106**, 1433-1452; b) A. H. Christian, P. Müller and S. Monfette, *Organometallics* 2014, **33**, 2134-2137; c) E. Carmona, J. M. Marín, P. Palma, M. Paneque and M. L. Poveda, *Inorg. Chem.* 1989, **28**, 1895-1900.

5 J. M. Jenkins, J. C. Verkade, *Inorg. Synth*. 1968, **11**, 108-111.

6 V. V. Grushin, H. Alper, *Organometallics* 1993, **12**, 1890-1901.

7 For characterization of VA-PNBs see: a) W. Kaminsky, A. Bark, M. Arndt, *Makromol. Chem. Macromol. Symp.* 1991, **41**, 83-93; b) M. Arndt, R. Engenhausen, W. Kaminsky, K. Zoumis, *J. Mol. Catal. A Chem.* 1995, **101**, 171-178; c) D. A. Barnes, G. M. Benedikt, B. L. Goodall, S. S. Huang, H. A. Kalamarides, S. Lenhard, L. H. McIntosh, K. T. Selvy, R. A. Shick, L. F. Rhodes, *Macromolecules* 2003, **36**, 2623-2632.

8 I. Pérez-Ortega, A. C. Albéniz, *Chem. Sci.,* 2022, **13**, 1823-1828.

9 A. Tenaglia, A. Terranova, B. Waegell, *J. Mol. Cat.* 1987, **40**, 281-287.

10 CrysAlisPro Software system, version 1.171.33.51, 2009, Oxford Diffraction Ltd, Oxford, UK.

11 G. M. Sheldrick, *Acta Cryst.*, 2015, **C71**, 3-8.

12 O. V Dolomanov, L. J. Bourhis, R. J. Gildea, J. A. K. Howard and H. Puschmann, *J. Appl. Crystallogr.* 2009, **42**, 339–34.